A Numerical Solutions of Some Nonlinear Fractional Flow Problems

PhD Thesis

By

Abdul Quayam Khan

Supervised By

Dr. Amer Rasheed

Department of Mathematics,

Lahore University of Management Sciences,

Lahore, Pakistan.

2021

. This work is submitted as a thesis in the partial fulfillment of the requirements for the degree of Doctor of Philosophy in Mathematics, to the Department of Mathematics, Lahore University of Management Sciences, Lahore, Pakistan.

DEDICATION

To all front line Doctors, Nurses and medical staff who are fighting with CoViD-19 and saving humans life.

Acknowledgement

I would like to thank my advisor Dr. Amer Rasheed for being a great mentor from whom I learned so much and for financially supporting me. I also wish to thank Dr. Zhilin Li, Dr. Shaheen Nazir and my committee members Dr. Sultan Sial and Dr. Imran Naeem for their time and wise opinions. My thanks also goes out to Asgher Ali, Muhammad Shoaib Anwar, my co-workers at the LUMS, who have been a great help. Finally, I would like to thank my family, for their constant support over the years.

Abdul Quayam Khan

October 6, 2021

ABSTRACT

Physical models of viscoelastic flow in terms of fractional order derivatives is a fascinating subject, especially in the fields of engineering, fluid mechanics and mathematical biology. These viscoelastic fluid models represent more realistic behavior as compared to the integer order derivatives in fluid dynamics. This is mainly because of the freedom one gets to choose either fractional order derivatives or integer order derivatives while formulating the flow problems. Mathematical modeling of engineering, fluid dynamics and industrial problems usually result in the form of fractional partial differential equations. These models are controlled within their domain of validity by fractional order Partial Differential Equations PDEs. Therefore, it is imperative to be familiar with previously developed methods for solving fractional order PDEs. In literature, there are several analytical methods – such as Laplace transformation as well as Fourier transformation – which had been used to solve linear fractional order PDEs. However, it is difficult to solve non-linear fractional order PDEs using these analytical methods. Consequently, most of viscoelastic flow problems with heat transfer analysis cannot be described in one fractional order PDE. Hence, researchers use numerical techniques to find approximate solutions for such fractional PDEs.

In this thesis, we have highlighted the numerical simulations and fractional order derivative effects on the fluid flow of three non-linear viscoelastic fluid problems: magnetohydrodynamics (MHD) flow of nanofluid with magnetic field, Maxwell's fluid flow through a space occupied by Forchheimer medium, and unsteady natural convection of Maxwell's viscoelastic fluid based on boundary layer heat transfer. The governing fractional PDE's for these viscoelastic flows are non-linear and coupled type fractional PDE's. Numerical methods, such as finite element and Euler backward approach, along with L_1 algorithm approximation, have also been used to find approximate solutions for non-linear coupled fractional PDEs. Finite element and Euler backward methods are used

to discretize space variables, whereas L_1 algorithm is used to discretize fractional order derivative with respect to time. A MATLAB code is designed for simulations. Moreover, the numerical results with physical and fractional parameter effects are presented in form of graphs.

Publications

1. A. Q. Khan, A. Rasheed, Mixed Convection Magnetohydrodynamics Flow of a Nanofluid with Heat Transfer: A Numerical Study, Mathematical Problems in Engineering. Hindawi **2019** 8129564.

2. A. Q. Khan, A. Rasheed, Numerical Simulation of Fractional Maxwell Fluid Flow Through Forchheimer Medium, International Communications in Heat and Mass Transfer. Volume 119, December 2020, 104872.

3. A. Q. Khan, A. Rasheed, Effects of Exponential Variable Viscosity on Heat Transfer Flow of MHD Fractional Maxwell Fluid, Internal Journal of Applied and Computational Mathematics, 6, 136 (2020).

Introduction

The structured of the thesis This structure of the thesis is the is following.

Chapter 1 In this chapter we briefly discuss flow problems with integer and non integer derivatives. The literature review is carried out for the solution and physical behavior of the flow problems.

Chapter 2 This chapter, is dedicated to provide some basic equations of motion and laws of fluid with their derivation of fractional momentum, fractional energy and Tensor equations, are discussed.

Chapter 3 In this chapter, a numerical techniques that we used to find solution of our problems. The discretization of fractional derivatives by using finite difference, finite element for space variable and finite difference methods are explained in detail.

Chapter 4 This chapter describes convection effects , the study of convection effects along with thermal radiations on the boundary layer flow of fractional Maxwell fluid. Numerical solutions for the fluid temperature and velocity are obtained by employing the Crank Nicolson finite difference method along with L1-algorithm. The problem solutions depend on the fractional order of time-fractional derivative as a parameter (the memory parameter). The influence of the memory parameter on the heat transfer and fluid motion has also been studied.

Chapter 5 In this chapter, a brief presentation of unsteady oscillatory flow of incompressible fluid with transfer of heat in a horizontal channel. Maxwell fluid is flowing through a space filled by Forchheimer medium. The Caputo time operator has been used in the formulation of governing a flow problem. A numerical solution has also been obtained using Finite Element Method for space variables and Finite Difference Method for fractional time derivatives.

Chapter 6 In this chapter, the unsteady mixed convection of Maxwell viscoelastic fluid based on boundary layer heat transfer, has been studied. The stretching sheet on lower wall of fluid with exponential time dependent viscosity has also been implemented. Moreover, the fractional equations of Maxwell fluid are carefully derived. These governing equations are then used to derive nonlinear coupled partial differential equations (PDEs) which involves space and time derivatives in convection terms. A comparative study of the fractional models and ordinary models has been carried out and results are presented in graphical illustrations. It has been found that the memory effects have a strong influence on the fluid motion and heat transfer.

Chapter 7 In this chapter, the immersed interface method for fractional one dimensional heat equation is introduced briefly. The numerical solution of this problem with the von Neuman stability analysis will be continued.

Contents

Chapter 1

Introduction

Fluid mechanics is one of the most significant branches of continuum mechanics. It falls under the umbrella of applied science with its applications in several practical domains, especially in the fields of engineering. Consequently, several mathematical models of fluid flow have been developed and applied to the problems. These models have helped us to look at the problems from different perspectives and identify any causal relationships that may affect the results. Hence, several techniques such as ventilation and air-conditioning procedure, drying and cooling method, thin-film and energy generation process, etc. have seemed to benefit the most from this progress. Fluids can generally be divided into two main categories: liquids and gases. Liquids have a higher density with their molecules having smaller distance amongst each other, thus making the fluid more viscous. Gases, on the other hand, are characterized by relatively lower densities and viscosities with large distances between their molecules. Fluids that obey Newton's law of viscosity are called Newtonian or linear fluids. Some examples of these fluids are water, air, oil, etc. In such type of fluids, rate of shear is directly proportional to the sheer stress. While these fluids may exhibit constant viscosity, they still fail to show elastic properties under typical processing conditions. For instance, polymeric materials, subjected to deformation, can remember their recent molecular configurations. These fluids tend to recover their original state and, in addition to viscosity, will exhibit elasticity. Other materials, however, such as toothpaste, drilling mud, etc. behave like solids and do not flow if they are a subject to small shear forces; these materials require higher shear forces

in order to flow properly. Similarly, fluids that exhibit significant elastic properties are called non-Newtonian or non-linear fluids. In such complex fluids, however, the viscosity does not remain constant. In fact, it decreases with the increase in temperature. Since solids exhibit similar properties, it can be said that solids are also non-Newtonian fluids with their viscosities approaching to infinity [1]. Some other examples of fluids exhibiting non-Newtonian behavior are biological fluids and cement slurries, chocolate and greases, plastic melts and paints, etc. In modern time, non Newtonian fluids have gained much attention due to their vast range of applications in industrial engineering. These fluids can be divided into three further types: pseudoplastic, dilitant, and visco-plastic fluids. Pseudoplastics or shear-thinning fluids are the ones whose viscosity decreases with an increase in shear rate. On the other hand, dilatant or shear thickening fluids' viscosity increases with an increase in shear rate. While visco-plastics are characterized as the ones with minimum stress threshold. These fluids are unique in the sense that they have a multi-phase nature (emulsions, dispersion, and suspensions) as well as polymeric (large molecule, or macromolecule) melt. Therefore, it is almost impossible to explain the complex behavior of non-linear fluids by the Newtonian models as the models are based on linear shear stress and strain relationship. Hence, this deficiency has led the researchers to depart from Newtonian models and hypothesize the limitations of non-Newtonian models. Fluids can be classified by either considering the effect of phase conditions on the flow, or by determining their rheological type. Phase condition can further be divided into three phenomena: homogeneity, pseudo homogeneity and heterogeneity. Similarly, rheological fluids are also identified by their three main types: purely viscous (viscosity responding instantaneously to a step change in shear rate or shear stress), thixotropic (having a rate or time dependent viscosity which decreases with time) and viscoelastic (having a time dependent viscosity which increases with time). Viscoelastic fluids are also unique in the sense that when stress applied on them is removed at once, the strain disappears gradually as opposed to other fluids whose strain fades away as soon as the applied stress is removed. James Clerk Maxwell [2], a Scottish scientist, introduced a model for viscoelastic fluids for the first time. This fluid model, also known as the "Rate Type Fluid Model", was published in his research paper on the dynamical theory of gases.

The Maxwell model has an advantage of being expressed as a differential model in its basic form. This permits a comparison between results of different methods. The model is still being used by researchers, especially to describe the response of some polymeric liquids, and its application is being thoroughly discussed in several research articles. Case in point: Maxwell fluid flow of heterogeneous and homogeneous processes, particularly in stagnation region over a stretched surface, was studied and the behavior of fluid flow was analyzed with several set of physical parameters [3]. The effect of magnetic field on a fractional Maxwell nano-fluid over a moving plate was also thoroughly investigated in a later study [4]. Moreover, Liu and Guo [5] studied MHD flow of Maxwell liquid with slip conditions pursued by a moving plate. Similarly, Maxwell fluid of unsteady flow with boundary layer approximation has been examined [6], MHD flow of a Maxwell nano-fluid with thermal radiation and stretching surface has been analyzed (Madhu et. al) [7], and slip coefficient effect on velocity has also been discussed [8]. In addition, Hsiao [9], in his experiment, studied the Maxwell fluid model of a thermal extrusion energy conversation problem and solved it by using numerical techniques . Magnetohydrodynamics (MHD) is defined as the dynamics of electrically conducted fluid in a magnetic field. The word "magnetohydrodynamics" is an embrace of magneto (magnetic), hydro (fluid) and dynamics (moment). MHD was initiated by Hannes Alfven, a Swedish Physicist, who received a Noble prize in 1970 for his fundamental work in physics. Since the flows in hydrodynamics do not explain the external magnetic field which creates a change in these flows, magnetohydrodynamics inspects this phenomenon and combines classical fluid mechanics and electrodynamics. It is relatively a new field and has many applications in science and engineering[10]-[13]..

The relationship of fluids and temperature is rather an important one. Temperature changes when a fluid moves. This is mainly because of the difference between boundaries or between an ambient fluid and boundary. These temperature variations can also exist due to variation of sources, such as absorption of thermal radiation, radioactivity, and condensation, etc. As we know that heat travels in three ways - conduction, convection and radiation - we will be considering radiation and convection only in our study. Radiation is a form of electromagnetic energy with some of its applications in nuclear power

generation, reactor cooling and combustion processes. Solar radiation has a lot of significance in advance energy conversation system which are performed at high temperature. Some examples of these are space vehicle re-entry, astrophysical flows, and solar power technology, etc. Such transfer, however, usually occurs when there is difference between the surface and surrounding temperatures. Bhattacharyya studied the effects of thermal radiation on micro-polar fluid flow as well as the heat transfer over a porous shrinking sheet [14] . In their study, Bhattacharyya [15] analyzed MHD flow of Casson fluid in the presence of radiative, stretching sheet in the stagnation region. Hayat, on the other hand, investigated the Maxwell flow of mixed convection near a stagnation point along with thermal radiation and convective boundary conditions [16].

In convection, on the other hand, heat energy passes due to difference in temperatures between the particles between surface and a moving liquid. The convection heat transfer occurs in two different ways: diffusion and advection. Diffusion is when fluid molecules move from higher concentration region to lower concentration region, whereas the movement of fluid molecules due to bulk motion is referred to as advection. Furthermore, convection can be divided into two parts: natural convection or free convection and forced convection. In free convection, energy transfers due to temperature derived density differences in a fluid motion. Whereas in forced convection, energy is transferred due to an external factor. In 1995, Choi and Eastman [17], who were working in a research group at the Argonne National Laboratory in USA, coined a new term for fluids that transfer heat – nanofluids. In their study, they referred to the liquid which is heated by diverged nanoparticles into a base fluid. Nanofluid is a fluid having nanometer (small diameters of nanoscale) sized elements, known as nanoparticles. These particles can be metallic (Fe, Al, Ag, Au, Cu), non-metallic (Al2O3, Fe2O3, CuO, TiO2, SiO2), or in the form of carbon nano-tubes (CNT, MWCNT, SWCNT). Nanofluids enhance thermal properties vis-a-vis base fluids, thus making them a better alternative. In other words, nanoparticles enhance thermal conductivity, viscosity and density but decrease specific heat capacity. There are two techniques that are used to synthesize nanofluids for production, namely single-step method and two-step method. In a single step method, nanoparticles are vaporized directly into the base fluid to produce stable nanofluids. There are several types of single-

step methods used for nanofluids preparation. For instance, Akhavan [18] used chemical vapour deposition process, Khoshvagh [19] and Rakhsha [20] used electrical explosion of wire (EEW) in liquid media, and Bahremand [21] used silver nanoparticles method. In second-step method, however, nanoparticles are first developed by different methods and then scattered into the base fluid. Case in point: Venkatachalapathy prepared CuO nanoparticles using a two-step method mixed with deionized water [22], and Naphon used ultrasonic method for the preparation of TiO2 nanofluids [23]. Similarly, many researchers have used two-step method for the preparation of nanoparticles. Nanofluids are now being used to explain fluid dynamics. For example, Kumar investigated the Marangoni effects on nanofluid in the presence of heat [24]. Turkyilmazoglu and Pop also studied heat and mass transfer of free convection flow of nanofluids containing Al2O3, Cu, Ag, CuO and TiO2 as nano particles [25]. Fluid flow through a porous medium continues to be an area of intensive research activity. It plays an important role in transport phenomena of fluid due to its large applications in applied science (filtration, rock mechanics, hydrogeology, etc.), and engineering (bio-remediation, petroleum engineering, construction engineering, etc.). Some examples of porous medium are rocks, soil, biological tissues such as bones, wood, cements and ceramics. The most important concept in the study of fluid transport under a porous medium, however, is the Darcy's Law, which has been widely used in petroleum industries. This law states that a fluid flow is linearly proportional to the pressure gradient. It is interesting to note that Darcy's law holds only for small velocities of both liquids and gases. At higher velocities, therefore, since the pressure gradient does not have a linear relationship, Darcy's law fails and is replaced by Dupuit [26] and Forchheimer's [27] study. Dupuit and Forchheimer noticed that drag is a quadratic function in the flow rate. Consequently, they proposed an equation which is commonly referred to as "Forchheimer equation". The main aim of this study, therefore, is to evaluate the validity of the Forchheimer model i.e. to add quadratic term of velocity into momentum equation. Several attempts have been made in past to validate the equation. For example, Seddeek investigated mixed convection flow with the presence of viscous dissipation and Darcy–Forchheimer in a vertical plate [28]; Sadiq and Hayat studied two dimensional Darcy-Forchheimer flow induced by stretched surface with magneto Maxwell fluid [29];

Anwar and Rasheed studied in compressible second grade fluid through a Forchheimer medium by emplying fractional derivative to their problem and found solution by using finite element and finite difference method [30].

Fractional calculus (FC) is a field of mathematics which deals with the study of integrals and derivatives of a non-integer order derivative. The history of fractional calculus begins when Leibniz wrote a letter to L'Hospital, in 1695, where the idea of non-integer order derivative was initially suggested. From that time until today, fractional calculus has been developed by many mathematicians, such as Liouville, Euler, Riemann, Grunwald, Lagrange, Heaviside, Fourier, Abel, Caputo etc . Almost all of them have proposed the definition of FC as per their understanding [31]. Nowadays, modeling with fractional derivatives are established experimentally as well as theoretically. Mathematical models that are derived with the help of fractional order derivatives simulate certain physical phenomenon more realistically. These phenomena are critical particularly for the systems wherein the hereditary effects are crucial as they depend on the past conditions. Fractional models have been developed and employed in many fields of science and engineering, such as fluid dynamics, electromagnetic, bio-population models, viscoelasticity, optics, electrochemistry and signal processing, etc. in order to establish behavior of several physical quantities [32]-[35]. Fractional models are also used for the accurate modelling of damping. Physical phenomena of fluid mechanics, electricity, and quantum mechanics models, etc. are controlled within their domain of validity by using integer order partial differential equations. Hence, Fractional Maxwell model of a viscoelastic fluid in a channel or cylinder has an area of keen interest for mathematicians who are working on fluid dynamics. In the flow motion, researchers are using fractional derivatives in rheological constitute equations of the momentum, where an ordinary time derivative is changed with fractional order derivative. Since Maxwell fluid model with ordinary derivatives could not give reasonable fit of data to be experimented or tested for complete range of frequencies, this gives a space to fractional Maxwell fluid model. Fractional Maxwell model can reveal better agreement of the data vis-a-vis ordinary derivative Maxwell model. Many researchers are using fractional calculus in their research work. For instance, Fetecau investigated the fractional model of nano-fluids with Caputo time derivative and discussed the influence

of a fractional parameter on velocity and temperature [36]. Shah also studied the Caputo fractional derivative model of a blood flow in a circular cylinder with magnetic particles. Numerical simulations were used to study the behavior of a fractional parameter on fluid and particles velocity [37].

Chapter 2

Fluid Dynamics

2.1 Fundamental of Fluid Dynamics

Fluid mechanics is the study of fluid motion (liquid and gases) and forces acting on it. Mathematical modeling of fluid mechanics makes some fundamental assumption about the material being analyzed. These assumptions or hypothesis are turned into mathematical equations that must be satisfied if hypothesis are true. Fluid mechanics can be separate into fluid static (a study of fluid when it is in rest), fluid kinematic (a study of the fluid when it is in motion) and fluid dynamics (study of different forces effect when fluid is in motion). This chapter describes some basic concepts of modeling, fractional Maxwell fluid constitute equations, fractional derivatives and solution methods of the flow problem.

2.1.1 Fundamental Equations of Fluid Dynamics

2.1.2 Navier-Stokes equation

The Navier-Stokes equations for motion are based on Newton second law of motion for fluids. In case of compressible non Newtonian fluid

$$\rho\left(u_t + u.\nabla u\right) = -\nabla p + \nabla.\mathbb{T} + \mathbb{F}, \tag{2.1}$$

where $u(x, y, t)$ is velocity, $\mathbb{T}(x, y, t)$ is Cauchy stress tensor, $\mathbb{F}(x, y, t)$ is force term, $\nabla = (\partial/\partial x, \partial/\partial y, \partial/\partial z)$ in three dimension, ρ is density and $p(x, y, t)$ is pressure. Term

(see details in [40]).$\rho\left(\frac{\partial u}{\partial t}+u.\nabla u\right)$ represent inertial forces, $\nabla.\mathbb{T}$ represent viscous force on fluid and $\mathbb{F}$ represent external force applied to fluid. Navier-Stokes equation was derived by Poisson, Navier, Saint-Venant, and Stokes. Navier-Stokes equations represent conservation of momentum.

2.1.3 Conservation of mass

This law (law of conservation of mass) was introduced by Antoine Lavoisier which means that mass is neither destroyed nor created in any chemical reaction. In other words, in any chemical reaction mass of a body or element in beginning of reaction will equal same at the end of reaction. In fluid mechanics, conservation of mass is also known as continuity equation

$$\frac{\partial \rho}{\partial t}+\nabla.(\rho u)=0, \tag{2.2}$$

where ρ is density. In case of incomprehensible flow the density becomes constant and continuity equation becomes

$$\nabla.u=0. \tag{2.3}$$

2.1.4 Conservation of energy

The fundamental law of physics known as conservation of energy, which states that, in a particular domain the energy remains constant, and energy can neither be created nor destroyed. Energy conservation can be set through the following equation:

$$\rho C_p\frac{\partial T}{\partial t}+\rho C_p u.\nabla T=\nabla \mathbf{q}, \tag{2.4}$$

here ρ is density, C_p is the specific heat, $\mathbf{q}$ is heat thermal flux and T denotes temperature. Fourier's law of conduction can be written as

$$\mathbf{q}=-k\nabla T, \tag{2.5}$$

where k is thermal conductivity. Using equation (2.5) into (2.4), the temperature equation become

$$\rho C_p\frac{\partial T}{\partial t}+\rho C_p u.\nabla T=-\nabla.(k\nabla T). \tag{2.6}$$

In fractional calculus case, the operator $(1+\lambda\frac{\partial^\alpha}{\partial t^\alpha})$ is applied on both side of equation (2.4)

$$\rho C_p(1+\lambda\frac{\partial^\alpha}{\partial t^\alpha})\frac{\partial T}{\partial t}+\rho C_p(1+\lambda\frac{\partial^\alpha}{\partial t^\alpha})u.\nabla T=-(1+\lambda\frac{\partial^\alpha}{\partial t^\alpha})\nabla.\mathbf{q}. \tag{2.7}$$

The expression for $\mathbf{q}$ is given by the fractional form of generalized Fourier's law introduced by Cattaneo [44].

$$(1+\lambda\frac{\partial^\alpha}{\partial t^\alpha})\mathbf{q}=-k\nabla T, \tag{2.8}$$

where λ denotes relaxation time.

2.1.5 Boussinesq approximation

In the Boussinesq Approximation, density is assumed to be very small such as $\Delta\rho << \rho_o$ for incompressible flow. Here ρ_0 represents reference density and $\Delta\rho$ is density variation. The deviatoric stress term $\nabla.\mathbb{T}$ can be written as $\nabla^2.u$ in momentum equation

$$\rho\left(\frac{\partial u}{\partial t}+u.\nabla u\right)=-\nabla p+\mu\nabla^2.u+F, \tag{2.9}$$

where $F=\rho g$. The bouncy term can be written as $(\rho_0+\Delta\rho)g$, this yields

$$\rho\left(\frac{\partial u}{\partial t}+u.\nabla u\right)=-\nabla p+\mu\nabla^2.u+(\rho_0+\Delta\rho)g, \tag{2.10}$$

where density can be expressed as a liner way as

$$\rho=\rho_0-\beta_0(T-T_0)$$

. , to avoid evaluating the fluid density on local or initial temperature, the bouncy term can further be rewritten as $(\rho-\rho_0)=-\rho_0\beta(T-T_0)$,

$$\rho\left(u_t+u.\nabla u\right)=-\nabla p+\mu\nabla^2.u+g\rho_0-g\rho_0\beta(T-T_0), \tag{2.11}$$

Here β is thermal expansion coefficient and g is gravitational force. To avoid potential round off errors, momentum equation are often written, The pressure and buoyancy terms on the right side of the Navier-Stokes equations, $-\nabla p+(\rho_0+\Delta\rho)g$ are written as $-\nabla P+\Delta\rho g$. Where $P=p+\rho g$. The change from P to p is referred as a pressure shift.

$$\rho\left(\frac{\partial u}{\partial t}+u.\nabla u\right)=-\nabla P+\mu\nabla^2.u-\rho_0\beta(T-T_0)g, \tag{2.12}$$

2.1.6 Cauchy stress tensor

Cauchy stress tensor named after Augus Louis, describes the state of force at a point inside the material. In a Cartesian coordinates, representing state of force in three dimensions requires nine number 3×3 matrix.

$$\tau_{ij} = \begin{bmatrix} \tau_{11} & \tau_{12} & \tau_{13} \\ \tau_{21} & \tau_{22} & \tau_{23} \\ \tau_{31} & \tau_{32} & \tau_{33} \end{bmatrix}$$

The above matrix is the representation of a stress tensor at a point. Stress tensor holds symmetric property that is $\tau_{ij} = \tau_{ji}$, in this we have six entries to calculate instead of nine.

2.1.7 Constitutive equations

In physics, the constitutive equations for a particular material, together with the conservation law of mass, linear momentum and energy, govern the response of that material. Unlike the conservation laws, however, the constitutive equations vary from material to material.

Newtonian fluid Constitutive equation of Newtonian fluid is:

$$\mathbb{T} = \mathbb{S} - p\mathbb{I}, \tag{2.13}$$

$$\mathbb{S} = \mu.\mathbb{A}_1, \tag{2.14}$$

where $\mathbb{I}$ is identity matrix, $\mathbb{S}$ is deviatoric tensor, p is pressure and $\mathbb{A}_1$ is first Rivlin Ericksen tensor given as

$$\mathbb{A}_1 = (\nabla u) + (\nabla u)^\intercal,$$

$$\mathbb{A}_1 = L + L^T$$

Maxwell fluid

$$\mathbb{T} = \mathbb{S} - p\mathbb{I}, \quad \mathbb{S} + \lambda \frac{\delta \mathbb{S}}{\delta t} = \mu \mathbb{A}_1, \tag{2.15}$$

here λ is relaxation time and if $\lambda \approx 0$ we get tensor of Newtonian fluid.

$$\frac{\delta \mathbb{S}}{\delta t} = \frac{d\mathbb{S}}{dt} - L\mathbb{S} - \mathbb{S}L^{\intercal} \tag{2.16}$$

Fractional Maxwell fluid In fractional Maxwell fluid constitutive equation , we have to replace time derivative with fractional order derivative

$$\mathbb{T} = -p\mathbb{I} + \mathbb{S}, \quad \mathbb{S} + \lambda^{\alpha} \frac{\delta^{\alpha} \mathbb{S}}{\delta t^{\alpha}} = \mu \mathbb{A}_1, \tag{2.17}$$

where α denotes fractional parameter.

2.1.8 Fractional boundary layer equation of Maxwell model

To formulate boundary layer equation for fractional Maxwell fluid, we have to use fractional constitutive equation of Maxwell fluid given above. One dimensional Continuity and momentum equation, for an incompressible fluid zero force term are:

$$\frac{\partial u}{\partial y} = 0, \tag{2.18}$$

from Equation (2.1), we have

$$\rho \left(\frac{\partial}{\partial t} + (\nabla . u) \right) u = \mu \frac{\partial u}{\partial y}, \tag{2.19}$$

now applying operator $(1 + \lambda^{\alpha} \frac{\partial^{\alpha}}{\partial t^{\alpha}})$ on both sides of Equation (2.19)

$$\rho (1 + \lambda^{\alpha} \frac{\partial^{\alpha}}{\partial t^{\alpha}}) \left(\frac{\partial}{\partial t} + (\nabla . u) \right) u = \mu \frac{\partial}{\partial y} (u + \lambda^{\alpha} \frac{\partial^{\alpha} u}{\partial t^{\alpha}}), \tag{2.20}$$

from fractional Maxwell model constitutive equation (2.17), we will replace right hand side term with $\mathbb{A}_1$

$$\rho (1 + \lambda^{\alpha} \frac{\partial^{\alpha}}{\partial t^{\alpha}}) \left(\frac{\partial}{\partial t} + (\nabla . u) \right) u = \mu \frac{\partial \mathbb{A}_1}{\partial y}. \tag{2.21}$$

For velocity u = $u(y, t)$, $\mathbb{A}_1$ is calculated as

$$\mathbb{A}_1 = \begin{pmatrix} 0 & u_y & 0 \\ u_y & 0 & 0 \\ 0 & 0 & 0 \end{pmatrix}$$

and for $\nabla.\mathbb{A}_1$,

$$\nabla.\mathbb{A}_1 = 2\frac{\partial^2 u}{\partial y^2}e_y \tag{2.22}$$

Substituting Equation (2.22) into (2.21)

$$\rho(1+\lambda^\alpha\frac{\partial^\alpha}{\partial t^\alpha})\left(\frac{\partial}{\partial t}+(\nabla.u)\right)u = \mu\frac{\partial^2 u}{\partial y^2}. \tag{2.23}$$

Similarly, when we have two dimensional flow problem then we have velocity field as $U(x,y,t) = u(x,y,t)e_x + v(x,y,t)e_y$. Continuity and momentum equations are

$$\frac{\partial u}{\partial x}+\frac{\partial v}{\partial y} = 0, \tag{2.24}$$

$$\rho\left(\frac{\partial u}{\partial t}+u\frac{\partial u}{\partial x}+v\frac{\partial u}{\partial y}\right) = \mu\frac{\partial \mathbb{T}}{\partial y}, \tag{2.25}$$

$$\rho\left(\frac{\partial v}{\partial t}+u\frac{\partial v}{\partial x}+v\frac{\partial v}{\partial y}\right) = \mu\frac{\partial \mathbb{T}}{\partial y}. \tag{2.26}$$

Applying operator $(1+\lambda^\alpha\frac{\partial^\alpha}{\partial t^\alpha})$ and using constitutive equation we have

$$\rho(1+\lambda^\alpha\frac{\partial^\alpha}{\partial t^\alpha})\left(\frac{\partial u}{\partial t}+u\frac{\partial u}{\partial x}+v\frac{\partial u}{\partial y}\right) = 2\mu\nabla\mathbb{A}_1, \tag{2.27}$$

$$\rho(1+\lambda^\alpha\frac{\partial^\alpha}{\partial t^\alpha})\left(\frac{\partial v}{\partial t}+u\frac{\partial v}{\partial x}+v\frac{\partial v}{\partial y}\right) = \mu\nabla\mathbb{A}_1. \tag{2.28}$$

Rivlin-Ericksen tensor A_1 for two dimensional is

$$\mathbb{A}_1 = \begin{bmatrix} 2\frac{\partial u}{\partial x} & \frac{\partial u}{\partial x}+\frac{\partial v}{\partial y} & 0 \\ \frac{\partial u}{\partial x}+\frac{\partial v}{\partial y} & 2\frac{\partial v}{\partial y} & 0 \\ 0 & 0 & 0 \end{bmatrix}$$

From continuity equation, we have $\frac{\partial u}{\partial x}+\frac{\partial v}{\partial y}=0$. There for replace in above matrix we get

$$\mathbb{A}_1 = \begin{bmatrix} 2\frac{\partial u}{\partial x} & 0 & 0 \\ 0 & 2\frac{\partial v}{\partial y} & 0 \\ 0 & 0 & 0 \end{bmatrix}$$

and $\nabla.\mathbb{A}_1$ is

$$\nabla.\mathbb{A}_1 = 2\frac{\partial^2 u}{\partial x^2}e_x + 2\frac{\partial^2 u}{\partial y^2}e_y, \tag{2.29}$$

Substituting Equation (2.29) into Equation (2.27), governing equations for fractional Maxwell fluid are:

$$\rho(1+\lambda^{\alpha}\frac{\partial^{\alpha}}{\partial t^{\alpha}})\left(\frac{\partial u}{\partial t}+u\frac{\partial u}{\partial x}+v\frac{\partial u}{\partial y}\right)=2\mu\frac{\partial^2 u}{\partial x^2}, \tag{2.30}$$

$$\rho(1+\lambda^{\alpha}\frac{\partial^{\alpha}}{\partial t^{\alpha}})\left(\frac{\partial v}{\partial t}+u\frac{\partial v}{\partial x}+v\frac{\partial v}{\partial y}\right)=\mu\frac{\partial^2 v}{\partial y^2}. \tag{2.31}$$

2.1.9 Dimensionless numbers

Few dimensionless numbers which are significant in fluid flow.

Grashof number Grashof number Gr was introduced by Franz Grashof. This non dimensional parameter is used in free convection flows and it is a ratio between the buoyancy force and the viscous force. Grashof number is

$$Gr=\frac{g\beta_t(T_w-T_\infty)h^3}{\nu^2},$$

where β_t is thermal expansion coefficient, g is gravity, h is length, ν is kinematic viscosity. And T_w and T_∞ are the reference and the free stream temperature.

Prandtl number Prandtl number Pr is a dimensionless parameter used in heat transfer, which was first introduced by Ludwig Prandtl. The Prandtl number Pr is the ratio between moving fluid and thermal diffusivity. Prandtl number is

$$Pr=\frac{\mu c_p}{k},$$

where k is thermal conductivity, c_p is specific heat capacity and μ is dynamic viscosity.

Reynolds number Reynolds number, Re is a dimensionless parameter and it is a ratio of inertial forces (resistance of any physical object) to viscous (viscosity of fluid) forces. It was introduced by Osborne Reynolds and it is define as

$$Re=\frac{\rho h U_0}{\mu},$$

here ρ denotes the density, h characteristic of length, U_0 characteristic of viscosity.

2.1.10 Fractional calculus

Fractional Calculus (FC) is the study of integrals and derivatives of non-integer or even complex order. Being an intensive developing area of calculus and it offers important features for research and becomes more useful in different applications.

Fractional derivatives Many mathematicians gave a different definitions of fractional operator, but two of them are most common, namely, Riemann-liouville and Caputo's one. In the present work, the Caputo's operator will be used to model the flow problems, because this derivative allows using initial conditions in terms of the function and its integer order derivatives. Additionally, derivatives take the same form as for integer order PDEs. While in Riemann-Liouville approach the initial conditions of fractional differential equations containing limiting value of Riemann-Liouville operator at lower terminal or lower bond $t = 0$. For example

$$\lim_{t\to 0} {}_0D_t^{\alpha-k} g(t) = c_k, \quad k = 1, 2, 3, ..., n$$

where c_k is constant. These initial condition can be solved mathematically but their solution are useless, because there is no such physical interpretation of such ICs. (See for further details [38])

Riemann-Liouville operator Suppose that the fraction term $\alpha > 0$, $t > a$ and $\alpha, a, t \in \mathbb{R}$ then

$$D^\alpha g(t) = \begin{cases} \dfrac{1}{\Gamma(n-\alpha)} \dfrac{d^n}{dt^n} \displaystyle\int_a^t \frac{g(\xi)}{(t-\xi)^{\alpha+1-n}} d\xi, & n-1 < \alpha < n, \quad n \in \mathbb{N}, \\ \dfrac{d^n}{dt^n} g(t), & \alpha = n, \quad n \in \mathbb{N} \end{cases} \tag{2.32}$$

Caputo operator Let $\alpha > 0$, $t > a$ and $\alpha, a, t \in \mathbb{R}$ then

$$D^\alpha g(t) = \begin{cases} \dfrac{1}{\Gamma(n-\alpha)} \displaystyle\int_a^t \frac{g^n(\xi)}{(t-\xi)^{\alpha+1-n}} d\xi, & n-1 < \alpha < n, \quad n \in \mathbb{N}, \\ \dfrac{d^n}{dt^n} g(t), & \alpha = n, \quad n \in \mathbb{N} \end{cases} \tag{2.33}$$

Gamma function The gamma function is the generalization of factorial function and it is denoted as $\Gamma(.)$. i.e., $\Gamma(m) = (m-1)!, \quad m \in \mathbb{N}$.

$$\Gamma(z) = \int_0^\infty e^{-y} y^{z-1} dy, \quad Re(z) > 0 \tag{2.34}$$

2.1.11 Numerical Algorithms

The governing equations of non Newtonian fluid for most problems are not unnecessary difficult, their exact solution may be difficult due to non linearity, geometry and material complexity. The numerical simulations means solution of a problem or mathematical model. There are some different methods in numerical analysis to solve ordinary and partial differential equations. In this study, We used Finite element and Euler backward difference methods for simulation of fractional non linear model. Finite element method is applied to solve the approximation of one dimensional problem, and Finite difference method is used to solve the two dimensional problems. The fractional derivatives of Caputo's operator are solved by newly developed $L-$algorithm [76].

The finite element method (FEM) is more general and power full method in its applications to engineering problems that involves complex domain or geometry and complex boundary conditions (BCs). In the FEM a given domain (regular or irregular) is divide into sub-domains, in each of which the mathematical model or governing equation is approximated by the variational method. The concept behind such approximation is related to the fact that it is a straightforward task to represent a non-linear (or complicated) function as a set of simple polynomials.

In Finite Difference Method (FDM) is one of the oldest numerical method to solve linear and non linear differential equations over regular domains. In FDM, the function (sufficiently smooth) is expanded by Taylor series that involve the values of the solution at mesh points. The algebraic equations are then solved by imposing the boundary conditions for the values of solution at each mesh point. [39].

Chapter 3

Numerical Techinques

The purpose of this chapter is introducing FEM and FDM for solving fractional partial differential equations of boundary value problems.

3.1 Finite Difference Method

It is possible to draw the FDM through the following steps:

1 Generate a grid.

A grid is a finite set of points (divided domain) on which we want to find the function values that represent an approximate solution to the partial differential equation. For example, given an positive integer parameter n, we can use a positive uniform Cartesian grid

$$x_i = ih, \quad i = 0, 1, 2, ..., n, \quad h = 1/n$$

The positive integer n can be chosen according to accuracy requirements. If we want the approximate solution has four significant digits, then we can take $n = 160$ or larger. (see details in [41])

2 Use a finite difference formula for the derivative.

Note that for a once differentiable (backward difference) function $v(x)$, we have

$$v^{'}(x) = lim_{\Delta x \to 0} \frac{v(x-h) - v(x)}{h} \tag{3.1}$$

At grid point x_i, $v^{'}(x_i)$ can be approximated using close function values as follows:

$$v^{'}(x_i) \approx \frac{v(x_i + h) - v(x_i)}{h} \tag{3.2}$$

Similarly, the approximation of second order derivative at x_i can be written as:

$$v^{''}(x_i) \approx \frac{v(x_i + h) - 2v(x_i) + v(x_i - h)}{h^2} \tag{3.3}$$

with some error in the approximation.

Consider the elliptic equation

$$v^{"}(x) = f(x)$$

with source term $f(x)$, here we assume $f(x)$ is continuous. In FDM, we replace the differential at each grid point x_i by

$$\frac{v(x_i + h) - 2v(x_i) + v(x_i - h)}{h^2} = f(x_i) + T(x_i) \tag{3.4}$$

where the $T(x_i)$ is called the local *truncation error*. Thus we define the finite difference solution (an approximation) for v(x) at all x_i as the solution V_i (if it exists) of the following linear system of algebraic equations: for i=0,1,2,3,....,n

$$\frac{v_0 - 2v_1 + v_2}{h^2} = f(x_1), \tag{3.5}$$

$$\frac{v_1 - 2v_2 + v_3}{h^2} = f(x_2), \tag{3.6}$$

$$\frac{v_2 - 2v_3 + v_4}{h^2} = f(x_3), \tag{3.7}$$

Similarly for i^{th} component

$$\frac{v_{i-1} - 2v_i + v_{i+1}}{h^2} = f(x_i), \tag{3.8}$$

and for $(n-1)^{th}$ component

$$\frac{v_{n-2} - 2v_{n-1} + v_n}{h^2} = f(x_{n-1}), \tag{3.9}$$

Note that the finite difference equation at every grid point involves solution values at three (stencil) grid points, rest are considered to be zero. i.e., at $x_i - 1$, x_i, and $x_i + 1$. The set of these three grid/mesh points is called the Finite Difference *stencil*.

3 Solution of Algebraic Equations

For approximate solution at every grid point. The system of above algebraic equations can be written in the tridiagonal matrix and vector form as given below

$$\begin{bmatrix} -2/h^2 & 1/h^2 & 0 & 0 & \dots & 0 \\ 1/h^2 & -2/h^2 & 1/h^2 & 0 & \dots & 0 \\ 0 & 1/h^2 & -2/h^2 & 1/h^2 & \dots & 0 \\ \dots & \dots & \dots & \dots & \dots & \dots \\ 0 & 0 & 0 & \dots & 1/h^2 & -2/h^2 \end{bmatrix} \begin{bmatrix} V_1 \\ V_2 \\ V_3 \\ \vdots \\ V_{n-1} \end{bmatrix} = \begin{bmatrix} f(x_1) - V_0/h^2 \\ f(x_2) \\ f(x_3) \\ \vdots \\ f(x_{n-1}) - V_n/h^2 \end{bmatrix}$$

The above tridiagonal system of linear equations $AV = F$ can be solved efficiently in $O(C_n)$ by the Crout or Cholesky algorithm.

4 Computer code.

Make a computer code, run the computer program to get the results. Analyze and visualize the resulting solutions.

5 Error Analysis.

Finite difference algorithmic stability and consistency defends on the convergence of the FDM scheme, The convergence is point-wise. The finite difference method requires the solution v(x) to have up to second-order continuous derivatives.

3.1.1 Stability, Consistency, Convergence, and Error Estimates of FDM

When a FDM is used to solve a partial differential equation (PDE), it is necessary to know how accurate the approximate or finite difference solution is compared to the true or analytical solution.

Global Error

Let $\mathbf{V} = [V_1, V_2, \dots, V_n]^T$ denotes approximate solutions generated by FDM at grid points $x_1, x_2, \dots, x_n$ and $\mathbf{v} = [v(x_1), v(x_2), \dots, v(x_n)]^T$ is the exact solution, then the global error is

$$\mathbf{E} = \mathbf{V} - \mathbf{v}$$

Naturally, we take the smallest/minimum upper bound for global error which is measured by following norms.

1 Infinity norm.

$$||E||_\infty = max_i\{|e_i|\}$$

is the largest norm at even one grid point. This norm is considered as the strongest norm.

2 The 1-norm.

1-norm is defined as

$$||E||_1 = \sum_i h_i|e_i|$$

is average norm, analogous to L^1 norm $\int |e(x)|dx$

3 The 2-norm.

2-norm is defined as

$$||E||_2 = (\sum_i h_i|e_i|^2)^{1/2}$$

is again an average norm and analogous to L^2 norm $(\int |e(x)|^2 dx)^{1/2}$.

If $||E||_2 \leq Ch^p$, $p > 0.$, then finite difference method is p^{th} order accurate.

Local Truncation Errors

Local truncation errors is differences between the differential equation and its finite difference approximations (finite difference formula) at each grid points. It measure how well a finite difference discretization approximates the differential equation. It is defined as

$$T(x) = P_h v - Pv$$

where v is exact solution. For Example, the three point central difference scheme and differential equation $v''(x) = f(x)$ the local truncation error is

$$T(x) = P_h v - Pv = \frac{v(x-h) - 2v(x) + v(x+h)}{h^2} - v''(x) \tag{3.10}$$

Defination

A finite difference scheme is called consistent if [41]

$$lim_{h\to 0}T(x) = lim_{h\to 0}(P_h v - Pv) = 0 \tag{3.11}$$

If $|T(x)| \leq Ch^p$, $p > 0$, then the finite difference discretization is p^{th} order accurate, where constant $C = O(1)$ is the error dependent on the solution $v(x)$. To check truncation error of a finite difference scheme is consistent, we will expand all the terms by using Taylor expansion in the local truncation error at a master grid point x_i. Finding a Truncation error for simple example, the three-point central finite difference scheme for $v''(x) = f(x)$ is

$$T(x) = \frac{v(x-h) - 2v(x) + v(x+h)}{h^2} - v''(x) = \frac{h^2}{12}v^{(4)}(x) + ... = O(h^2) \tag{3.12}$$

such that

$$|T(x)| \leq Ch^2$$

where $C = max_{0\leq x\leq 1}|\frac{h^2}{12}v^{(4)}(x)|$. The finite difference scheme is consistent and the discretization is second order accurate.

3.1.2 The Euler Method

The Euler method (also know as Forward Euler method) is a first order numerical procedure for solving ODEs with a given initial value or initial conditions. One of the good aspect of the forward Euler's method is that it is easy to understand a differential equation with construction of a solution. The first idea is that, from initial condition we have already know the solution up to some time point t^k. The second is, we want to find the solution from $t^k$to t^{k+1} as a straight line. To study this method, let's consider heat equation with initial and boundary value problem.

$$v_t = \beta v_{xx} + f(x,t), \quad t > 0, \tag{3.13}$$

$$v(a,t) = f_1(t), \quad v(b,t) = f_2(t), \quad v(x,o) = v_0(x) \tag{3.14}$$

Let us find finite difference solution for $v(x,t)$ at time $T > 0$.
As a first step, we have to generate a grid

$$x_i = a + ih, \quad i = 0, 1, 2, ..., n, \quad h = \frac{b-a}{n},$$
$$t^k = k\Delta t, \quad k = 0, 1, 2, ..., m, \quad \Delta t = \frac{T}{m}$$

In above method, we cannot take arbitrary or even a small Δt for explicit methods due to numerical instability concerns. The second step is to approximate the both derivatives (with respect to space and time) with finite difference scheme. As we know in this section, how to discretize the space derivatives, so let focus on finite difference formulas for the time derivative.

Forward Euler Method

At a grid (x_i, t^k), $k > 0$, using the forward finite difference approximation for v_t and central finite difference for v_{xx} we have,

$$\frac{v(x_i, t^k + \Delta t) - v(x_i, t^k)}{\Delta t} = \beta \frac{v(x_{i-1}, t^k) - 2v(x_i, t^k) + v(x_{i+1}, t^k)}{h^2} + f(x_i, t^k) + T(x_i, t^k) \quad (3.15)$$

where the local truncation error is

$$T(x_i, t^k) = -\frac{h^2\beta}{12} v_{xxxx}(x_i, t^k) + \frac{\Delta t}{2} v_{tt}(x_i, t^k) + ... \quad (3.16)$$

In above equation, dots denotes the higher order terms and discretization is $O(h^2 + \Delta t)$.

$$\frac{v_i^{k+1} - v_i^k}{\Delta t} = \beta \frac{v_{i-1}^k - 2v_i^k + v_{i+1}^k}{h^2} + f_i^k, \quad (3.17)$$

where $f_i^k = f(x_i, t^k)$, with v_i^k denoting approximate solution for $v(x_i, t^k)$. when we take $k = 0$, v_i^0 is the initial condition at grid (x_i, t^0). From the values v_i^k at time step k to the solution of the finite difference equation at the next time step $k + 1$ is

$$v_i^{k+1} = v_i^k + \Delta t \left(\beta \frac{v_{i-1}^k - 2v_i^k + v_{i+1}^k}{h^2} + f_i^k \right), \quad i = 1, 2, 3, ..., n-1 \quad (3.18)$$

The solution of the finite difference equations can be obtained directly from the approximate solution at previous time $(k-1)$ steps and we do not need to solve a system of

algebraic/linear equations, so this method is called explicit. In fact, we compute the solution at t^1 from the initial condition (IC) at t^0, and then at t^2 using the approximate solution at t^1. Such an approach is often called a time marching method.
When testing the forward Euler's method with different Δt and keep checking the errors in a problem with a known exact or analytical solution, we find out that the method works well when we take Δt grater then zero and less or equal to $\frac{h^2}{2\beta}$ ($0 < \Delta t \leq \frac{h^2}{2\beta}$) but results blows up when we take $\Delta t > h^2$.

3.1.3 The Crank-Nicolson method

The time step constraint for het equation with source term is $\Delta t = \frac{h^2}{2\beta}$ for the explicit Euler's method is generally considered to be a severe restriction, e.g., In above initial and boundary value problem if we take $h = 0.01$, final time is $T = 10$ and constant $\beta = 100$, then we need 2×10^7 steps to get the solution at the final time. The backward Euler's method does not have the time step constraint (can find details of backward Euler method in [41]), but it is only first order $O(h)$ accurate. If someone wants second-order accuracy $O(h^2)$, we have to take $\Delta t = O(h^2)$. For finite difference scheme that is second-order $O(h^2 + \Delta^2)$ accurate both in space variable and time, without compromising stability and increasing computational cost, is the Crank–Nicolson scheme.
The following lemma is based on Crank–Nicolson scheme,

Lemma 3.1.1. *Let $\Phi(t)$ be a continuous function that has first- and second-order continuous derivatives, i.e., $\Phi(t) \in c^2$. Then*

$$\Phi(t) = \frac{1}{2}(\Phi(t - \frac{\Delta t}{2}) + \Phi(t + \frac{\Delta t}{2})) + \frac{(\Delta t)^2}{8} v''(t) + H.O.T \tag{3.19}$$

The Crank–Nicolson scheme approximates the heat equation with source term

$$v_t = v_{xx} + f(x, t) \tag{3.20}$$

at $(x_i, t^k + \Delta t/2)$, by averaging the time level t^k and t^{k+1} of the diffusion term or spatial

derivative $\nabla.(\beta\nabla v)$ and $f(x,t)$.

$$\frac{v(x_i,t^k+\Delta t)-v(x_i,t^k)}{\Delta t}=\frac{\beta^k_{i-\frac{1}{2}}v(x_{i-1},t^k)-(\beta^k_{i-\frac{1}{2}}+\beta^k_{i+\frac{1}{2}})v(x_i,t^k)+\beta^k_{i+\frac{1}{2}}v(x_{i+1},t^k)}{2h^2} \quad (3.21)$$

$$\frac{\beta^{k+1}_{i-\frac{1}{2}}v(x_{i-1},t^{k+1})-(\beta^{k+1}_{i-\frac{1}{2}}+\beta^{k+1}_{i+\frac{1}{2}})v(x_i,t^{k+1})+\beta^{k+1}_{i+\frac{1}{2}}v(x_{i+1},t^{k+1})}{2h^2}+\frac{1}{2}(f(x_i,t^k)+f(x_i,t^{k+1})) \quad (3.22)$$

The discretization is of second order time and space. Taking $\beta=1$ and using the Taylor expansion.

$$\frac{v(x,t+\Delta t)-v(x,t)}{\Delta t}=v_t(x,t+\Delta t/2)+\frac{1}{3}(\frac{\Delta t}{2})^2v_{tttt}(x,t+\Delta t/2)+O((\Delta t)^4) \quad (3.23)$$

$$\frac{v(x+h,t)-2v(x,t)+v(x-h,t)}{h^2}=\frac{\partial^2v(x,t)}{\partial x^2}+O(h^2) \quad (3.24)$$

$$\frac{v(x+h,t+\Delta t)-2v(x,t+\Delta t)+v(x-h,t+\Delta t)}{h^2}=v_{xx}(x,t+\Delta t)+O(h^2) \quad (3.25)$$

$$\frac{1}{2}\left(v_{xx}(x,t)+v_{xx}(x,t+\Delta t)\right)=\frac{\partial^2v(x,t+\Delta t/2)}{\partial x^2}+O((\Delta t)^2) \quad (3.26)$$

$$\frac{f(x,t)+f(x,t+\Delta t)}{2}=f(x,\frac{t+\Delta t}{2})+O((\Delta t)^2) \quad (3.27)$$

For every time step, we have to solve a (tridiagonal) system of linear equations to get V_i^{k+1}. The computational cost is slightly more than that of the explicit Euler method in 1D, and we can take $\Delta t=h$ and have second order $O((\Delta t)^2)$ accuracy. Although the Crank–Nicolson (CR) method is an implicit method, it is much more efficient than the explicit Euler's method since it is second order $O(h^2+(\Delta t)^2)$ accurate both in space and time with the same computational cost or complexity.

3.2 Discretization of fractional derivative in time

Let us consider the numerical resolution of a fractional derivative w.r.t time, which is derived from the integer order derivative by replacing the derivative with a non integer

order derivative of order α, here α is: $0 \leq \alpha \leq 1$.

Let $T > 0$, consider the time-fractional derivative of Caputo definition

$$\frac{\partial^\alpha v}{\partial t^\alpha} = \frac{1}{\Gamma(1-\alpha)} \int_0^t \frac{\frac{\partial v(x,s)}{\partial s}}{(t-x)^\alpha} ds, \quad 0 < \alpha < 1, \tag{3.28}$$

when $\alpha = 1$ then derivative in (3.28) will become ordinary derivatives.

For the discritization of Caputo fractional derivative, first, we will introduce a finite difference formula to discretize the fractional derivative. Let $t_k = k\Delta t$, $k = 0, 1, 2, ..., K$ and $\Delta t = \frac{T}{K}$. k is step size w.r.t t. For the construction of our scheme, take $0 \leq k < K$

$$\frac{\partial^\alpha v(x, t_{k+1})}{\partial t^\alpha} = \frac{1}{\Gamma(1-\alpha)} \sum_{j=0}^{k} \int_{t_j}^{t_{j+1}} \frac{\frac{\partial v(x,s)}{\partial s}}{(t_{k+1}-x)^\alpha} ds, \quad 0 < \alpha < 1, \tag{3.29}$$

$$\frac{\partial^\alpha v(x, t_{k+1})}{\partial t^\alpha} = \frac{1}{\Gamma(1-\alpha)} \sum_{j=0}^{k} \frac{v(x, t_{j+1}) - v(x, t_j)}{\Delta t} \int_{t_j}^{t_{j+1}} \frac{ds}{(t_{k+1}-x)^\alpha} + T_{\Delta t}^{k+1} \tag{3.30}$$

where $T_{\Delta t}^{k+1}$ is the truncation error. This error can be find [65].

$$T_{\Delta t}^{k+1} \leq C_v \left[\frac{1}{\Gamma(1-\alpha)} \sum_{j=0}^{k} \int_{t_j}^{t_{j+1}} \frac{v(x, t_{j+1}) - v(x, t_j) - 2s}{(t_{k+1}-x)^\alpha} ds \right] \tag{3.31}$$

where C_v is a constant depending only on v. Further solving right hand side of the equation (3.31)

$$\frac{1}{\Gamma(1-\alpha)} \sum_{j=0}^{k} \int_{t_j}^{t_{j+1}} \frac{v(x, t_{j+1}) - v(x, t_j) - 2s}{(t_{k+1}-x)^\alpha} ds = -$$

$$\frac{1}{\Gamma(1-\alpha)} \sum_{j=0}^{k} \frac{1}{(1-\alpha)} (2j+1)(\Delta t)^{(2-\alpha)} [(k-j)^{(1-\alpha)} - (k+1-j)^{(1-\alpha)}] + \tag{3.32}$$

$$\frac{1}{\Gamma(1-\alpha)} \sum_{j=0}^{k} \frac{2}{(1-\alpha)} (\Delta t)^{(2-\alpha)} [(j+1)(k-j)^{1-\alpha} - j(k+1-j)^{(1-\alpha)}] +$$

$$\frac{1}{\Gamma(1-\alpha)} \sum_{j=0}^{k} \frac{2}{((2-\alpha))(1-\alpha)} (\Delta t)^{(2-\alpha)} [(k-j)^{(2-\alpha)} - (k+1-j)^{(2-\alpha)}]$$

$$= (\Delta t)^{(2-\alpha)} \frac{1}{\Gamma(2-\alpha)} [(k+1)^{(1-\alpha)} + 2(k^{(1-\alpha)} + (k-1)^{(1-\alpha)} + (k-2)^{(1-\alpha)} + ... + 1^{(1-\alpha)})] - \tag{3.33}$$

$$(\Delta t)^{(2-\alpha)} \frac{1}{\Gamma(3-\alpha)} (k+1)^{(2-\alpha)}$$

$$= (\Delta t)^{2-\alpha}\frac{1}{\Gamma(2-\alpha)}[(k+1)^{1-\alpha} + 2(k^{(1-\alpha)} + (k-1)^{(1-\alpha)} + (k-2)^{(1-\alpha)} + ... + 1^{(1-\alpha)}) - \frac{2(k+1)^{(2-\alpha)}}{(2-\alpha)}] \quad (3.34)$$

Let

$$S(k) = (k+1)^{(1-\alpha)} + 2(k^{(1-\alpha)} + (k-1)^{(1-\alpha)} + (k-2)^{(1-\alpha)} + ... + 1^{(1-\alpha)}) - \frac{2(k+1)^{2-\alpha}}{(2-\alpha)},$$

Proof of the bounded $|S(k)|$ for $0 \leq \alpha \leq 1$ and for $k \geq 1$ is given in the following lemma.

Lemma 3.2.1. *For all $0 \leq \alpha \leq 1$ and for all $k \geq 1$, then $|S(k)| \leq c$, for some constant c.*

Proof

Taking $\alpha = 0$, we get $S(k) = 0$ for all k. Now we will show that for $\alpha \in (0, 1]$.

$$S(k) = (k+1)^{(1-\alpha)} + 2(k^{(1-\alpha)} + (k-1)^{(1-\alpha)} + (k-2)^{(1-\alpha)} + ... + 1^{1-\alpha}) - \frac{2(k+1)^{2-\alpha}}{(2-\alpha)},$$

$$S(k) = \sum_{k=0}^{K} \beta_k$$

where $\beta_k = (k+1)^{(1-\alpha)} + k^{(1-\alpha)} - \frac{2}{(2-\alpha)}((k+1)^{2-\alpha} - k^{2-\alpha})$.
This leads us to show $\sum_{k=0}^{K} \beta_k$ converges. Since we know the series $\sum_{k=0}^{K} \frac{1}{k^p}$ convergence for all $p > 1$. By consequence, it suffices to prove $|\beta_k| \leq \frac{1}{k^{1+\alpha}}$ for $k \geq 2$.

$$\begin{aligned}
|\beta_k| &= k^{1-\alpha}\big|(1+\frac{1}{k})^{1-\alpha} + 1 - \frac{2k}{2-\alpha}((1+\frac{1}{k})^{1-\alpha} - 1)\big|, \\
&= k^{1-\alpha}\big|1 + 1 + (1-\alpha)\frac{1}{k} + \frac{(1-\alpha)(-\alpha)}{2!k^2} + \frac{(1-\alpha)(-\alpha)(-\alpha-1)}{3!k^3} + ... \\
&-\frac{2k}{2-\alpha}(-1 + 1 + (2-\alpha)\frac{1}{k} + \frac{(2-\alpha)(1-\alpha)}{2!k^2} + \frac{(2-\alpha)(1-\alpha)(-\alpha)}{3!k^3} + ...\big|, \\
&= k^{1-\alpha}\big|(\frac{1}{2!} - \frac{1}{3!})(1-\alpha)(-\alpha)\frac{1}{k^2} + (\frac{1}{3!} - \frac{1}{4!})\frac{(1-\alpha)(-\alpha)(-\alpha-1)}{k^3} + ...\big|, \\
&\leq k^{1-\alpha}\frac{1}{3!}(1-\alpha)(\alpha)\frac{1}{k^2}(1 + \frac{2(1+\alpha)}{4k} + \frac{3(1+\alpha)(2+\alpha)}{20k^2} + ...), \\
&\leq \frac{1}{3!}(1-\alpha)(\alpha)\frac{1}{k^{1+\alpha}}(1 + \frac{1}{k} + \frac{1}{k^2} + ...) \leq \frac{2}{3!}(1-\alpha)(\alpha)\frac{1}{k^{1+\alpha}} \leq \frac{1}{k^{1+\alpha}}
\end{aligned}$$

Proof is completed.

Using Lemma (3.2.1), and we know that $\frac{1}{\Gamma(2-\alpha)}$ for all $\alpha \in [0, 1]$,

$$\left|\frac{1}{\Gamma(1-\alpha)}\sum_{j=0}^{k}\int_{t_j}^{t_{j+1}}\frac{v(x,t_{j+1})-2s-v(x,t_j)}{(t_{k+1}-x)^{\alpha}}ds\right| \leq 2\Delta t^{2-\alpha} \tag{3.35}$$

holds.

$$T_{\Delta t}^{k+1} \leq 2\Delta t^{2-\alpha}$$

Solving directly equation (3.30), RHS is

$$\frac{1}{\Gamma(1-\alpha)}\sum_{j=0}^{k}\frac{v(x,t_{j+1})-v(x,t_j)}{\Delta t}\int_{t_j}^{t_{j+1}}\frac{ds}{(t_{k+1}-x)^{\alpha}} = \tag{3.36}$$

$$\frac{1}{\Gamma(1-\alpha)}\sum_{j=0}^{k}\frac{v(x,t_{j+1})-v(x,t_j)}{\Delta t}\int_{t_{k-j}}^{t_{k-j+1}}\frac{ds}{t^{\alpha}},$$

$$= \frac{1}{\Gamma(1-\alpha)}\sum_{j=0}^{k}\frac{v(x,t_{k-j+1})-v(x,t_{k-j})}{\Delta t}\int_{t_j}^{t_{j+1}}\frac{ds}{t^{\alpha}}, \tag{3.37}$$

$$= \frac{1}{\Gamma(1-\alpha)}\sum_{j=0}^{k}\frac{v(x,t_{k-j+1})-v(x,t_{k-j})}{\Delta t}[(j+1)^{1-\alpha}-j^{1-\alpha}] \tag{3.38}$$

Let $\gamma_j = (j+1)^{(1-\alpha)} - j^{(1-\alpha)}, j = 0, 1, 2, ..., K$ and define the operator L_t^{α}

$$L_t^{\alpha}v(x,t_{k+1}) = \frac{1}{\Gamma(1-\alpha)}\sum_{j=0}^{k}\gamma_j\frac{v(x,t_{k-j+1})-v(x,t_{k-j})}{\Delta t} \tag{3.39}$$

Equation (3.30) will become

$$\frac{\partial^{\alpha}v(x,t_{k+`1})}{\partial t^{\alpha}} = L_t^{\alpha}v(x,t_{k+1}) + T_{\Delta t}^{k+1} \tag{3.40}$$

3.3 Finite element method

The finite element method (FEM) is more general and power full method in its applications to engineering problems that involves complex geometry and complex boundary conditions

(BCs). In finite element method (FEM), given domain (regular or non regular) divide into sub domains and over each sub domain the mathematical model or governing equation is approximated by variational method (weak form) or Ritz method (minimization form). The concept behind approximation of solution over each sub domain is fact that it is easier to represent a complicated or non linear function as a collection of simple polynomials. We will use the following 1D boundary value problem to introduce the FEM.

$$-v^{''}(x) = f(x), \quad 0 < x < 1, \quad v(0) = 0, \quad v(1) = 0 \tag{3.41}$$

The *Galerkin* Finite Element Method for the 1D BVP

We will explain the FE method for the 1D boundary vale problem (BVP) using the *Galerkin* FE method is explained in these steps.

1 Construct a variational form (weak formulation).

In this step, we multiply a test function $\phi(x)$ to a partial differential equation (3.41) which also satisfy the boundary conditions (BCs) of the PDE, $\phi(0) = 0, \quad \phi(1) = 0$.

$$-v^{''}(x)\phi(x) = f(x)\phi(x), \tag{3.42}$$

then integrate from 0 to 1 to have following form (using integration by parts),

$$\int_0^1 -v^{''}(x)\phi(x)dx = -v^{'}\phi^{'}|_0^1 + \int_0^1 v^{'}(x)\phi^{'}(x)dx, \tag{3.43}$$

$$= \int_0^1 v^{'}(x)\phi^{'}(x)dx, \tag{3.44}$$

$$\implies \int_0^1 v^{'}(x)\phi^{'}(x)dx = \int_0^1 f(x)\phi(x)dx \tag{3.45}$$

which is weak form.

2 Generate a mesh,

A (uniform) cartesian mesh is $x_i = a + ih$, $i = 0, 1, ..., n$,where $h = (b-a)/n, (b = 1, a = 0)$, defining the intervals (or element in FEM) (x_{i-1}, x_i) , $i = 1, 2, ..., n$.

3 Construct a set of basis functions,

A basis function based on mesh is piece wise linear functions $j = 1, 2, 3, ..., n-1$

$$\phi(x)_j = \begin{cases} \frac{x-x_{j-1}}{h}, & x_{j-1} \leq x < x_j, \\ \frac{x_{j+1}-x}{h}, & x_j \leq x < x_{j+1}, \\ 0, & x < x_j, x > x_{j+1} \end{cases} \tag{3.46}$$

These basis functions often called the hat functions.

4 Approximate Finite Element,

The finite element solution by a linear combination of the basis functions.

$$v_h(x) = \sum_{i=1}^{n-1} c_i \phi_i(x), \tag{3.47}$$

where the coefficients in summation c_i are the unknowns of the ODE to be find. Here considering a basis functions, obviously $v_h(x)$ is also a piece-wise continuous linear function, though there are infinite many different cases of basis functions. We have to find a system of linear equations by substituting $v_h(x)$ for the exact solution $v(x)$. For the coefficients in the weak form $\int_0^1 v^{'}(x)\phi^{'}(x)dx = \int_0^1 f(x)(x)\phi(x)dx$.

$$\int_0^1 v_h^{'}(x)\phi^{'}(x)dx = \int_0^1 f(x)\phi(x)dx, \tag{3.48}$$

Error introduced in this step.

$$\begin{aligned} \implies & \int_0^1 (\sum_{i=1}^{n-1} c_i \phi_i^{'}(x)\phi^{'}(x))dx = \int_0^1 f(x)\phi(x)dx, \\ \implies & \sum_{i=1}^{n-1} c_i \int_0^1 \phi_i^{'}(x)\phi^{'}(x)dx = \int_0^1 f(x)\phi(x)dx, \end{aligned} \tag{3.49}$$

Next, use test function $\phi(x)$ as $\phi_1, \phi_2, ..., \phi_{n-1}$, to get the system of linear equations.

$$\left[\int_0^1 (\phi_1^{'}(x)\phi_1^{'}(x))dx\right] c_1 + ... + \left[\int_0^1 (\phi_1^{'}(x)\phi_{n-1}^{'}(x))dx\right] c_{n-1} = \int_0^1 f(x)\phi_1(x)dx,$$
$$\left[\int_0^1 (\phi_2^{'}(x)\phi_1^{'}(x))dx\right] c_1 + ... + \left[\int_0^1 (\phi_2^{'}(x)\phi_{n-1}^{'}(x))dx\right] c_{n-1} = \int_0^1 f(x)\phi_2(x)dx,$$
$$\ldots \quad \ldots \quad \ldots \quad \ldots \quad \ldots \quad \ldots \quad \ldots \quad \ldots$$
$$\left[\int_0^1 (\phi_{n-1}^{'}(x)\phi_1^{'}(x))dx\right] c_1 + ... + \left[\int_0^1 (\phi_{n-1}^{'}(x)\phi_{n-1}^{'}(x))dx\right] c_{n-1} = \int_0^1 (f(x)\phi_{n-1}(x))dx,$$

The matrix form is

$$\begin{bmatrix} a(\phi_1,\phi_1) & a(\phi_1,\phi_2) & a(\phi_1,\phi_3) & a(\phi_1,\phi_4) & \ldots & a(\phi_1,\phi_{n-1}) \\ a(\phi_2,\phi_1) & a(\phi_2,\phi_2) & a(\phi_2,\phi_3) & a(\phi_2,\phi_4) & \ldots & a(\phi_2,\phi_{n-1}) \\ a(\phi_3,\phi_1) & a(\phi_3,\phi_2) & a(\phi_3,\phi_3) & a(\phi_3,\phi_4) & \ldots & a(\phi_3,\phi_{n-1}) \\ \ldots & & & & & \\ a(\phi_{n-1},\phi_1) & a(\phi_{n-1},\phi_2) & a(\phi_{n-1},\phi_3) & a(\phi_{n-1},\phi_4) & \ldots & a(\phi_{n-1},\phi_{n-1}) \end{bmatrix} \begin{bmatrix} c_1 \\ c_2 \\ c_3 \\ \vdots \\ c_{n-1} \end{bmatrix}$$
$$= \begin{bmatrix} (f,\phi_1) \\ (f,\phi_2) \\ (f,\phi_3) \\ \vdots \\ (f,\phi_{n-1}) \end{bmatrix}$$

Where $a(\phi_i,\phi_j) = \int_0^1 \phi_i^{'}(x)\phi_j^{'}(x)dx$ and $(f,\phi_i) = \int_0^1 f(x)\phi_i(x)dx$. The bilinear form $a(\phi_i,\phi_j)$ is linear with each variable (hat function), and (f,ϕ) is a linear form. If ϕ_i are the basis (hat) functions, then further solving $a(\phi_i,\phi_j) = \int_0^1 \phi_i^{'}(x)\phi_j^{'}(x)dx$ and plugin values in matrix form, we get

$$\begin{bmatrix} 2/h & -1/h & 0 & 0 & \ldots & 0 \\ -1/h & 2/h & 1/h & 0 & \ldots & 0 \\ 0 & -1/h & 2/h & 1/h & \ldots & 0 \\ \ldots & & & & & \\ 0 & 0 & 0 & \ldots & -1/h & 2/h \end{bmatrix} \begin{bmatrix} c_1 \\ c_2 \\ c_3 \\ \vdots \\ c_{n-1} \end{bmatrix} = \begin{bmatrix} \int_0^1 f\phi_1 dx \\ \int_0^1 f\phi_2 dx \\ \int_0^1 f\phi_3 dx \\ \vdots \\ \int_0^1 f\phi_{n-1} dx \end{bmatrix}$$

5 Solve linear system of Equations,

Solve linear system of equation for the coefficients of c_i $(AC = F)$ and find approximate solution of $v_h(x) = \sum_{i=1}^{n-1} c_i \phi_i(x)$.

6 Find error analysis.

3.3.1 Key Components of the FEM

We will discuss BVP (3.41) using FEM.

1 *Galerkin* method (variational formulation).

2 *Ritz* method (minimization formula.)

We will also highlight important aspects of FEM, such as how to assemble the stiffness matrix for element.
Consider the integral form $\int_0^1 v'(x)\phi'(x)dx = \int_0^1 f(x)\phi(x)dx$ for any $\phi(x)$ in the Sobolev space $H^1(0,1)$.

Meshing and basis functions

A mesh in one dimensional problem is a set of points or elements in the interval of interest, like , $x_0 = 0, x_1, x_2, ..., x_N = 1$. Let $h_i = x_{i+1} - x_1$, for $i = 0, 1, 2, ..., N-1$

1 x_i is called nodal point or node.

2 $(x_{i+1} - x_1)$ is an element.

3 $h = max_{0 \le i \le N-1} h_i$ is the mesh size.

Finite dimensional space (Sobolve space) on the Mesh

Suppose the solution (of PDE) space is W, which is $H_0^1(0,1)$ in the (3.41) problem. Let us construct a subspace

$$W_h \subset V$$

, where W_h is finite dimensional space and W is the solution space.

This type of FEM is known as conforming one. A different type of a finite dimensional solution spaces generate different FE solutions. Since W_h has finite dimensional space, we can constract a set of independent functions.

$$\phi_1(x), \quad \phi_2(x), ..., \phi_{N-1}(x) \subset W_h \tag{3.50}$$

if

$$\sum_{i=1}^{N-1} \phi_i(x)\alpha_i = 0 \tag{3.51}$$

then

$$\alpha_1 = \alpha_2 = ... = \alpha_{N-1} = 0$$

, As basis $\phi_1(x), \quad \phi_2(x), ..., \phi_{N-1}(x)$ are independent. Thus W_h is the spanned by the basis function.

$$W_h =< \phi_1(x), \quad \phi_2(x), ..., \phi_{N-1}(x) >$$

$$W_h = \{w_h(x), w_h(x) = \sum_{i=1}^{N-1} \phi_i(x)\alpha_i\} \tag{3.52}$$

A linear piecewise function is the simplest finite dimensional space defined over the mesh is:

$$W_h = \{w_h(x), w_h(0) = w_h(1) = 0\}, \tag{3.53}$$

where $w_h(x)$ is continuous pice wise linear.

To Find Dimensions of W_h

A linear function g(x) in an interval (x_i, x_{i+1}) is uniquely determined by its values at x_i and x_{i+1}:

$$g(x) = g(x_i)\frac{x - x_{i+1}}{x_i - x_{i+1}} + g(x_{i+1})\frac{x - x_i}{x_{i+1} - x_i} \tag{3.54}$$

Here are N-1 nodal values, $g(x_1), g(x_2), ..., g(x_{N-1})$. For a piece-wise linear function over the mesh, in addition to $g(x_0) = g(x_N) = 0$ Given a vector

$$[g(x_1), g(x_2), ..., g(x_{N-1})]^T \in R^{N-1}$$

, we can construct a $w_h(x) \in W_h$ by taking $w_h(x_i) = g(x_i), i = 1, ..., N-1$. On the other side, given $w_h(x) \in W_h$, we have a vector

$$[w(x_1), w(x_2), ..., w(x_{N-1})]^T \in R^{N-1}$$

So there is a one to one corresponding between W_h and R^{N-1}. Consequently

$$W_h \equiv R^{N-1}$$

A set of basis functions

The solution space for finite dimension can be generate by a set of linearly independent basis functions. Infinite sets of basis functions exists, but we have to choose the ones who

1 is simple;

2 has compact (or minimum) support, that is., non zero in a element and zero everywhere; and third

3 meets the regular requirements, that is, continuous and differentiable, other then at nodal points.

Simplest form of set of a functions is hat functions,

$$\begin{aligned}
\phi_1(x_1) = 1, \quad \phi_1(x_i) = 0, \quad i = 0, 2, 3, ..., N, \\
\phi_2(x_2) = 1, \quad \phi_2(x_i) = 0, \quad i = 0, 1, 3, ..., N, \\
\dots \\
\phi_j(x_j) = 1, \quad \phi_j(x_i) = 0, \quad i = 0, 2, 3, ..., j-1, j+1, ..., N, \\
\dots \\
\phi_{N-1}(x_{N-1}) = 1, \quad \phi_{N-1}(x_i) = 0, \quad i = 0, 2, 3, ..., N-2, N,
\end{aligned}$$

It can be represented as one function

$$\phi_j(x_i) = \begin{cases} 1, & if \quad i = j, \\ 0, & if \quad i \neq j \end{cases} \tag{3.55}$$

The mathematical form of basis function is,

$$\phi_j(x) = \begin{cases} 0, & if \quad x < x_{j-1}, \\ \frac{x - x_{j-1}}{h_j}, & if \quad x_{j-1} \leq x < x_j \\ \frac{x_{j+1} - x}{h_j}, & if \quad x_j \leq x < x_{j+1} \\ 0, & if \quad x_{j+1} \leq x, \end{cases} \tag{3.56}$$

and FE solution is

$$v_h(x) = \sum_{i=1}^{N-1} \alpha_i \phi_i(x) \tag{3.57}$$

and either the variational or weak form (V) or the minimization form or Ritz method (M) can be used to find a system of linear equations for the coefficients of test functions α_i. Applying the basis (hat) functions, we have

$$v_h(x_j) = \sum_{i=1}^{N-1} \alpha_i \phi_i(x_j) = 0 + 0 + ... + \alpha_j \phi_j(x_j) + 0 + ... + 0 = \alpha_i \tag{3.58}$$

so α_j is numerical/approximate solution of FEM to the exact solution at $x = x_j$.

3.3.2 Ritz Method

This method was one of the earliest or oldest method and has proven a successful method, although every PDE has not a minimization form, minimization form for equation (3.41) is

$$\begin{aligned} F(v) &= \frac{1}{2} \int_0^1 (v^{'} v^{'}) dx - \int_0^1 f v dx, \\ min_{v \in H_0^1(0,1)} : \quad F(v) &= \frac{1}{2} \int_0^1 (v^{'})^2 dx - \int_0^1 f v dx, \end{aligned} \tag{3.59}$$

As in variational method, the approximate solution is

$$v_h(x) = \sum_{i=1}^{N-1} \alpha_i \phi_i(x), \tag{3.60}$$

substituting into the functional form

$$F(v_h) = \frac{1}{2} \int_0^1 \left(\sum_{i=1}^{N-1} \alpha_i \phi_i^{'}(x) \right)^2 dx - \int_0^1 f \left(\sum_{i=1}^{N-1} \alpha_i \phi_i(x) \right) dx, \tag{3.61}$$

which is a multivariate function of $\alpha_1, \alpha_2, ..., \alpha_{N-1}$ and can be written as

$$F(v_h) = F(\alpha_1, \alpha_2, ..., \alpha_{N-1}),$$

where as necessary conditions for minimum is

$$\frac{\partial F}{\partial \alpha_1} = 0, \quad \frac{\partial F}{\partial \alpha_2} = 0, \quad , ..., \frac{\partial F}{\partial \alpha_{N-1}} = 0, \tag{3.62}$$

Taking partial derivatives of (3.61) w.r.t α_i

$$\frac{\partial F}{\partial \alpha_1} = \int_0^1 \left(\sum_{i=1}^{N-1} \alpha_i \phi_i^{'}(x) \right) \phi_1^{'} dx - \int_0^1 f \phi_1 dx = 0, \tag{3.63}$$

$$\frac{\partial F}{\partial \alpha_2} = \int_0^1 \left(\sum_{i=1}^{N-1} \alpha_i \phi_i^{'}(x) \right) \phi_2^{'} dx - \int_0^1 f \phi_2 dx = 0, \tag{3.64}$$

$$\dots \tag{3.65}$$

$$\frac{\partial F}{\partial \alpha_{N-1}} = \int_0^1 \left(\sum_{i=1}^{N-1} \alpha_i \phi_i^{'}(x) \right) \phi_{N-1}^{'} dx - \int_0^1 f \phi_{N-1} dx = 0, \tag{3.66}$$

exchanging order of integration and summation,

$$\sum_{i=1}^{N-1} \int_0^1 \left(\phi_i^{'}(x) \right) \alpha_i \phi_1^{'} dx = \int_0^1 f \phi_1 dx, \tag{3.67}$$

$$\dots \tag{3.68}$$

$$\sum_{i=1}^{N-1} \int_0^1 \left(\phi_i^{'}(x) \right) \alpha_i \phi_{N-1}^{'} dx = \int_0^1 f \phi_{N-1} dx, \tag{3.69}$$

this system is equaling to the

$$\int_0^1 v^{'} \phi^{'} dx = \int_0^1 f \phi dx, \tag{3.70}$$

which is same as weak form of Galerkin method. Ritz and Galerkin methods are same for many problems.

3.3.3 Assembling the stiffness matrix element by element

Let's consider a BVP problem in equation (3.41), after deriving the minimization (for Ritz method) or weak form (for Galerkin method) and constructed a mesh and then basis functions for the problem, in final stage we need to find:

. The coefficient matrices of diffusion and advection terms $A = \{a_{ij}\} = \{\int_0^1 \phi_i' \phi_j' dx\}$, often called the stiffness matrix , and

. the coefficient vector of source term f, known as load vector $F = \{\int_0^1 f\phi_j dx\} = \{f_i\}$.

It is difficult in FEM to assemble global matrix A and global load vector F. For the (3.41) problem, assembling matrix element one by one is:

$$(x_0, x_1) = \Omega_1, \quad (x_1, x_2) = \Omega_2, \quad \ldots, \quad (x_{i-1}, x_i) = \Omega_i, \quad \ldots (x_{N-1}, x_N) = \Omega_N,$$

For any integrable function v(x) we break up the integration element by element or in pieces,

$$\int_0^1 v(x)dx = \sum_{j=1}^{N} \int_{j-1}^{j} v(x)dx$$

The stiffness matrix can be written as

$$S = \begin{bmatrix} \int_0^1 (\phi_1')^2 dx & \int_0^1 \phi_1'\phi_2' dx & \int_0^1 \phi_1'\phi_3' dx & \int_0^1 \phi_1'\phi_4' dx & \ldots & \int_0^1 \phi_1'\phi_{N-1}' dx \\ \int_0^1 \phi_2'\phi_1' dx & \int_0^1 (\phi_2')^2 dx & \int_0^1 \phi_2'\phi_3' dx & \int_0^1 \phi_2'\phi_4' dx & \ldots & \int_0^1 \phi_2'\phi_{N-1}' dx \\ \int_0^1 \phi_3'\phi_1' dx & \int_0^1 \phi_3'\phi_2' dx & \int_0^1 (\phi_3')^2 dx & \int_0^1 \phi_3'\phi_4' dx & \ldots & \int_0^1 \phi_3'\phi_{N-1}' dx \\ \ldots & \ldots & \ldots & \ldots & \ldots & \ldots \\ \int_0^1 \phi_{N-1}'\phi_1' dx & \int_0^1 \phi_{N-1}'\phi_2' dx & \int_0^1 \phi_{N-1}'\phi_3' dx & \ldots & \int_0^1 \phi_{N-1}'\phi_{N-2}' dx & \int_0^1 (\phi_{N-1}')^2 dx \end{bmatrix}$$

$$= \begin{bmatrix} \int_{x_0}^{x_1} (\phi_1')^2 dx & \int_{x_0}^{x_1} \phi_1'\phi_2' dx & \int_{x_0}^{x_1} \phi_1'\phi_3' dx & \ldots & \int_{x_0}^{x_1} \phi_1'\phi_{N-1}' dx \\ \int_{x_0}^{x_1} \phi_2'\phi_1' dx & \int_{x_0}^{x_1} (\phi_2')^2 dx & \int_{x_0}^{x_1} \phi_2'\phi_3' dx & \ldots & \int_{x_0}^{x_1} \phi_2'\phi_{N-1}' dx \\ \int_{x_0}^{x_1} \phi_3'\phi_1' dx & \int_{x_0}^{x_1} \phi_3'\phi_2' dx & \int_{x_0}^{x_1} (\phi_3')^2 dx & \ldots & \int_{x_0}^{x_1} \phi_3'\phi_{N-1}' dx \\ \ldots & \ldots & \ldots & \ldots & \ldots \\ \int_{x_0}^{x_1} \phi_{N-1}'\phi_1' dx & \int_{x_0}^{x_1} \phi_{N-1}'\phi_2' dx & \ldots & \int_{x_0}^{x_1} \phi_{N-1}'\phi_{N-2}' dx & \int_{x_0}^{x_1} (\phi_{N-1}')^2 dx \end{bmatrix}$$

$$+\begin{bmatrix} \int_{x_1}^{x_2}(\phi_1')^2dx & \int_{x_1}^{x_2}\phi_1'\phi_2'dx & \int_{x_1}^{x_2}\phi_1'\phi_3'dx & \dots & \int_{x_1}^{x_2}\phi_1'\phi_{N-1}'dx \\ \int_{x_1}^{x_2}\phi_2'\phi_1'dx & \int_{x_1}^{x_2}(\phi_2')^2dx & \int_{x_1}^{x_2}\phi_2'\phi_3'dx & \dots & \int_{x_1}^{x_2}\phi_2'\phi_{N-1}'dx \\ \int_{x_1}^{x_2}\phi_3'\phi_1'dx & \int_{x_1}^{x_2}\phi_3'\phi_2'dx & \int_{x_1}^{x_2}(\phi_3')^2dx & \dots & \int_{x_1}^{x_2}\phi_3'\phi_{N-1}'dx \\ \dots & \dots & \dots & \dots & \dots \\ \int_{x_1}^{x_2}\phi_{N-1}'\phi_1'dx & \int_{x_1}^{x_2}\phi_{N-1}'\phi_2'dx & \dots & \int_{x_1}^{x_2}\phi_{N-1}'\phi_{N-2}'dx & \int_{x_1}^{x_2}(\phi_{N-1}')^2dx \end{bmatrix}$$

$$\dots \quad \dots \quad \dots$$

$$+\begin{bmatrix} \int_{x_{N-1}}^{x_N}(\phi_1')^2dx & \int_{x_{N-1}}^{x_N}\phi_1'\phi_2'dx & \int_{x_{N-1}}^{x_N}\phi_1'\phi_3'dx & \dots & \int_{x_{N-1}}^{x_N}\phi_1'\phi_{N-1}'dx \\ \int_{x_{N-1}}^{x_N}\phi_2'\phi_1'dx & \int_{x_{N-1}}^{x_N}(\phi_2')^2dx & \int_{x_{N-1}}^{x_N}\phi_2'\phi_3'dx & \dots & \int_{x_{N-1}}^{x_N}\phi_2'\phi_{N-1}'dx \\ \int_{x_{N-1}}^{x_N}\phi_3'\phi_1'dx & \int_{x_{N-1}}^{x_N}\phi_3'\phi_2'dx & \int_{x_{N-1}}^{x_N}(\phi_3')^2dx & \dots & \int_{x_{N-1}}^{x_N}\phi_3'\phi_{N-1}'dx \\ \dots & \dots & \dots & \dots & \dots \\ \int_{x_{N-1}}^{x_N}\phi_{N-1}'\phi_1'dx & \int_{x_{N-1}}^{x_N}\phi_{N-1}'\phi_2'dx & \dots & \int_{x_{N-1}}^{x_N}\phi_{N-1}'\phi_{N-2}'dx & \int_{x_{N-1}}^{x_N}(\phi_{N-1}')^2dx \end{bmatrix}$$

Since we are using the hat basis functions, then each element has only two nonzero basis functions. Which leads to

$$S = \begin{bmatrix} \int_{x_0}^{x_1}(\phi_1')^2dx & 0 & 0 & \dots & 0 \\ 0 & 0 & 0 & \dots & 0 \\ 0 & 0 & 0 & \dots & 0 \\ \dots & \dots & \dots & \dots & \dots \\ 0 & 0 & \dots & 0 & 0 \end{bmatrix} + \begin{bmatrix} \int_{x_1}^{x_2}(\phi_1')^2dx & \int_{x_1}^{x_2}\phi_1'\phi_2'dx & 0 & \dots & 0 \\ \int_{x_1}^{x_2}\phi_2'\phi_1'dx & \int_{x_1}^{x_2}(\phi_2')^2dx & 0 & \dots & 0 \\ 0 & 0 & 0 & \dots & 0 \\ \dots & \dots & \dots & \dots & \dots \\ 0 & 0 & \dots & 0 & 0 \end{bmatrix}$$

$$\dots \quad \dots \quad \dots$$

$$+\begin{bmatrix} 0 & 0 & 0 & \dots & 0 \\ 0 & \int_{x_2}^{x_3}(\phi_2')^2dx & \int_{x_2}^{x_3}\phi_2'\phi_3'dx & \dots & 0 \\ 0 & \int_{x_2}^{x_3}\phi_3'\phi_2'dx & \int_{x_2}^{x_3}(\phi_3')^2dx & \dots & 0 \\ \dots & \dots & \dots & \dots & \dots \\ 0 & 0 & \dots & 0 & 0 \end{bmatrix} + \begin{bmatrix} 0 & 0 & 0 & \dots & 0 \\ 0 & 0 & 0 & \dots & 0 \\ 0 & 0 & 0 & \dots & 0 \\ \dots & \dots & \dots & \dots & \dots \\ 0 & 0 & \dots & 0 & \int_{x_{N-1}}^{x_N}(\phi_{N-1}')^2dx \end{bmatrix}$$

The nonzero contribution stiffness two by two matrix from a particular element x_{i+1}, x_i is

$$K_i^e = \begin{bmatrix} \int_{x_i}^{x_{i+1}} (\phi_i^{'})^2 dx & \int_{x_i}^{x_{i+1}} \phi_i^{'}\phi_{i+1}^{'} dx \\ \int_{x_i}^{x_{i+1}} \phi_{i+1}^{'}\phi_i^{'} dx & \int_{x_i}^{x_{i+1}} (\phi_{i+1}^{'})^2 dx \end{bmatrix}$$

Similarly, two by one local load vector for particular element x_{i+1}, x_i is

$$F_i^e = \begin{bmatrix} \int_{x_i}^{x_{i+1}} f\phi_i dx \\ \int_{x_i}^{x_{i+1}} f\phi_{i+1} dx \end{bmatrix}$$

Assembling of a global load vector can be:

$$F = \begin{bmatrix} \int_{x_0}^{x_1} f\phi_1 dx \\ 0 \\ 0 \\ 0 \\ \vdots \\ 0 \\ 0 \end{bmatrix} + \begin{bmatrix} \int_{x_1}^{x_2} f\phi_1 dx \\ \int_{x_1}^{x_2} f\phi_2 dx \\ 0 \\ 0 \\ \vdots \\ 0 \\ 0 \end{bmatrix} + \begin{bmatrix} 0 \\ \int_{x_2}^{x_3} f\phi_2 dx \\ \int_{x_2}^{x_3} f\phi_3 dx \\ 0 \\ \vdots \\ 0 \\ 0 \end{bmatrix} + ... + \begin{bmatrix} 0 \\ 0 \\ 0 \\ 0 \\ \vdots \\ 0 \\ \int_{x_{N-1}}^{x_N} f\phi_{N-1} dx \end{bmatrix}$$

Computing local stiffness matrix and local load vector

In the element $\Omega_i = (x_i, x_{i+1})$, there are only two nonzero hat functions between x_i and x_{i+1}.

$$\phi_i^e = \frac{x_{i+1} - x}{x_{i+1} - x_i}, \qquad \phi_{i+1}^e = \frac{x - x_i}{x_{i+1} - x_i},$$

$$(\phi_i^e)^{'} = \frac{-1}{x_{i+1} - x_i} = \frac{-1}{h_i}, \qquad (\phi_{i+1}^e)^{'} = \frac{1}{x_{i+1} - x_i} = \frac{1}{h_i},$$

where ϕ_i^e and ϕ_{i+1}^e are defined only on one particular element $\Omega_i = (x_i, x_{i+1})$. It is easy to verify that

$$\int_{x_i}^{x_{i+1}} (\phi_i^{'})^2 dx = \int_{x_i}^{x_{i+1}} (\frac{1}{h_i})^2 dx = \frac{1}{h_i},$$
$$\int_{x_i}^{x_{i+1}} \phi_i^{'}\phi_{i+1}^{'} dx = \int_{x_i}^{x_{i+1}} -(\frac{1}{h_i})^2 dx = \frac{-1}{h_i},$$
$$\int_{x_i}^{x_{i+1}} (\phi_{i+1}^{'})^2 dx = \int_{x_i}^{x_{i+1}} (\frac{1}{h_i})^2 dx = \frac{1}{h_i},$$

The local stiffness matrix K_i^e is

$$K_i^e = \begin{bmatrix} \frac{1}{h_i} & \frac{-1}{h_i} \\ \frac{-1}{h_i} & \frac{1}{h_i} \end{bmatrix}$$

and Global stiffness matrix S is

$$S = 0^{(N-1)\times(N-1)} = \begin{bmatrix} \frac{1}{h_0}+\frac{1}{h_1} & \frac{-1}{h_1} & 0 & 0 & \dots & 0 \\ \frac{-1}{h_1} & \frac{1}{h_1}+\frac{1}{h_2} & \frac{-1}{h_2} & 0 & \dots & 0 \\ 0 & \frac{-1}{h_2} & \frac{1}{h_2}+\frac{1}{h_3} & \frac{-1}{h_3} & \dots & 0 \\ \dots & \dots & \dots & \dots & \dots & \dots \\ 0 & 0 & \dots & \frac{-1}{h_{N-3}} & \frac{1}{h_{N-3}}+\frac{1}{h_{N-2}} & \frac{-1}{h_{N-2}} \\ 0 & 0 & \dots & 0 & \frac{-1}{h_{N-2}} & \frac{1}{h_{N-2}}+\frac{1}{h_{N-1}} \end{bmatrix}$$

Chapter 4

Mixed convection magnetohydrodynamics flow of a nanofluid with heat transfer: A numerical study

4.1 Introduction

The aim of present study is to investigate the convection effects along with the magnetic field and thermal radiations on the boundary layer flow of fractional Maxwell fluid over a moving plate. The fluid motion is initiated by moving the plate impulsively along the $x-axis$. In order to capture memory effects during the motion of fluid, fractional calculus approach has been employed in order to derive the mathematical model which finally gives fractional coupled non linear partial differential equations. The numerical simulations of the underlying model have been carried out by using Euler backward difference method for space variables and $L1$-algorithm discretization for fractional derivative . Various flow and fractional parameters effects on velocity variation and temperature variation presented via graphs. Moreover, fractional and other physical parameters effects have also been discussed on average skin friction coefficient and average Nusselt number with the help of tables.

4.2 Mathematical formulation

The incompressible momentum and conservation of mass equations along with the energy conservation equation have been utilized in order to model the underlying physical phenomenon of two dimensional boundary layer Maxwell flow of nanofluid with heat transfer over. Uniform magnetic field $(0, B_0, 0)$ in the positive $y-$ direction has been introduced in the model using Lorentz force and radiation $\mathbf{q}_r$ have been applied externally while the fluid motion is considered along y coordinate. The velocity is taken as:

$$\mathbf{V} = (u(x, y, t), v(x, y, t), 0)$$

It is to be noted that the viscous dissipation effects are ignored in the derived model. Moreover, the fluid motion along vertical direction is investigated, therefore the equation of velocity component v is ignored by using the boundary layer assumptions and Boussinesq approximations, the equations for conservation of mass and momentum for nano-fluid in the presence of magnetic field can be:

$$\frac{\partial u}{\partial x} + \frac{\partial v}{\partial y} = 0, \tag{4.1}$$

$$\frac{\partial u}{\partial t} + u\frac{\partial u}{\partial x} + v\frac{\partial u}{\partial y} = \nu_{nf}\frac{\partial \tau_{xy}}{\partial y} - \frac{\sigma_{nf}B_0^2}{\rho_{nf}}u - \frac{\nu_{nf}}{k}u + \beta_{nf}g\left(T - T_0\right). \tag{4.2}$$

where nf stands for nano-fluid, ν_{nf} is dynamic viscosity, ρ_{nf} is density, β_{nf} is thermal expansion coefficient, k_{nf} is thermal conductivity, σ_{nf} is electrical conductivity of nano-fluid and g is the gravitational acceleration. The fractional order derivation is introduced into the constitutive equations for the Maxwell model as proposed by Friedrich [42]

$$\tau_{xy} + \lambda_1^{\alpha}\frac{\partial^{\alpha}\tau_{xy}}{\partial t^{\alpha}} = \mu\frac{\partial u}{\partial y},$$

which leads to

$$\left(1 + \lambda_1^{\alpha}\frac{\partial^{\alpha}}{\partial t^{\alpha}}\right)\tau_{xy} = \mu\frac{\partial u}{\partial y}, \tag{4.3}$$

where λ_1 is the relaxation time, α is fractional derivative such that $0 < \alpha < 1$ and τ_{xy} is shear stress. The operator $\partial^{\alpha}/\partial t^{\alpha}$ is Caputo time derivative of order α given as [71]

$$\partial_t^{\alpha}u(t) := \frac{1}{\Gamma(n-\alpha)}\int_0^t \frac{1}{(t-\xi)^{-n+\alpha+1}}\frac{\partial^n u(\xi)}{\partial \xi^n}d\xi, \quad n-1 < \Re e\{\alpha\} < n, \quad n \in \mathbb{N}, \tag{4.4}$$

with $\Gamma(\cdot)$ Gamma function defined as:

$$\Gamma(z) := \int_{\mathbb{R}} \xi^{z-1} e^{-\xi} d\xi, \quad z \in \mathbb{C}, \quad \Re\{z\} > 0.$$

In order to eliminate τ_{xy} from equations (4.2) and (4.3), applying the operator $\left(1 + \lambda_1^{\alpha} \frac{\partial^{\alpha}}{\partial t^{\alpha}}\right)$ on both sides of (4.2) and then using (4.3), we finally arrive at

$$\begin{aligned} \frac{\partial u}{\partial t} &+ u\frac{\partial u}{\partial x} + v\frac{\partial u}{\partial y} + \lambda_1^{\alpha}\frac{\partial^{\alpha+1} u}{\partial t^{\alpha+1}} + \lambda_1^{\alpha}\frac{\partial^{\alpha}}{\partial t^{\alpha}}\left(u\frac{\partial u}{\partial x}\right) + \lambda_1^{\alpha}\frac{\partial^{\alpha}}{\partial t^{\alpha}}\left(v\frac{\partial u}{\partial y}\right) = \nu_{nf}\frac{\partial^2 u}{\partial y^2} \\ &+ \beta_{nf} g\left(1 + \lambda_1^{\alpha}\frac{\partial^{\alpha}}{\partial t^{\alpha}}\right)(T - T_0) - \left(1 + \lambda_1^{\alpha}\frac{\partial^{\alpha}}{\partial t^{\alpha}}\right)\left(\frac{\sigma_{nf} B_0^2}{\rho_{nf}} + \frac{\nu_{nf}}{k_{nf}}\right) u, \end{aligned} \tag{4.5}$$

The temperature on the plate is presumed to be T_0 and on the surface of the fluid the temperature is considered to be the ambient. The change of temperature within the fluid is modeled by using

$$\frac{\partial T}{\partial t} + u\frac{\partial T}{\partial x} + v\frac{\partial T}{\partial y} = -\nabla \cdot \mathbf{q} - \frac{1}{(\rho c_p)_{nf}}\frac{\partial \mathbf{q}_r}{\partial y},$$

where $\mathbf{q}$ is the heat flux, $c_{p_{nf}}$ is heat capacity and q_r is the thermal radiation. Since the heat flux is supposed to be towards vertical direction, therefore the above equation can further be written as

$$\frac{\partial T}{\partial t} + u\frac{\partial T}{\partial x} + v\frac{\partial T}{\partial y} = -\frac{\partial \mathbf{q}}{\partial y} - \frac{1}{(\rho c_p)_{nf}}\frac{\partial \mathbf{q}_r}{\partial y}, \tag{4.6}$$

The expression for $\mathbf{q}$ is given by the fractional form of generalized Fourier's law introduced by Cattaneo [44]

$$\left(1 + \lambda_2^{\gamma}\frac{\partial^{\gamma}}{\partial t^{\gamma}}\right)\mathbf{q} = -k_{nf}\frac{\partial T}{\partial y}, \tag{4.7}$$

In order to eliminate $\mathbf{q}$, first applying the operator $\left(1 + \lambda_2^{\gamma}\frac{\partial^{\gamma}}{\partial t^{\alpha}}\right)$ on both side of equation (4.6) and then using (4.7), we have obtained

$$\begin{aligned} \frac{\partial T}{\partial t} + u\frac{\partial T}{\partial x} + v\frac{\partial T}{\partial y} + \lambda_2^{\gamma}\frac{\partial^{\gamma+1} T}{\partial t^{\gamma+1}} + \lambda_2^{\gamma}\frac{\partial^{\gamma}}{\partial t^{\gamma}}\left(u\frac{\partial T}{\partial x}\right) + \lambda_2^{\gamma}\frac{\partial^{\gamma}}{\partial t^{\gamma}}\left(v\frac{\partial T}{\partial y}\right) \\ = \frac{k_{nf}}{(\rho c_p)_{nf}}\frac{\partial^2 T}{\partial y^2} - \frac{1}{(\rho c_p)_{nf}}(1 + \lambda_2^{\alpha}\frac{\partial^{\gamma}}{\partial t^{\gamma}})\frac{\partial \mathbf{q}_r}{\partial y}, \end{aligned} \tag{4.8}$$

where the expression $\mathbf{q}_r$ defined by [45]

$$\mathbf{q}_r = -\frac{4\sigma}{3\beta}\frac{\partial T^4}{\partial y}$$

introduces the radiation contribution in the flow field. Expanding T^4 by a Taylor series about T_0 and neglecting higher orders of T, we can write $T^4 = 4T_0^3T - 3T_0^4$. Therefore $\mathbf{q}_r$ can eventually be defined as

$$\mathbf{q}_r = -\frac{4\sigma}{3\beta}\frac{\partial T^4}{\partial y} \cong -\frac{16\sigma T_0^3}{3\beta}\frac{\partial T}{\partial y} \tag{4.9}$$

Using equations (4.9) and (4.7), the equation (4.8) can be written as

$$\begin{aligned}\frac{\partial T}{\partial t} + u\frac{\partial T}{\partial x} + v\frac{\partial T}{\partial y} + \lambda_2^\gamma\frac{\partial^{\gamma+1}T}{\partial t^{\gamma+1}} + \lambda_2^\gamma\frac{\partial^\gamma}{\partial t^\gamma}\left(u\frac{\partial T}{\partial x}\right) + \lambda_2^\gamma\frac{\partial^\gamma}{\partial t^\gamma}\left(v\frac{\partial T}{\partial y}\right)\\ = \left(\frac{k_{nf}}{(\rho c_p)_{nf}} - \frac{16\sigma T_0^3}{3\beta(\rho c_p)_{nf}}\right)\frac{\partial^2 T}{\partial y^2}.\end{aligned} \tag{4.10}$$

Finally, the equations (4.1), (4.5) and (4.10) constitutes the model problem which describes the underlying physical phenomenon addressed in this work

$$\begin{cases}\dfrac{\partial u}{\partial x} + \dfrac{\partial v}{\partial y} = 0,\\ \dfrac{\partial u}{\partial t} + u\dfrac{\partial u}{\partial x} + v\dfrac{\partial u}{\partial y} + \lambda_1^\alpha\dfrac{\partial^{\alpha+1}u}{\partial t^{\alpha+1}} + \lambda_1^\alpha\dfrac{\partial^\alpha}{\partial t^\alpha}\left(u\dfrac{\partial u}{\partial x}\right) + \lambda_1^\alpha\dfrac{\partial^\alpha}{\partial t^\alpha}\left(v\dfrac{\partial u}{\partial y}\right) = \nu_{nf}\dfrac{\partial^2 u}{\partial y^2}\\ \qquad\qquad +\beta_{nf}g\left(1+\lambda_1^\alpha\dfrac{\partial^\alpha}{\partial t^\alpha}\right)(T-T_0) - B_1^2\left(1+\lambda_1^\alpha\dfrac{\partial^\alpha}{\partial t^\alpha}\right)u,\\ \dfrac{\partial T}{\partial t} + u\dfrac{\partial T}{\partial x} + v\dfrac{\partial T}{\partial y} + \lambda_2^\gamma\dfrac{\partial^{\gamma+1}T}{\partial t^{\gamma+1}} + \lambda_2^\gamma\dfrac{\partial^\gamma}{\partial t^\gamma}\left(u\dfrac{\partial T}{\partial x}\right) + \lambda_2^\gamma\dfrac{\partial^\gamma}{\partial t^\gamma}\left(v\dfrac{\partial T}{\partial y}\right) = K_{nf}^1\dfrac{\partial^2 T}{\partial y^2}.\end{cases} \tag{4.11}$$

where

$$B_1^2 = \left(\frac{\sigma_{nf}B_0^2}{\rho_{nf}} + \frac{\nu_{nf}}{k_{nf}}\right), \quad K_{nf}^1 = \left(\frac{k_{nf}}{(\rho c_p)_{nf}} - \frac{16\sigma T_0^3}{3\beta(\rho c_p)_{nf}}\right)$$

and ρ_{nf} is density of nanofluid, μ_{nf} is dynamic viscosity of nanofluid and other parameters for the nanofluid are defined as[46]

$$\begin{aligned}\rho_{nf} &=: (1-\phi)\rho_f + \phi\rho_s,\\ \frac{k_{nf}}{k_f} &= \left(\frac{k_s(1+2\phi)+2k_f(1-\phi)}{k_s(1+\phi)+k_f(2+\phi)}\right),\\ \rho_{nf}\beta_{nf} = (\rho\beta)_f - \phi(\rho\beta)_f + \phi\rho_s\beta_s, &\quad \sigma_{nf} = k_f\left(1+(\sigma-1)\phi\right),\\ (\rho c_p)_{nf} = \phi(\rho c_p)_s + (1-\phi)(\rho c_p)_f, &\quad \mu_{nf} = \frac{\mu_f}{(1-\phi)^{2.5}}.\end{aligned}$$

In the above equations, ϕ denotes the volume fraction of the nanoparticles in nanofluid. ρ_s, k_s, μ_s and $(c_p)_s$ denotes density, thermal conductivity, viscosity and specific heat capacities of surfactant respectively. Similarly ρ_f, k_f and $(c_p)_f$ denotes density,thermal

conductivity and specific heat capacities of base fluid respectively.

As described earlier, the fluid motion at time $t = 0$ is initiated by a impulsive movement of the plate with the time dependent velocity tU_0, the temperature of the plate is also dependent on time t, therefore the initial and boundary conditions which best suit the physical phenomenon can be given by

$$\begin{aligned} t \leqslant 0 : v = 0, \quad u = 0, \quad T = 0, \\ t > 0 : v = 0, \quad u = 0, \quad T = 0 \quad at \quad x = 0, \\ t > 0 : u = tU_0, \quad T = \frac{T_d - T_0}{T_0} t \quad at \quad y = 0, \\ t > 0 : u \to 0, \quad T \to T_0 \quad at \quad y \to \infty. \end{aligned} \tag{4.12}$$

4.2.1 Non-dimensionalization

In order to understand physics of the proposed problem in an easy way we have nondimensionalized the governing problem. It helps to comprehend the underlying physical phenomenon with nondimensional parameters of interest without giving any weightage to units of involved quantities. Non dimensionalization of the model (4.11)-(6.20) can be obtained by considering the following nondimensional variables and parameters

$$t^* = \frac{t\nu}{d^2}, \quad y^* = \frac{y}{d}, \quad x^* = \frac{x\nu}{d^2 U_0}, \quad u^* = \frac{u}{U_0}, \quad v^* = \frac{dv}{\nu}, \quad \lambda_1^* = \lambda_1(\frac{\nu}{d^2}),$$
$$\lambda_2^* = \lambda_2(\frac{\nu}{d^2}), \quad \theta = \frac{T - T_0}{T_d - T_0}$$

with the use of chain rule

$$\frac{\partial u}{\partial t} = U_0 \frac{\partial u^*}{\partial t^*} \frac{\partial t^*}{\partial t}, \qquad \frac{\partial u}{\partial y} = U_0 \frac{\partial u^*}{\partial y^*} \frac{\partial y^*}{\partial y}, \qquad \frac{\partial^\alpha u}{\partial t^\alpha} = U_0 \frac{\nu^\alpha}{d^{2\alpha}} \frac{\partial^\alpha u^*}{\partial t^{*\alpha}}.$$

Using above expressions, the model (4.11)-(6.20) takes the following form (after removing the asteric (*) sign)

$$\begin{cases} \dfrac{\partial u}{\partial x} + \dfrac{\partial v}{\partial y} = 0, \\ \dfrac{\partial u}{\partial t} + u\dfrac{\partial u}{\partial x} + v\dfrac{\partial u}{\partial y} + \lambda_1^\alpha \dfrac{\partial^{\alpha+1} u}{\partial t^{\alpha+1}} + \lambda_1^\alpha \dfrac{\partial^\alpha}{\partial t^\alpha}\left(u\dfrac{\partial u}{\partial x}\right) + \lambda_1^\alpha \dfrac{\partial^\alpha}{\partial t^\alpha}\left(v\dfrac{\partial u}{\partial y}\right) \\ \qquad = \dfrac{\partial^2 u}{\partial y^2} + G_r \lambda_1^\alpha \dfrac{\partial^\alpha}{\partial t^\alpha}\theta + G_r\theta - (M + \Phi_2)\, u - (M + \Phi_2)\, \lambda_1^\alpha \dfrac{\partial^\alpha u}{\partial t^\alpha}, \\ \dfrac{\partial \theta}{\partial t} + u\dfrac{\partial \theta}{\partial x} + v\dfrac{\partial \theta}{\partial y} + \lambda_2^\gamma \dfrac{\partial^{\gamma+1}\theta}{\partial t^{\gamma+1}} + \lambda_2^\gamma \dfrac{\partial^\gamma}{\partial t^\gamma}\left(u\dfrac{\partial \theta}{\partial x}\right) + \lambda_2^\gamma \dfrac{\partial^\gamma}{\partial t^\gamma}\left(v\dfrac{\partial \theta}{\partial y}\right) = \left(\dfrac{1 - \Phi_3}{P_r}\right)\dfrac{\partial^2 \theta}{\partial y^2}. \end{cases} \tag{4.13}$$

Where $\Phi_2 = \frac{d^2}{U_0 \nu k_{nf}}$, $\Phi_3 = -\frac{16T_0^3(T_d - T_0)\sigma}{3\beta(\rho C_p)_{nf} k_{nf}}$, $M = \frac{\sigma_{nf} B_0^2 d^2}{U_0 \nu \mu_{nf}}$, $G_r = \frac{\beta_{nf} g(T_d - T_0)d^2}{U_0 \nu}$ Grashof number and $P_r = \frac{U_0 \nu c_p \mu}{k d^2}$ Prandtl number respectively.

Dimensionless form of boundary and initial conditions are

$$\begin{aligned} t \leqslant 0 : v = 0, \quad u = 0, \quad \theta = 0, \\ t > 0 : v = 0, \quad u = 0, \quad \theta = 0 \quad at \quad x = 0, \\ t > 0 : u = t, \quad \theta = t \quad at \quad y = 0, \\ t > 0 : u \to 0, \quad \theta \to 0 \quad at \quad y \to \infty. \end{aligned} \tag{4.14}$$

The subsequent section elucidates the numerical scheme employed to solve the non-dimensional mathematical model derived in this section.

4.3 Numerical Method

This section elucidates briefly the numerical scheme employed to solve the developed model 4.13-4.14. The finite difference approximations have been utilized along with L_1 scheme in order to discretize the mixed fractional derivatives which appears in the model. Other numerical schemes can also be utilized in order to solve the model 4.13-4.14, for example V. E. Lynch et. al. [47] have discussed two numerical schemes, namely $L2$ and $L2C$, for solving partial differential equations of fractional order. The authors have investigated explicit and semi implicit techniques along with two types of discretization schemes. It is found that these techniques depend on the correct choice of discretization methods as well as on the choice of α. The $L2$ scheme demonstrates good convergence results for $\alpha > 1.5$ whereas $L2C$ shows adequate convergence for $\alpha < 1.5$.

$L1$ scheme is a newly introduced technique by F. Liu et. al. [48] wherein the authors have devised a method of discretizing the nonlinear convection terms as well as the terms which involve fractional order derivative of nonlinear terms using finite difference approximations. The $L1$ scheme does not depend on the particular choice of discretization or on the values of fractional order α. The technique has been successfully applied on various models and obtained significant results, see for example [4], [49] and references therein. The $L1$ scheme is best suited for the problems of the type considered in this manuscript. The scheme is described briefly in the subsequent section.

4.3.1 Discretization method

Define $t_k = k\Delta t,\ k = 0,1,2,3,...,r$, time steps with Δt being a time step size and $x_i = i\Delta x,\ i = 0,1,2,3,...,m$; $y_j = j\Delta y,\ j = 0,1,2,3,...,n$, where $\Delta x = \frac{L_x}{m}$ and $\Delta y = \frac{L_y}{n}$ are space step sizes. Let u_{ij}^k and θ_{ij}^k be numerical approximations of $u(t,x,y)$ and $\theta(t,x,y)$ at point (x_i, y_j) and time t_k in the model 4.13-4.14.

The Caputo time fractional derivative in equation 4.4 is discretized at time t_k as follows

$$\begin{aligned}\partial_t^\alpha u(t_k) &= \frac{1}{\Gamma(2-\alpha)}\sum_{s=0}^{k}\int_{t_k}^{t_{k+1}}(t_k-\xi)^{1-\alpha-1}\frac{\partial u(\xi)}{\partial\xi}d\xi, \quad 0<\Re e\{\alpha\}<1,\\ &= \frac{\Delta t^{-\alpha}}{\Gamma(2-\alpha)}\left[b_0u(t_k) - b_{k-1}u(t_0) + \sum_{s=1}^{k-1}(b_{s-1}-b_s)\,u(t_{k-s})\right] + O(\Delta t) \quad (4.15)\end{aligned}$$

where $b_s = s^{(1-\alpha)} - (s-1)^{(1-\alpha)},\ s = 0,1,2,...,r$.

The non-fractional derivatives terms are discretized using Euler backward finite difference approximations as [48], [78]

$$\begin{aligned}\left.\frac{\partial u}{\partial t}\right|_{t=t_k} &= \frac{u(x_i,y_j,t_k)-u(x_i,y_j,t_{k-1})}{\Delta t} + O(\Delta t),\\ u\left.\frac{\partial u}{\partial x}\right|_{t=t_k} &= u(x_i,y_j,t_{k-1})\frac{u(x_i,y_j,t_k)-u(x_{i-1},y_j,t_k)}{\Delta x} + O(\Delta x), \quad (4.16)\\ v\left.\frac{\partial u}{\partial y}\right|_{t=t_k} &= v(x_i,y_j,t_{k-1})\frac{u(x_i,y_j,t_k)-u(x_i,y_{j-1},t_k)}{\Delta y} + O(\Delta y),\\ \frac{\partial^2 u}{\partial y^2} &= \frac{u_{i,j+1}^k - 2u_{i,j}^k + u_{i,j-1}^k + u_{i,j+1}^{k-1} - 2u_{i,j}^{k-1} + u_{i,j-1}^{k-1}}{2(\Delta y)^2} + O(\Delta y^2) \quad (4.17)\end{aligned}$$

where $u_{i,j}^k = u(x_i,y_j,t_k)$ and the nonlinear terms have been linearized. Moreover the fractional derivatives of the above terms at time t_k can be defined in the following way (see for details [48])

$$\begin{aligned}\frac{\partial^{\alpha+1}u(t_k)}{\partial t^{\alpha+1}} &= \frac{\Delta t^{-1-\alpha}}{\Gamma(2-\alpha)}\left[u_{ij}^k - u_{ij}^{k-1} - \sum_{s=1}^{k-1}(B_s)(u_{ij}^{k-s} - u_{ij}^{k-s-1})\right],\\ \frac{\partial^\alpha}{\partial t^\alpha}\left(u\frac{\partial u}{\partial x}\right) &= \frac{\Delta t^{-\alpha}}{\Delta x\Gamma(2-\alpha)}\left[u_{ij}^{k-1}\left(u_{ij}^k - u_{i-1j}^k\right) - \sum_{s=1}^{k-1}(B_s)u_{ij}^{k-s-1}\left(u_{ij}^{k-s} - u_{i-1j}^{k-s}\right)\right],\\ \frac{\partial^\alpha}{\partial t^\alpha}\left(v\frac{\partial u}{\partial y}\right) &= \frac{\Delta t^{-\alpha}}{\Delta y\Gamma(2-\alpha)}\left[v_{ij}^{k-1}\left(u_{ij+1}^k - u_{ij}^k\right) - \sum_{s=1}^{k-1}(B_s)v_{ij}^{k-s-1}\left(u_{ij+1}^{k-s} - u_{ij}^{k-s}\right)\right],\end{aligned}$$

Assume that

$$B_s = (b_{s-1} - b_s), \quad \delta_1 = \lambda^\alpha\frac{\Delta t^{-\alpha}}{\Gamma(2-\alpha)}, \quad \delta_2 = \frac{1}{2\Delta y^2}, \quad \delta_3 = \lambda^\gamma\frac{\Delta t^{-\gamma}}{\Gamma(2-\gamma)}, \quad (4.18)$$

and in order to simplify notations, we write

$$\begin{aligned}
A_1 &= \sum_{s=1}^{k-1}(b_{s-1}-b_s)(u_{ij}^{k-s}-u_{ij}^{k-s-1}),\\
A_2 &= \sum_{s=1}^{k-1}(b_{s-1}-b_s)u_{ij}^{k-s-1}\left(u_{ij}^{k-s}-u_{i-1j}^{k-s}\right), \qquad (4.19)\\
A_3 &= \sum_{s=1}^{k-1}(b_{s-1}-b_s)v_{ij}^{k-s-1}\left(u_{ij+1}^{k-s}-u_{ij}^{k-s}\right),\\
A_4 &= \theta_{ij}^{k-1}-\sum_{s=1}^{k-1}(b_{s-1}-b_s)\theta_{ij}^{k-s}, \qquad (4.20)\\
A_5 &= -\sum_{s=1}^{k-1}(b_{s-1}-b_s)u_{ij}^{k-s}.
\end{aligned}$$

By using similar conventions, we can easily obtain the approximations for the fractional derivatives terms involved in the temperature equation given below

$$\begin{aligned}
\frac{\partial^{\alpha+1}\theta(t_k)}{\partial t^{\alpha+1}} &= \frac{\Delta t^{-1-\alpha}}{\Gamma(2-\alpha)}\left[\theta_{ij}^{k}-\theta_{ij}^{k-1}-\sum_{s=1}^{k-1}(c_{s-1}-c_s)(\theta_{ij}^{k-s}-\theta_{ij}^{k-s-1})\right],\\
\frac{\partial^{\alpha}}{\partial t^{\alpha}}\left(u\frac{\partial\theta}{\partial x}\right) &= \frac{\Delta t^{-\alpha}}{\Delta x\Gamma(2-\alpha)}\left[u_{ij}^{k-1}\left(\theta_{ij}^{k}-\theta_{i-1j}^{k}\right)-\sum_{s=1}^{k-1}(c_{s-1}-c_s)u_{ij}^{k-s-1}\left(\theta_{ij}^{k-s}-\theta_{i-1j}^{k-s}\right)\right],\\
\frac{\partial^{\alpha}}{\partial t^{\alpha}}\left(v\frac{\partial\theta}{\partial y}\right) &= \frac{\Delta t^{-\alpha}}{\Delta y\Gamma(2-\alpha)}\left[v_{ij}^{k-1}\left(\theta_{ij+1}^{k}-\theta_{ij}^{k}\right)-\sum_{s=1}^{k-1}(c_{s-1}-c_s)v_{ij}^{k-s-1}\left(\theta_{ij+1}^{k-s}-\theta_{ij}^{k-s}\right)\right],
\end{aligned}$$

where $c_s = s^{(1-\alpha)}-(s-1)^{(1-\alpha)}$, $s =: 0,1,2,...,r$. In order to simplify the notations, we assume that

$$\begin{aligned}
B_1 &= \sum_{s=1}^{k-1}(c_{s-1}-c_s)(\theta_{ij}^{k-s}-\theta_{ij}^{k-s-1}),\\
B_2 &= \sum_{s=1}^{k-1}(c_{s-1}-c_s)u_{ij}^{k-s-1}\left(\theta_{ij}^{k-s}-\theta_{i-1j}^{k-s}\right),\\
B_3 &= \sum_{s=1}^{k-1}(c_{s-1}-c_s)v_{ij}^{k-s-1}\left(\theta_{ij+1}^{k-s}-\theta_{ij}^{k-s}\right),
\end{aligned}$$

Finally, by substituting the approximations 4.16-4.21 in the model equations (4.13), we can obtain the following discretization scheme

$$
\begin{aligned}
v_{ij}^{k} &= v_{ij-1}^{k} + v_{ij-1}^{k-1} - v_{ij}^{k-1} + 2\frac{h_y}{h_x}\left(u_{i-1j-1}^{k-1} - u_{ij-1}^{k-1}\right) \\
&+2\frac{h_y}{h_x}\left(u_{i-1j}^{k-1} - u_{ij}^{k-1} + u_{i-1j-1}^{k} - u_{ij-1}^{k} + u_{i-1j}^{k} - u_{ij}^{k}\right),
\end{aligned} \tag{4.21}
$$

$$
\begin{cases}
u_{ij}^{k}\left(\dfrac{1}{\Delta t} + \dfrac{u_{ij}^{k-1}}{\Delta x} + \dfrac{v_{ij}^{k-1}}{\Delta y} + \dfrac{\delta_1}{\Delta t} + u_{ij}^{k-1}\dfrac{\delta_1}{\Delta x} - v_{ij}^{k-1}\dfrac{\delta_1}{\Delta y} + 2\delta_2 + (M+\Phi_2)(1+\dfrac{\delta_1}{\Delta t})\right) \\
+u_{i-1j}^{k}\left(-\frac{u_{ij}^{k-1}}{\Delta x} - u_{ij}^{k-1}\frac{\delta_1}{\Delta x}\right) + u_{ij-1}^{k}\left(-\frac{v_{ij}^{k-1}}{\Delta y} - \delta_2\right) + u_{ij+1}^{k}\left(-\delta_2 + \frac{\delta_1 v_{ij}^{k-1}}{\Delta y}\right) \\
\quad = u_{ij}^{k-1}\left(\frac{1}{\Delta t} + \frac{\delta_1}{\Delta t} - 2\delta_2\right) + \frac{\delta_1}{\Delta t}A_1 + \frac{\delta_1}{\Delta x}A_2 + \dfrac{\delta_1}{\Delta y}A_3 + \delta_2 u_{ij+1}^{k-1} + \delta_2 u_{ij-1}^{k-1} \\
+\delta_1 G_r A_4 + G_r\theta_{ij}^{k-1} + (M+\phi_2)\,\delta_1 A_5,
\end{cases} \tag{4.22}
$$

$$
\begin{cases}
\theta_{ij}^{k}\left(\dfrac{1}{\Delta t} + u_{ij}^{k-1}\dfrac{1}{\Delta x} + v_{ij}^{k-1}\dfrac{1}{\Delta y} + \delta_3\dfrac{1}{\Delta t} + \delta_3 u_{ij}^{k-1}\dfrac{1}{\Delta x} + \delta_3 v_{ij}^{k-1}\dfrac{1}{\Delta y} + \delta_2\dfrac{2}{p_r}(1-\phi_3)\right) \\
+\theta_{i-1j}^{k}\left(-\dfrac{u_{ij}^{k-1}}{\Delta x} - \dfrac{u_{ij}^{k-1}\delta_3}{\Delta x}\right) + \theta_{ij-1}^{k}\left(-\dfrac{v_{ij}^{k-1}}{\Delta y} - \dfrac{v_{ij}^{k-1}\delta_3}{\Delta y} - \dfrac{\delta_2}{P_r}(1-\phi_3)\right) \\
-\dfrac{\delta_2}{P_r}(1-\phi_3)\theta_{ij+1}^{k} = \theta_{ij}^{k-1}\left(\dfrac{1}{\Delta t} + \delta_3\dfrac{1}{\Delta t} - 2\dfrac{\delta_2}{P_r}(1-\phi_3)\right) + \delta_3\left(B_1\dfrac{1}{\Delta t} + B_2\dfrac{1}{\Delta x} + B_3\dfrac{1}{\Delta y}\right) \\
+\dfrac{\delta_2}{P_r}(1-\phi_3)\left(\theta_{ij+1}^{k-1} + \theta_{ij-1}^{k-1}\right),
\end{cases} \tag{4.23}
$$

and the initial and boundary conditions can evidently be defined as

$$
\begin{aligned}
v_{ij}^{0} = 0, \quad u_{ij}^{0} = 0, \quad \theta_{ij}^{0} = 0, \\
v_{0j}^{k} = 0, \quad u_{0j}^{k} = 0, \quad \theta_{0j}^{k} = 0, \\
v_{i0}^{k} = 0, \quad u_{i0}^{k} = t_k, \quad \theta_{i0}^{k} = 0, \\
v_{iL_y}^{k} = 0, \quad u_{iL_y}^{k} = 0, \quad \theta_{iL_y}^{k} = 0,
\end{aligned} \tag{4.24}
$$

Solution procedure

The computational domain is considered as a rectangle with sizes $L_x = 1$ and $L_y = 5$ where L_y corresponds to $y \to \infty$ as the solution approaches to zeros in the vicinity of $L_y = 5$, see Fig. 6.5 for validation. Th solution has been computed with mesh sizes $\Delta x = 0.01$, $\Delta y = 0.01$ and $\Delta t = 0.01$. The iteration process in the numerical scheme (4.21)-(4.23) has been initiated by initial values u_{ij}^0, v_{ij}^0 and θ_{ij}^0 given by equation (4.24).

Assuming that the earlier values u_{ij}^{k-1}, v_{ij}^{k-1} and θ_{ij}^{k-1} at time $t = t_{k-1}$ are known for the $k - level$ iteration. The memory terms $A_1,\ A_2,\ A_3$ and $B_1,\ B_2,\ B_3$ are also known as these terms are defined till the $(k-1)th$ time step. Finally, the iteration at each kth time step can be written in the form of five diagonal linear system by placing each term of $(k-1)th$ step on the right hand side of the systems. The linear systems are then solved by using a classical direct method. A MATLAB code has been developed in order to find solution of the scheme (4.21)-(4.24).

4.3.2 Skin Friction Coefficient

The fluid layer adjacent to the boundary (plate) is characterized by the skin friction coefficient or shear stress coefficient denoted as $\mathcal{C}_f$ and defined by [49]

$$\mathcal{C}_f = \frac{\mu_{nf}}{\rho_f U_0^2}\tau_w, \tag{4.25}$$

with the stress at the boundary is defined by

$$\tau_w = \left.\frac{\partial u}{\partial y}\right|_{y=0}, \tag{4.26}$$

whereas the fractional form of the stress can be defined using equation (4.3) as

$$\left(1 + \lambda_1^\alpha \frac{\partial^\alpha}{\partial t^\alpha}\right)\tau_w = \left.\frac{\partial u}{\partial y}\right|_{y=0}, \tag{4.27}$$

Therefore the skin friction coefficient $\mathcal{C}_f$ can finally be defined as

$$\left(1 + \lambda_1^\alpha \frac{\partial^\alpha}{\partial t^\alpha}\right)\mathcal{C}_f = \frac{\mu_{nf}}{\rho_f U_0^2}\left.\frac{\partial u}{\partial y}\right|_{y=0}, \tag{4.28}$$

Using the nondimensional quantities defined in section 4.2.1, the dimensionless form of the skin friction is given by

$$\left(1 + \lambda_1^\alpha \frac{\partial^\alpha}{\partial t^\alpha}\right)\mathcal{C}_f = \frac{1}{Re}\left.\frac{\partial u}{\partial y}\right|_{y=0}, \tag{4.29}$$

Using $L1$-discretization of Caputo derivative defined in 6.22, the skin friction coefficient $\mathcal{C}_f$ can be written as

$$\mathcal{C}_f = \frac{\delta_1 \sum_{s=1}^{k-1}(b_{s-1} - b_s)\mathcal{C}_f(t_{k-s}) + \frac{1}{Re}\left.\frac{\partial u}{\partial y}\right|_{y=0}}{1 + \delta_1} \tag{4.30}$$

where $Re = U_0 d/\nu$ is the Reynolds number. The Average skin friction coefficient can further be defined as

$$\bar{\mathcal{C}_f} = \frac{\delta_1 \sum_{s=1}^{k-1}(b_{s-1} - b_s)\bar{\mathcal{C}_f}(t_{k-s}) + \frac{1}{Re}\int_0^1 \frac{\partial u}{\partial y}\Big|_{y=0} dx}{1 + \delta_1} \tag{4.31}$$

The skin friction coefficient has been calculated for different values of physical parameters and the results have been shown in Table (5.1).

4.3.3 Local Nusselt Number

A ratio between convective and conductive heat transfer in the fluid is known as local Nusselt number denoted by Nu. The large values of the Nusselt number shows the dominated heat transfer by convection in the fluid. The Nusselt number for Maxwell fluid is[49].

$$Nu = -\frac{dk_{nf}}{k_f(T_d - T_0)}\mathbf{q}_w, \tag{4.32}$$

with the expression for $\mathbf{q}_w$ defined by

$$\mathbf{q}_w = \frac{\partial T}{\partial y}\bigg|_{y=0} \tag{4.33}$$

and for the fractional Maxwell fluid, we can define (see for details [33])

$$\left(1 + \lambda_2^\alpha \frac{\partial^\alpha}{\partial t^\alpha}\right)\mathbf{q}_w = \frac{\partial T}{\partial y}\bigg|_{y=0} \tag{4.34}$$

Applying operator $\left(1 + \lambda_2^\gamma \frac{\partial^\gamma}{\partial t^\gamma}\right)$ on both side of equation (4.32) and using above relations, the Nusselt number Nu can be written as

$$\left(1 + \lambda_2^\alpha \frac{\partial^\gamma}{\partial t^\gamma}\right) Nu = -\frac{dk_{nf}}{k_f(T_d - T_0)}\frac{\partial T}{\partial y}\bigg|_{y=0} \tag{4.35}$$

The dimensionless form of Nussult number can be defined using relations in section 4.2.1 as

$$\left(1 + \lambda_2^\gamma \frac{\partial^\gamma}{\partial t^\gamma}\right) Nu = -\frac{k_{nf}}{k_f}\frac{\partial \theta}{\partial y}\bigg|_{y=0} \tag{4.36}$$

Using $L1$-discretization of Caputo derivative defined in 6.22, the Nusselt number Nu can be discretized as

$$Nu = \frac{\delta_3 \sum_{s=1}^{k-1}(c_{s-1} - c_s)Nu(t_{k-s}) - \frac{k_{nf}}{k_f}\frac{\partial\theta}{\partial y}\Big|_{y=0}}{1+\delta_3} \tag{4.37}$$

Moreover, the average Nusselt number can be given as

$$\bar{Nu} = \frac{\delta_3 \sum_{s=1}^{k-1}(c_{s-1} - c_s)\bar{Nu}(t_{k-s}) - \frac{k_{nf}}{k_f}\int_0^1 \frac{\partial\theta}{\partial y}\big|_{y=0}dx}{1+\delta_3} \tag{4.38}$$

The Nusselt number has been calculated for various values of physical quantities and the outcomes have been shown in Table (5.2).

4.4 Results and discussion

In this section, the effects of heat transfer flow of fractional Maxwell fluid with magnetic field and radiation over a moving plate is studied. The non linear coupled equations are numerically solved by newly developed $L1$ technique along with the finite difference approximations as described earlier. The parameters involved in the model which are discussed are mainly the fractional parameters α, γ, Maxwell or the relaxation time parameters λ_1, λ_2, Prandtl number P_r, magnetic field M, radiation parameter Φ_3 and nanofluid parameter Φ_2. The effect of these physical and fractional parameters on the velocity variation and temperature variation along with Skin friction coefficient $\mathcal{C}_f$ and Nusselt number Nu have been investigated and explained via graphs and tables.

4.4.1 Effects on velocity field

Fig 4.1(a) indicates that fractional parameter α effects on velocity profile with final time $t_f = 1$ and $t_f = 2$. For grater values of α, the velocity of the fluid increases. This implies that increase in the fractional parameter α give rise in the thickness of velocity for the both short and long times. Change in behavior can be noted for some other values of involved parameters. Similar pattern can be seen for boundary layer thickness of the flow domain.

In Fig. 4.1(b) shows relaxation time λ_1 effects on velocity profile. Velocity of the fluid decreases for larger values of λ_1. For time $t_f = 1$, velocity of the fluid decreases quickly when we have larger values of λ_1. Increasing the values of λ_1 result as increase in the boundary layer thickness and velocity variation decreases. The relaxation time parameter is stronger for large λ_1. Hence velocity profile decreases by the increase of λ_1. Influence of magnetic field on fluid velocity shown in Fig. 4.2(a). The increase of magnetic field parameter M tends to decrease velocity profile. The Lorentz force increases is directly proportional of magnetic number, where has magnetic number makes resistance to the motion of fluid. Due to magnetic number, magnitude of the local skin friction and velocity variation decreases. Effects of nano-particles volume ϕ on nanofluids are shown in 4.2(b). The increase in the volumic concentration ϕ of nano particles decreases velocity which is physically adequate as observed in experimental findings.

4.4.2 Effects on temperature profile

The dimensionless form of a temperature is considered because of the fact that the natural or free convection is operate by temperature gradient. In Fig. 4.3(a) demonstrate fractional parameter effects of γ on temperature is same like in α case on velocity profile. Decreasing γ values from 1 to 0 quickly decrease temperature. This shows non integer order derivatives weakens the effects of heat conduction. Relaxation time parameter λ_2 effects on temperature field shown in Fig. 4.3(b). A small change occurs in temperature for small values of λ_2. Petit increase in λ_2 decrease temperature profile slightly. Radiation effects on temperature profile shown in Fig. 5.3(b). Radiation parameter Φ_3 minor increment makes a larger change in temperature field. The Prandtl number is the ratio of momentum diffusivity and thermal diffusivity. Prandtl number Pr effects on temperature are shown in Fig. 4.4(b). A petit increase in Prandtl number demonstrate decrease in temperature profile. It is also noted that for large values of Prandtl parameter Pr the thickness thermal boundary layer goes down. Using Pr, we can control the thickness of momentum and thermal boundary layers. Heat disperses slowly and thermal boundary layer reach to lower level when Pr has large values and opposite behavior is observed for thermal boundary layer at smaller values of Pr.

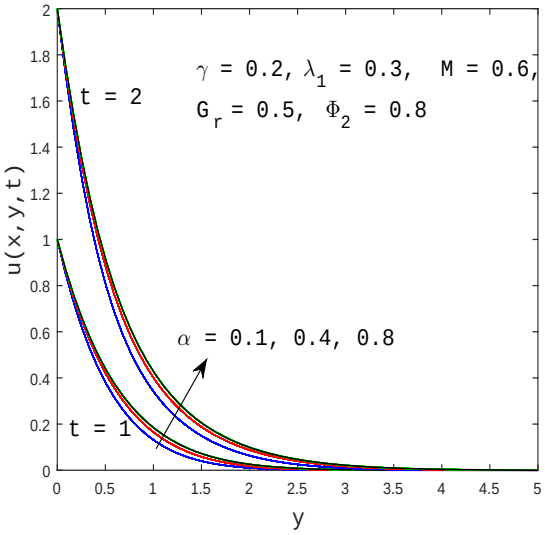

(a) velocity distribution with α variation.

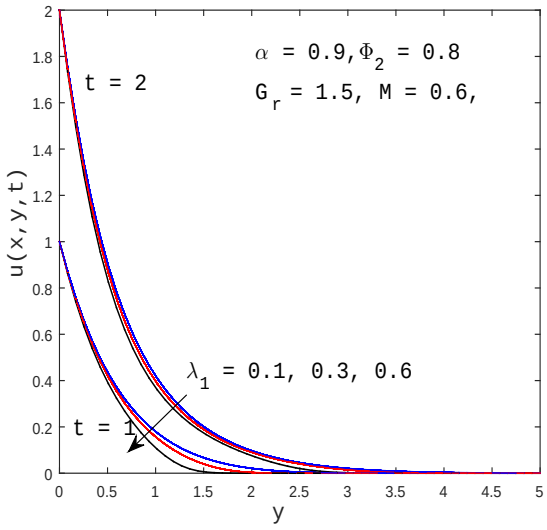

(b) Velocity distribution for λ_1

Figure 4.1

Fig. 5.5(a) and Fig. 6.5(b) shows three dimensional velocity and temperature distribution which demonstrate convergence and good stability in space and time variables.

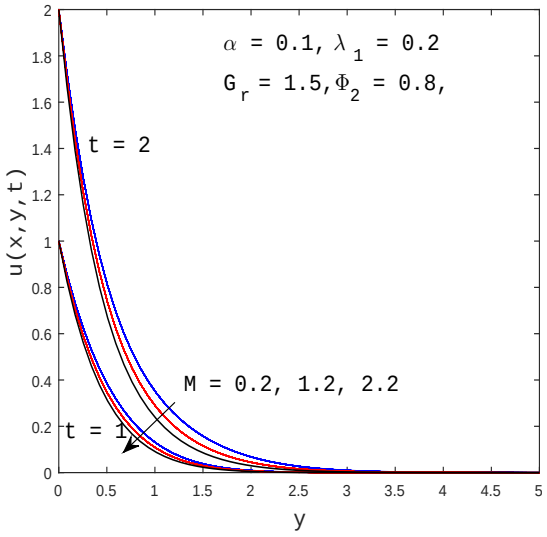

(a) Velocity distribution for M.

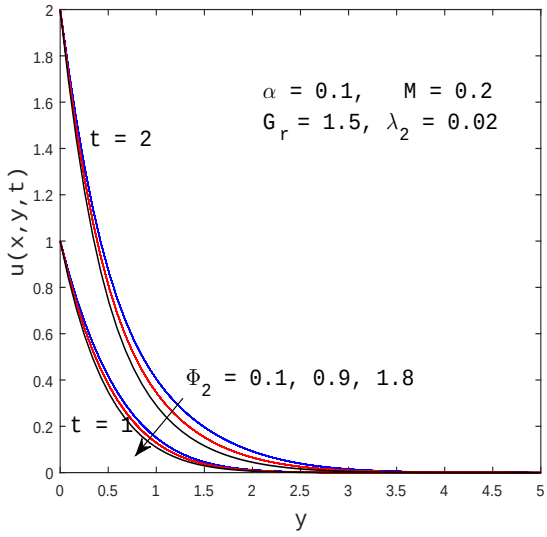

(b) Velocity distribution for Φ_2

Figure 4.2

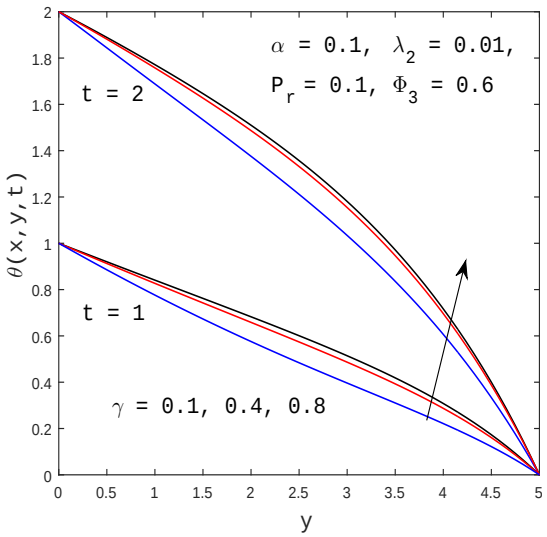

(a) Temperature distributions with γ variation.

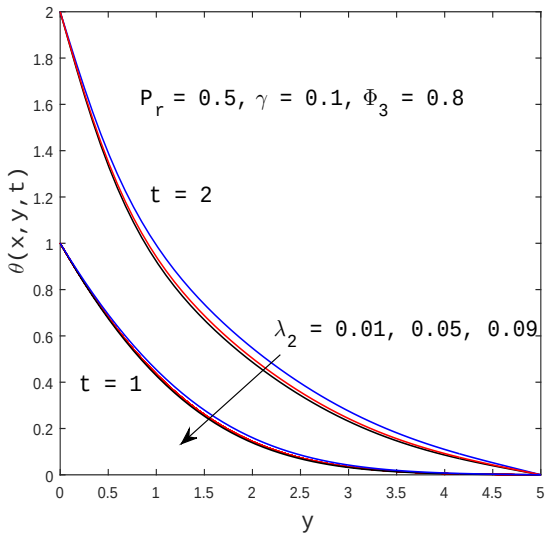

(b) Temperature distribution for λ_2.

Figure 4.3

4.4.3 Average skin friction coefficient

The average skin friction coefficient for different parameters are shown in Table 4.1. Skin friction plays a vital role in prediction the behavior of flow nearer the boundary. Realistic

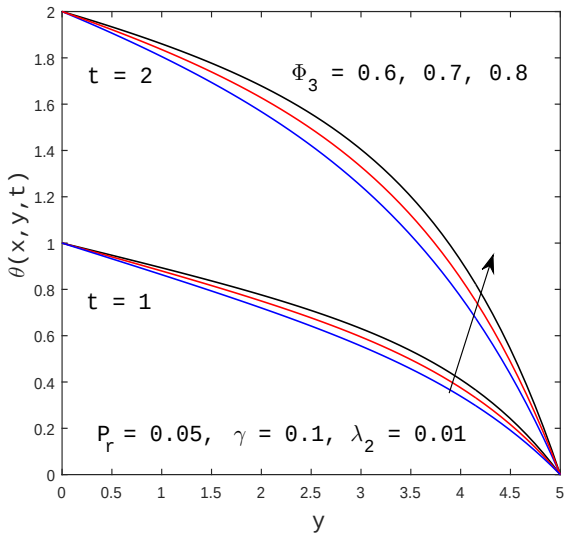

(a) Temperature distribution for Φ_3.

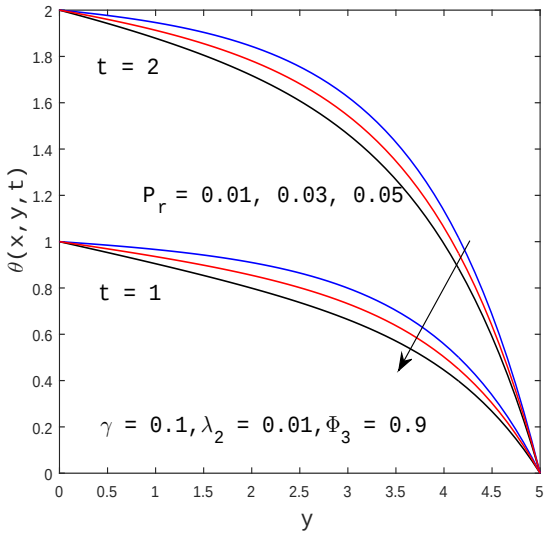

(b) Temperature distribution for P_r.

Figure 4.4

physical simulations can be done if we taken into account the skin friction while calculating the flow field particularly velocity field. Effects of different parameters on the skin friction coefficient can be used for the controlled environment. Finally here we calculate the numerical values of skin friction coefficient for different values of involved parameters. These numeric values will be helpful to show the cumulative trend of friction in the flow

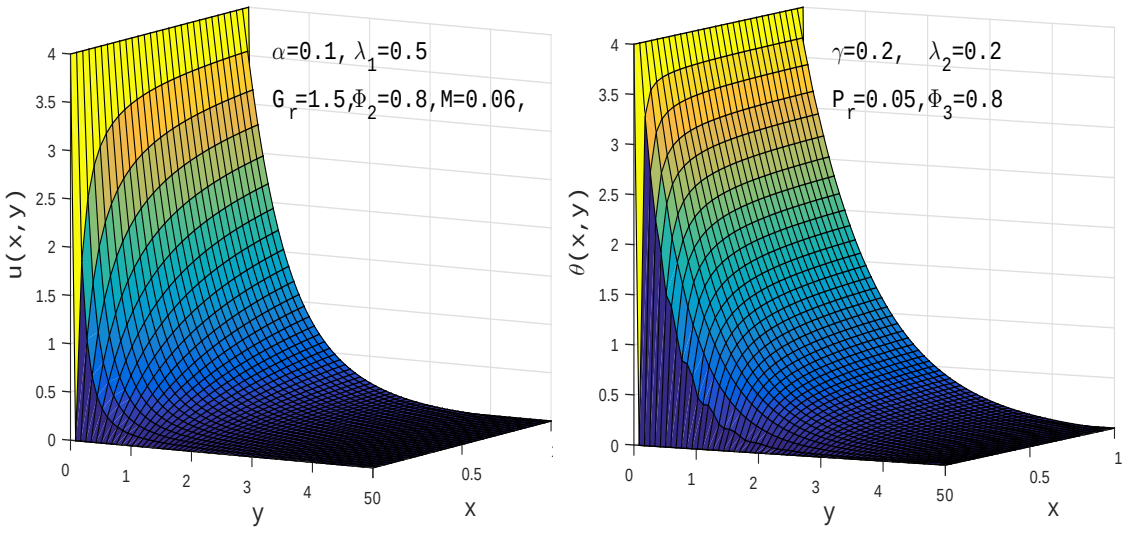

(a) Three dimensional velocity distribution. (b) Three dimensional temperature distribution.

Figure 4.5

domain. For each velocity fractional derivative, average skin friction coefficient decreases with the increase of fractional parameter α. This shows that velocity fractional derivative monotonically decreases average skin friction coefficient. It seems velocity gradient is not related to decrease of velocity fractional derivative, which is shown in Fig. 5.1(a). Skin friction coefficient is function of a velocity gradient shown in Eq. 4.31. Maxwell parameter λ_1 increases average skin friction coefficient slowly but uniform magnetic field M and nano fluid parameter Φ_2 decrease average skin friction coefficient.

4.4.4 Average Nusselt number

Table 4.2 illustrates the influence of physical and fractional parameters on average Nusselt number. Nusselt number plays an extensive role for the caculation of thermal field. Realistic physical simulations can be done if we taken into account the Nusselt number while calculating the thermal field. Here we calculate the numerical values of Nusselt number for different values of involved parameters. These numeric values will be helpful to show the cumulative trend of temperature gradient in the flow domain. As shown in table, for each temperature fractional derivative parameter γ, average Nusselt number

Table 4.1: Average skin friction coefficient for different parameters.

α	λ_1	M	Φ_2	$\bar{Cf}$
0.1	0.2	0.01	0.01	-8.2201
0.3	0.2	0.01	0.01	-9.3333
0.6	0.2	0.01	0.01	-10.5056
0.9	0.2	0.01	0.01	-11.1255
0.1	**0.2**	0.01	0.01	-8.2201
0.1	**0.4**	0.01	0.01	-8.0712
0.1	**0.6**	0.01	0.01	-7.9827
0.1	**0.8**	0.01	0.01	-7.9193
0.1	0.2	**0.01**	0.01	-8.2201
0.1	0.2	**0.05**	0.01	-8.2399
0.1	0.2	**0.1**	0.01	-8.2647
0.1	0.2	**0.5**	0.01	-8.4069
0.1	0.2	0.01	**0.01**	-8.2201
0.1	0.2	0.01	**0.1**	-8.2647
0.1	0.2	0.01	**1.1**	-8.7495
0.1	0.2	0.01	**2.1**	-9.2150

monotonically decreases with the increase of fractional parameter γ. Average Nusselt number is irrelevant to temperature gradient as shown in Fig. 5.1(b) where temperature has different values. Average Nusselt number is comprehensive function of temperature gradient as shown in Eq. 4.38. Maxwell parameter λ_2, Prandtl number Pr and radiation parameter Φ_3 has a small variation on average Nusselt number.

In Table 4.3, We have presented the comparison for different values of Prandtl number Pr with already published papers for assessment and accuracy of the numerical results and good compatibility was observed. The Prandtl Number is often used in heat transfer and free and forced convection calculations. As it is the ratio of molecular diffusivity

Table 4.2: Average Nusselt number for different parameters.

γ	λ_2	P_r	Φ_3	$\bar{Nu}$
0.1	0.2	0.01	0.01	-52.0576
0.3	0.2	0.01	0.01	-76.5177
0.6	0.2	0.01	0.01	-1.9658e+02
0.9	0.2	0.01	0.01	-1.1654e+03
0.1	**0.2**	0.01	0.01	-52.0576
0.1	**0.4**	0.01	0.01	-51.4028
0.1	**0.6**	0.01	0.01	-51.0632
0.1	**01**	0.01	0.01	-50.6861
0.1	0.2	**0.01**	0.01	-52.0576
0.1	0.2	**0.05**	0.01	-52.1020
0.1	0.2	**0.09**	0.01	–52.1483
0.1	0.2	**0.1**	0.01	–52.1594
0.1	0.2	0.01	**0.01**	-52.0576
0.1	0.2	0.01	**0.05**	-52.0518
0.1	0.2	0.01	**0.1**	-52.0466
0.1	0.2	0.01	**0.5**	-52.0193

of momentum to the molecular diffusivity of heat, it shows the relative thickness of the velocity boundary layer to the thermal boundary layer. Crepeau and Clarksean [51], Chamkha and khaled [52] and Chen [53] compared Prandtl number Pr results with some previously published results.

Table 4.3: Comparison of $-\frac{\partial\theta}{\partial y}\Big|_{y=0}$ at $x = 1$, with $\alpha = 1$, $\gamma = 1$, $M = 0$, $\phi_3 = 0$, $\lambda_1 = \lambda_2 = 0$.

Pr	Crepeau and clarksean [51]	Chamkha and khaled [52]	Chen [53]	present work
0.01	0.0805	0.0600	0.0806	0.0585
0.1	0.2302	0.2119	0.23014	0.2460
1	0.5671	0.5649	0.5671	0.6631
10	1.1690	1.1720	1.1693	1.1412
100	2.1910	2.1943	2.1913	2.1126

Chapter 5

Numerical simulation of fractional Maxwell fluid flow through Forchheimer medium

5.1 Introduction

In this article, we examined the unsteady flow of incompressible oscillatory fluid with heat transfer in a vertical channel. Maxwell fluid is flowing through a space filled by Forchheimer medium. The Caputo time operator has been used in the formulation of governing flow problem. A numerical solution has been obtained using Finite Element Method for space variables and Finite Difference Method for fractional time derivatives. The effects of pertinent physical parameters like Forchheimer parameter, Grashof number, Reynolds number, fractional parameters α and β on velocity and temperature distribution are considered and demonstrated through graphs.

5.2 Mathematical formulation

In this problem, we considered one-dimensional, unsteady incompressible viscoelastic flow of fractional Maxwell fluid in a channel of infinite length. Fluid is supposed to move by the movment of lower plate of a channel in the presence of Forchhimer medium. Plates

are separated by distance h and planes $y = 0$ and $y = h$ denotes lower and upper plates. Fluid flows along y direction and x direction is taken as normal to the plates. Induced magnetic field effect is ignored due to small Reynolds number.
Flow velocity is:

$$\mathbf{U} = u(y,t)\mathbf{e}_x + v(y,t)\mathbf{e}_y + w(y,t)\mathbf{e}_z$$

Flow is moving only in a positive vertical direction, therefore $v(y,t) \equiv 0 \equiv w(y,t)$ will become zero. So, governing velocity field is

$$\mathbf{U} = u(y,t)\mathbf{e}_x. \tag{5.1}$$

5.2.1 Conservation of mass

Continuity equation [54]

$$\frac{\partial \rho}{\partial t} + div(\rho u) = 0, \tag{5.2}$$

where ρ is density of the fluid, $\nabla\cdot$ is divergence operator and u is velocity. For incompressible fluid, we have

$$\nabla.\bar{u} = 0. \tag{5.3}$$

5.2.2 Stress tensor

Cauchy stress tensor for the Maxwell model has the following form [55].

$$\mathbb{T} = -p\mathbb{I} + \mathbb{S}, \quad \mathbb{S} + \lambda_1 \frac{\delta \mathbb{S}}{\delta t} = \mu \mathbb{A}_1, \tag{5.4}$$

where $-p$ denotes pressure, $\mathbb{I}$ denotes identity matrix, μ is viscosity, $\mathbb{A}_1$ is the first Rivlin-Eriksen tensor defined as

$$\mathbb{A}_1 = \nabla u + \nabla u^T, \tag{5.5}$$

$$\frac{\delta \mathbb{S}}{\delta t} = \frac{D\mathbb{S}}{Dt} - L\mathbb{S} - \mathbb{S}L^T, \tag{5.6}$$

where $\frac{D}{Dt}$ is material time derivative, u is the velocity of the fluid and L is gradient of a velocity.

Fractional stress tensor for Maxwell fluid on the plate with fractional time Caputo derivative ([56],[59]),

$$\tau + \lambda_1^\alpha \frac{\partial^\alpha \tau}{\partial t^\alpha} = \mu \frac{\partial u}{\partial y}, \quad 0 < y < h, t > 0, \tag{5.7}$$

where $\tau = \mathbb{S}_{xy}$ is the nonzero component of extra stress tensor $\mathbb{S}$ and $\partial^\alpha / \partial t^\alpha$ is Caputo derivative of non integer order α. Suppose $\alpha \in \mathbb{R}$ and $m \in \mathbb{N}$, then Caputo operator is defined as [59]

$$\frac{\partial^\alpha g(t)}{\partial t^\alpha} = \frac{1}{\Gamma(m-\alpha)} \int_0^t (t-\eta)^{m-\alpha-1} \frac{\partial^m g(\eta)}{\partial \eta^m} d\eta, \quad m-1 < \alpha < m,$$

where Gamma function denoted by $\Gamma(\cdot)$ is:

$$\Gamma(z) = \int_0^\infty \eta^{z-1} e^{-\eta} d\eta, \quad z \in \mathbb{C}, \quad \Re\{z\} > 0.$$

5.2.3 Momentum equation

Navier-Stokes equation is ([57])

$$\rho \left(\frac{\partial u}{\partial t} + u.(\nabla u) \right) = -\nabla p + \mu \frac{\partial \tau}{\partial y}. \tag{5.8}$$

The boundary layer flow with boussinesq approximations and Darcy Forchheimer porous resistance (see ([60]), page 1) and also applying operator $(1 + \lambda_1^\alpha \frac{\partial^\alpha}{\partial t^\alpha})$ to equation (5.8).

$$\begin{aligned} \rho(1 + \lambda_1^\alpha \frac{\partial^\alpha}{\partial t^\alpha}) \left[\frac{\partial u}{\partial t} + u.(\nabla u) \right] &= (1 + \lambda_1^\alpha \frac{\partial^\alpha}{\partial t^\alpha})(-\nabla p) + \mu(1 + \lambda_1^\alpha \frac{\partial^\alpha}{\partial t^\alpha}) \frac{\partial \tau}{\partial y} \\ +\rho g \beta (1 + \lambda_1^\alpha \frac{\partial^\alpha}{\partial t^\alpha})(T - T_h) - \frac{\mu}{k_1}(1 + \lambda_1^\alpha \frac{\partial^\alpha}{\partial t^\alpha})u - \frac{\rho c_F}{\sqrt{k_1}}(1 + \lambda_1^\alpha \frac{\partial^\alpha}{\partial t^\alpha})u^2, \end{aligned} \tag{5.9}$$

where u is velocity along x-axis, ρ is density, g is gravitational force, λ_1 is the Maxwell parameter, β is the volumetric coefficient of thermal expansion, k_1 is permeability of porous medium, c_F is dimensionless Forchheimer coefficient.

Using equations 5.3 and 5.7 into equation 5.9, we get

$$\begin{aligned} \frac{\partial u}{\partial t} + \lambda_1^\alpha \frac{\partial^{\alpha+1} u}{\partial t^{\alpha+1}} &= \frac{\mu}{\rho} \frac{\partial^2 u}{\partial y^2} + g\beta(T - T_h) + \lambda_1^\alpha \frac{\partial^\alpha}{\partial t^\alpha} g\beta(T - T_h) \\ &\quad - \frac{\mu}{\rho k_1}(1 + \lambda_1^\alpha \frac{\partial^\alpha}{\partial t^\alpha})u - \frac{c_F}{\sqrt{k_1}}(1 + \lambda_1^\alpha \frac{\partial^\alpha}{\partial t^\alpha})u^2, \end{aligned} \tag{5.10}$$

5.2.4 Conservation of energy

Energy equation for constant temperature T_m on lower plate and T_h on upper plate define as ([58])

$$\rho c_p \left(\frac{\partial T}{\partial t}\right) = -\frac{\partial q}{\partial y}, \tag{5.11}$$

where c_p is specific heat at constant pressure, ρ is density and q is heat flux.
For fractional energy equation, we are applying operator $(1 + \lambda_2^\beta \frac{\partial^\beta}{\partial t^\beta})$ on both sides of equation (6.10) and using equation (5.3)

$$(1 + \lambda_2^\beta \frac{\partial^\beta}{\partial t^\beta})\frac{\partial T}{\partial t} = -\frac{1}{\rho c_p}\frac{\partial}{\partial y}(1 + \lambda_2^\beta \frac{\partial^\beta}{\partial t^\beta})q, \tag{5.12}$$

generalization of fractional Cattaneo's law ([62])

$$(1 + \lambda_2^\beta \frac{\partial^\beta}{\partial t^\beta})q = -k\frac{\partial T}{\partial y}, \tag{5.13}$$

here k is thermal conductivity

$$\frac{\partial T}{\partial t} + \lambda_2^\beta \frac{\partial^{\beta+1} T}{\partial t^{\beta+1}} = \frac{1}{\rho c_p}\frac{\partial}{\partial y}\left(k\frac{\partial T}{\partial y}\right). \tag{5.14}$$

BCs and initial conditions for Equation (5.10) and Equation (5.14) are

$$y = 0, \quad u = \frac{U_0 \nu}{h^2} t, \quad T = \frac{\nu t (T_m - T_h)}{h} + T_h, \tag{5.15}$$

$$y = h, \quad u = 0, \quad T = T_h, \tag{5.16}$$

$$t = 0, \quad u = 0, \quad T = 0. \tag{5.17}$$

5.2.5 Non-Dimensionalization

In order to solve the developed partial differential equations (5.10) and (5.14), it is important to write these equations in nondimensional form. For this we need characteristic quantities that describe flow problem and nondimensional groups, such as characteristic length h, characteristic temperature T_h and characteristic velocity U_0. Nondimensional parameters are defined by using these characteristic quantities

$$t^* = \frac{\nu t}{h^2}, \quad y^* = \frac{y}{h}, \quad u^* = \frac{u}{U_0}, \quad \lambda_1^* = \frac{\lambda_1 \nu}{h^2}, \quad \lambda_2^* = \frac{\lambda_2 \nu}{h^2}, \quad T^* = \frac{T - T_h}{T_m - T_h},$$

nondimensional form of equations 5.10 and 5.14 are given as (dropping the $*$)

$$\frac{\partial u}{\partial t}+\lambda_1^{\alpha}\frac{\partial^{\alpha+1}u}{\partial t^{\alpha+1}} = \frac{\partial^2 u}{\partial y^2}+GrT+Gr\lambda_1^{\alpha}\frac{\partial^{\alpha}}{\partial t^{\alpha}}T-\phi(1+\lambda_1^{\alpha}\frac{\partial^{\alpha}}{\partial t^{\alpha}})u-\phi_r(1+\lambda_1^{\alpha}\frac{\partial^{\alpha}}{\partial t^{\alpha}})u^2, \quad (5.18)$$

$$\frac{\partial T}{\partial t}+\lambda_2^{\beta}\frac{\partial^{\beta+1}T}{\partial t^{\beta+1}} = \frac{1}{Pr}\frac{\partial^2 T}{\partial y^2}, \quad (5.19)$$

where $Pr=\frac{\mu c_p}{k}$, $Gr=g\beta\frac{(T_m-T_h)h^2}{U_0\nu}$, $\phi=\frac{h^2}{k_1}$ and $\phi_r=\frac{C_F U_0 h^2}{\sqrt{k_1}\nu}$ are Prandtl number, Grashof number and Reynolds number respectively.

Initial and boundary conditions are

$$\begin{cases} u=t, \quad T=t, \quad y=0. \quad t>0 \\ u=0, \quad T=0, \quad y=1, \quad t>0 \\ u=0, \quad T=0, \quad t=0, \quad 0\le y\le 1. \end{cases} \quad (5.20)$$

To reduce initial and boundary conditions of equations (5.18) and (5.19) into homogeneous Dirichlet BC's, we introduce following transformations,

$$\begin{cases} v(y,t)=u(y,t)-t(1-y), \\ \theta(y,t)=T(y,t)-tcos(\frac{\pi y}{2}), \end{cases} \quad (5.21)$$

applying these transformation into (5.18) and (5.19). We get

$$\frac{\partial v}{\partial t}+\lambda_1^{\alpha}\frac{\partial^{\alpha+1}v}{\partial t^{\alpha+1}}-\frac{\partial^2 v}{\partial y^2}-Gr\theta-Gr\lambda_1^{\alpha}\frac{\partial^{\alpha}\theta}{\partial t^{\alpha}}+\phi v+\phi\lambda_1^{\alpha}\frac{\partial^{\alpha}v}{\partial t^{\alpha}}+\phi_r v^2+2\phi_r t(1-y)v \quad (5.22)$$
$$+\phi_r\lambda_1^{\alpha}\frac{\partial^{\alpha}v^2}{\partial t^{\alpha}}+2\phi_r(1-y)\lambda_1^{\alpha}\frac{\partial^{\alpha}v}{\partial t^{\alpha}}=g_1(y,t),$$
$$\frac{\partial\theta}{\partial t}+\lambda_2^{\beta}\frac{\partial^{\beta+1}\theta}{\partial t^{\beta+1}}-\frac{1}{Pr}\frac{\partial^2\theta}{\partial y^2}=g_2(y,t), \quad (5.23)$$

where

$$g_1(y,t)=-\left(1+\frac{t^{-\alpha}}{\Gamma(1-\alpha)}\right)(1-y)+Gr.cos(\frac{\pi y}{2})\left(\frac{t^{1-\alpha}}{\Gamma(2-\alpha)}+t\right)$$
$$-\phi(1-y)\left(\lambda_1\frac{t^{1-\alpha}}{\Gamma(2-\alpha)}+t\right)-\phi_r(1-y)^2\left(\lambda_1\frac{t^{2-\alpha}}{\Gamma(3-\alpha)}+t^2\right),$$
$$g_2(y,t)=-cos(\frac{\pi y}{2})-\frac{t^{-\beta}}{\Gamma(1-\beta)}cos(\frac{\pi y}{2})-\frac{\pi^2 t}{4}cos(\frac{\pi y}{2}),$$

with initial and BCs

$$\begin{cases} v = 0, \quad \theta = 0, \quad y = 0, \quad t > 0 \\ v = 0, \quad \theta = 0, \quad y = 1, \quad t > 0 \\ v = 0, \quad \theta = 0, \quad t = 0, \quad 0 \leq y \leq 1. \end{cases} \tag{5.24}$$

Local skin friction coefficient which measures the surface shear stress and Nusselt number that measure heat transfer effect, are defined for integer order derivative are [61].

$$C_f = \frac{\mu}{\rho U_0^2} \frac{\partial u}{\partial y}\bigg|_{y=0}, \tag{5.25}$$

$$Nu = \frac{-kh}{T_m - T_h} \frac{\partial T}{\partial y}\bigg|_{y=0}. \tag{5.26}$$

Skin friction coefficient and local Nusselt number for fractional Maxwell fluid model are derived from constitutive equation (5.7) (See details in [63]).

$$C_f + \lambda_1^\alpha \frac{\partial^\alpha}{\partial t^\alpha} C_f = \frac{\mu}{\rho U_0^2} \frac{\partial u}{\partial y}\bigg|_{y=0}, \tag{5.27}$$

$$Nu + \lambda_2^\beta \frac{\partial^\beta}{\partial t^\beta} Nu = \frac{-kh}{T_m - T_h} \frac{\partial T}{\partial y}\bigg|_{y=0}. \tag{5.28}$$

Non-dimensional form of equations (5.27) and 5.28 are given as.

$$C_f + \lambda_1^\alpha \frac{\partial^\alpha}{\partial t^\alpha} C_f = \frac{1}{Re} \frac{\partial u}{\partial y}\bigg|_{y=0}, \tag{5.29}$$

$$Nu + \lambda_2^\beta \frac{\partial^\beta}{\partial t^\beta} Nu = k \frac{\partial T}{\partial y}\bigg|_{y=0}. \tag{5.30}$$

Solving (5.29) and (5.30) at each t_k time step and also using transformations (5.21), we get local skin friction coefficient and local Nusselt number as

$$C_f = \frac{1}{1 + r1} \left(r1 \sum_{s=1}^{k-1} (\alpha_{s-1} - \alpha_s) C_{f(t_{k-s})} + \frac{1}{Re} \frac{\partial v}{\partial y}\bigg|_{y=0} - \frac{t}{Reh} \right), \tag{5.31}$$

$$Nu = \frac{1}{1 + r3} \left(r3 \sum_{s=1}^{k-1} (\beta_{q-1} - \beta_q) Nu(t_{k-q}) - k \frac{\partial \theta}{\partial y}\bigg|_{y=0} \right), \tag{5.32}$$

where

$$\alpha_s = (s+1)^{1-\alpha} - s^{1-\alpha}, \quad s = 0, 1, 2, ..., r, \tag{5.33}$$

$$\beta_q = (q+1)^{1-\beta} - q^{1-\beta}, \quad q = 0, 1, 2, ..., r \tag{5.34}$$

and similar way, we can find average skin friction and average Nusselt number:

$$\bar{C_f} = \frac{1}{1+r1}\left(r1\sum_{s=1}^{k-1}(\alpha_{s-1}-\alpha_s)\bar{C}_{f(t_{k-s})} + \frac{1}{Re}\int_0^1 \frac{\partial v}{\partial y}\bigg|_{y=0} dx - \frac{t}{Reh}\right), \tag{5.35}$$

$$\bar{Nu} = \frac{1}{1+r3}\left(r3\sum_{s=1}^{k-1}(\beta_{q-1}-\beta_q)\bar{Nu}(t_{k-q}) - k\int_0^1 \frac{\partial \theta}{\partial y}\bigg|_{y=0} dx\right), \tag{5.36}$$

Here $r1$ and $r2$ are defined as

$$r1 = \lambda_1^{\alpha}\frac{\Delta t^{-\alpha}}{\Gamma(2-\alpha)}, \quad r3 = \lambda_2^{\beta}\frac{\Delta t^{-\beta}}{\Gamma(2-\beta)}.$$

5.3 Numerical scheme

Numerical scheme is used to solve the coupled PDEs (5.22) and (5.23). In this section, $L1-$algorithm ([76]) used to discretize Caputo derivative and finite element method (FEM) is employed to discretize special variable y. For further details, reader is referred to ([65, 66]). The well-posedness of the problem is discussed in details in ([67]), where continuity of the solution can be proved in suitable functional spaces. Lebesgue space denoted as $\mathcal{L}^2([a,b])$ denotes set of complexed value function, squared integrable functions over $[a,b]$ in real number together with $\mathcal{L}^2$ norm. Sobolev space is subspace of Lebesgue space and is denoted by $\mathcal{H}^p([a,b])$ where $p>0$. $\mathcal{H}_0^p([a,b])$ is a finite dimensional subspace of Sobolev space $\mathcal{H}^p([a,b])$. The closure of $\mathcal{H}^p([a,b])$ is $\mathcal{C}_0^{\infty}(\overline{[a,b]})$ where $\mathcal{C}_0^{\infty}(\overline{[a,b]})$ is the set of all functions, such that $f \in \mathcal{C}_0^{\infty}(\overline{[a,b]})$ has finite norm. Further details regarding properties of sobolev space are discussed in ([68]). Further, Let we define the following spaces

$$\mathbb{L}^2([a,b]) = \mathcal{L}^2([a,b]) \times \mathcal{L}^2([a,b]),$$

and

$$\mathbb{H}([a,b]) = \mathcal{H}_0^p([a,b]) \times \mathcal{H}_0^p([a,b]).$$

Let $\mathcal{C}^k([0,t_f];\mathcal{V}([a,b]))$, for $k \in \mathbb{N}$, is $k-$ times continuously differentiable functional space, defined from $[0,t_f]$ to $\mathcal{V}([a,b])$ as

$$\mathcal{C}^k([0,t_f];\mathcal{V}([a,b])) := \left\{v \in \mathcal{C}^0([0,t_f];\mathcal{V}([a,b])) \,\middle|\, \partial_t^j v \in \mathcal{C}^0([0,t_f];\mathcal{V}([a,b])) : j \in \mathbb{N}, \forall j \le k\right\},$$

with norm defined as

$$\|v\|_{\mathcal{C}^k\left([0,t_f];\mathcal{V}([a,b])\right)} := \max_{j=0}^{k}\left(\left\|\partial_t^j v\right\|_{\mathcal{C}^0\left([0,t_f];\mathcal{V}([a,b])\right)}\right).$$

where $\mathcal{C}^0$ denotes the space of continuous functions with norm

$$\|v\|_{\mathcal{C}^0\left([0,t_f];\mathcal{V}([a,b])\right)} := \max_{t\in[0,t_f]}\|v\|_{\mathcal{V}}.$$

5.3.1 Finite difference discretizations

In this section, we discretize fractional time variable in the equations (5.22) and (5.23), uniformly partitioned time mesh $[0,t_f]$ (here t_f denotes final time) into $m+1$ points $t_k = k\tau$ for $k = 0,1,2,\cdots,m$ where $\tau = \dfrac{t_f}{m}$ is the time step size. For t approximation at time t_k, for $k\in[0,m]$, given as:

$$\frac{\partial\sigma}{\partial t}(y,s) \simeq \frac{\partial\sigma}{\partial t}(y,t_k) \simeq \frac{\sigma(y,t_{k+1})-\sigma(y,t_k)}{\tau}, \quad t_k \le s \le t_{k+1}, \tag{5.37}$$

and for t_0,

$$\frac{\partial\sigma}{\partial t}(y,t_0) \simeq \frac{\sigma(y,t_1)-\sigma(y,t_0)}{\tau}.$$

The given initial conditions at $t=0$ in (5.24) yield

$$\sigma(y,t_1)\simeq 0 \quad \text{and} \quad \sigma(y,t_0)\simeq 0. \tag{5.38}$$

Moreover, fractional derivative ∂_t^α $(0<\alpha<1)$ at each k, $0\le k<m$ can be approximated by using the scheme given in ([65, 66]) Also for

$$\begin{aligned}\frac{\partial^\alpha\sigma}{\partial t^\alpha}(y,t_{m+1}) &= \frac{1}{\Gamma(1-\alpha)}\sum_{p=0}^{m}\frac{\sigma(y,t_{m-p+1})-\sigma(y,t_{m-p})}{\tau}\int_{p\tau}^{(p+1)\tau}\frac{d\varepsilon}{\varepsilon^\alpha},\\ &= \frac{\tau^{-\alpha}}{\Gamma(2-\alpha)}\Big[\sigma(y,t_{m+1})-\sigma(y,t_m)\Big]+\frac{\tau^{-\alpha}}{\Gamma(2-\alpha)}\Big[\zeta_m^\alpha[\sigma]\Big],\end{aligned} \tag{5.39}$$

where as

$$b_p^\alpha := (p+1)^{1-\alpha}-p^{1-\alpha}, \quad p=0,1,2,...,m$$

and

$$\zeta_m^\alpha[\sigma] := \sum_{p=1}^{m} b_p^\alpha\Big[\sigma(y,t_{m+1-p})-\sigma(y,t_{m-p})\Big] \tag{5.40}$$

$$\text{with} \qquad \zeta_0^\alpha[\sigma] := 0. \tag{5.41}$$

From equation (5.38), we have $\zeta_1^\alpha[\sigma] := 0$

$$\begin{aligned}\frac{\partial^{\alpha+1}\sigma}{\partial t^{\alpha+1}}(y,t_{m+1}) &= \frac{1}{\Gamma(-\alpha)}\sum_{k=1}^{m}\int_{k\tau}^{(k+1)\tau}\frac{\partial\sigma(y,\xi)}{\partial\xi}\frac{d\xi}{(t_{k+1}-\xi)^{-\alpha-1}},\\ &\simeq \frac{1}{\Gamma(-\alpha)}\sum_{k=1}^{m}\frac{\sigma(y,t_{k+1})-\sigma(y,t_k)}{\tau}\int_{k\tau}^{(k+1)\tau}\frac{d\xi}{(t_{k+1}-\xi)^{-\alpha-1}}, \quad (5.42)\end{aligned}$$

Using the substitution $t_{k+1}-\xi=\varepsilon$ in equation (5.42). We have

$$\begin{aligned}\frac{\partial^{\alpha+1}\sigma}{\partial t^{\alpha+1}}(y,t_{m+1}) &= \frac{1}{\Gamma(-\alpha)}\sum_{p=0}^{m-1}\frac{\sigma(y,t_{m-p+1})-\sigma(y,t_{m-p})}{\tau}\int_{p\tau}^{(p+1)\tau}\frac{d\varepsilon}{\varepsilon^{-\alpha-1}},\\ &= \frac{\tau^{-1-\alpha}}{\Gamma(1-\alpha)}\Big[\sigma(y,t_{m+1})-\sigma(y,t_m)\Big]+\frac{\tau^{-1-\alpha}}{\Gamma(1-\alpha)}\left(\zeta_m^\alpha[\sigma]\right), \quad (5.43)\end{aligned}$$

$$\zeta_m^\alpha[\sigma] := \sum_{p=1}^{m-1} b_p^\alpha\Big[\sigma(y,t_{m+1-p})-\sigma(y,t_{m-p})\Big] \quad \text{with} \qquad \zeta_0^\alpha[\sigma] := 0. \quad (5.44)$$

From equation (5.38), we have $\zeta_1^\alpha[\sigma] \simeq 0$.

Let us introduce the operators $\mathcal{L}_t^{\alpha+1}[\sigma]$, $\mathcal{L}_t^\alpha[\sigma]$ and $\mathcal{L}_t[\sigma]$ as

$$\begin{aligned}\mathcal{L}_t^{\alpha+1}[\sigma](t) &= \lambda_1^\alpha\left(\frac{\partial^{\alpha+1}}{\partial t^{\alpha+1}}\right)[\sigma](t),\\ \mathcal{L}_t^{\alpha}[\sigma](t) &= \lambda_1^\alpha\left(\frac{\partial^{\alpha}}{\partial t^{\alpha}}\right)[\sigma](t),\\ \mathcal{L}_t[\sigma](t) &= \frac{\partial}{\partial t},\end{aligned}$$

which can be approximated, at t_m, using equations 5.39 and 5.43 as

$$\begin{aligned}\mathcal{L}_t^{\alpha+1}[\sigma](t_m) &= \lambda_1^\alpha\left(\frac{\partial^{\alpha+1}}{\partial t^{\alpha+1}}\right)[\sigma](t_m),\\ \mathcal{L}_t^{\alpha}[\sigma](t_m) &= \lambda_1^\alpha\left(\frac{\partial^{\alpha}}{\partial t^{\alpha}}\right)[\sigma](t_m),\\ \mathcal{L}_t^{\alpha+1}[\sigma](t_m) &= \lambda_1^\alpha C_{\alpha+1}\Big[\sigma(t_{m+1})-\sigma(t_m)\Big]+\lambda_1^\alpha C_{\alpha+1}\Big[\zeta_m^\alpha[\sigma]\Big], \quad (5.45)\\ \mathcal{L}_t^{\alpha}[\sigma](t_m) &= \lambda_1^\alpha C_\alpha\zeta_m^\alpha[\sigma]+\lambda_1^\alpha C_\alpha\Big[\sigma(t_{m+1})-\sigma(t_m)\Big], \quad (5.46)\\ \mathcal{L}_t[\sigma](t) &= C\Big[\sigma(t_{m+1})-\sigma(t_m)\Big], \quad (5.47)\end{aligned}$$

with $C_{\alpha+1} = \dfrac{\tau^{-1-\alpha}}{\Gamma(1-\alpha)}$, $C_\alpha = \dfrac{\tau^{-\alpha}}{\Gamma(2-\alpha)}$ and $C = \tau^{-1}$
Also for

$$\begin{aligned}\frac{\partial^{\beta+1}\sigma}{\partial t^{\beta+1}}(y,t_{m+1}) &= \frac{1}{\Gamma(-\beta)}\sum_{k=1}^{m}\int_{k\tau}^{(k+1)\tau}\frac{\partial\sigma(y,\xi)}{\partial\xi}\frac{d\xi}{(t_{k+1}-\xi)^{-\beta-1}},\\ &\simeq \frac{1}{\Gamma(-\beta)}\sum_{k=1}^{m}\frac{\sigma(y,t_{k+1})-\sigma(y,t_k)}{\tau}\int_{k\tau}^{(k+1)\tau}\frac{d\xi}{(t_{k+1}-\xi)^{-\beta-1}}, \quad (5.48)\end{aligned}$$

Let us substitute $t_{k+1} - \xi = \varepsilon$ into equation (5.48), we have

$$\begin{aligned}\frac{\partial^{\beta+1}\sigma}{\partial t^{\beta+1}}(y,t_{m+1}) &= \frac{1}{\Gamma(-\beta)}\sum_{p=0}^{m-1}\frac{\sigma(y,t_{m-p+1})-\sigma(y,t_{m-p})}{\tau}\int_{p\tau}^{(p+1)\tau}\frac{d\varepsilon}{\varepsilon^{-\beta-1}},\\ &= \frac{\tau^{-1-\beta}}{\Gamma(1-\beta)}\Big[\sigma(y,t_{m+1})-\sigma(y,t_m)\Big]+\frac{\tau^{-1-\beta}}{\Gamma(1-\beta)}\Big[\zeta_m^\beta[\sigma]\Big], \quad (5.49)\end{aligned}$$

where $b_p^\beta := (p+1)^{-\beta} - (p)^{-\beta}$, $\quad 0 \le p \le m-1$ and

$$\zeta_m^\beta\sigma] := \sum_{p=1}^{m-1} b_p^\beta\Big[\sigma(y,t_{m+1-p})-\sigma(y,t_{m-p})\Big] \quad \text{with} \qquad \zeta_0^\beta[\sigma] := 0. \quad (5.50)$$

We also introduce an operator $\mathcal{R}_t^\beta[\sigma]$ as

$$\mathcal{R}_t^\beta[\sigma](t) = \gamma_2^\beta\left(\frac{\partial^{\beta+1}}{\partial t^{\beta+1}}\right)[\sigma](t),$$

which can be approximated, at t_k for $0 < k < m$, using equation 5.49 as

$$\begin{aligned}\mathcal{R}_{t_k}^\beta[\sigma](t_k) &= \gamma_2^\beta\left(\frac{\partial^{\beta+1}}{\partial t^{\beta+1}}\right)[\sigma](t_k),\\ &\simeq C_\beta\Big[\sigma(t_{k+1})-\sigma(t_k)\Big]+C_\beta\zeta_k^\beta[]. \quad (5.51)\end{aligned}$$

with $C_\beta = \dfrac{\tau^{-1-\beta}}{\Gamma(1-\beta)}$.

5.3.2 Finite Element Discretization

The spatial variable y in the equations (5.22) and (5.23) has been discretized by dividing domain $\Omega = [0,1]$ in equal nodes. For discretization of our scheme, the domain $\Omega = [0,1]$

is divided into a number of n elements Ω_i with fix length. The elements are divided such as there is no space between them.

$$\overline{\Omega} = \bigcup_{i=1}^{n} \overline{\Omega}_i \quad \text{and} \qquad \forall i \neq j : Int(\Omega_i) \bigcap Int(\Omega_j) = 0,$$

here, $Int(\Omega_i)$ denotes set of all points of Ω_i.
A subspace $\left\{\mathcal{V}_0^h(\Omega = [0,1])\right\}_{h>0}$ of $\mathcal{H}_0^1(\Omega = [0,1])$ as

$$\mathcal{V}_0^h(\Omega = [0,1]) := \left\{ \phi \in \mathcal{H}_0^1(\Omega = [0,1]) \;\middle|\; \phi_{|\Omega_i} \in P_r(\Omega_i),\ \forall i = 0, 1, 2, \cdots, n \right\}, \tag{5.52}$$

where $P_r(\Omega_i)$ denotes finite dimensional space of Lagrange polynomials of degree r. Furthermore we denote $\mathbb{V}_0^h(\Omega) = \mathcal{V}_0^h(\Omega) \times \mathcal{V}_0^h(\Omega)$. The weak formulation of the PDEs (5.22) and (**??**) can then be defined by:

Variational Formulation. Find $(v, \theta) \in \mathbb{C}^1\left([0,T]; \mathbb{H}_0^1(\Omega)\right)$ such that

$$\mathcal{L}_t^{\alpha+1}(v,\xi) - Gr\mathcal{L}_t^{\alpha}(\theta,\xi) + \phi\mathcal{L}_t^{\alpha}(v,\xi) + \phi_r\mathcal{L}_t^{\alpha}\left(v^2,\xi\right) + \langle v,\xi\rangle + \phi(v,\xi) \tag{5.53}$$
$$+\phi_r(v^2,\xi) - Gr(\theta,\xi) + \mathcal{L}_t(v,\xi) + \phi_r 2t((1-y)v,\xi) + \phi_r 2\frac{t^{1-\alpha}}{\Gamma(2-\alpha)}\mathcal{L}_t^{\alpha}((1-y)v,\xi) = (g_1,\xi),$$

$$\mathcal{R}_t^{\beta}(\theta,\zeta) + \frac{1}{Pr}\langle\theta,\zeta\rangle + \mathcal{L}_t(\theta,\zeta) = (g_2,\xi), \tag{5.54}$$

$$v(y,0) = 0, \quad \theta(y,0) = 0,$$

for all $(\xi, \zeta) \in \mathbb{H}_0^1(\Omega = [0,1])$. □

Eventually, we have derived weak form of the equations (5.22) and (5.23) in equations(5.53) and (5.54). Let (v_h, θ_h) represents space approximations of (v, θ) in $\mathbb{C}^1\left([0,T]; \mathbb{V}_0^h\right)$,

Discrete Variational Formulation. Find $(v_h, \theta_h) \in \mathbb{C}^1\left([0,L]; \mathbb{V}_0^h(\Omega)\right)$ and $(v_h, \theta_h) \in \mathbb{C}^1\left([0,L]; \mathbb{V}_0^h(\Omega)\right)$ such that

$$\mathcal{L}_t^{\alpha+1}(v_h,\xi) - Gr\mathcal{L}_t^{\alpha}(\theta_h,\xi) + \phi\mathcal{L}_t^{\alpha}(v_h,\xi) + \phi_r\mathcal{L}_t^{\alpha}\left(v_h^2,\xi\right) + \langle v_h,\xi\rangle + \phi(v_h,\xi) + \phi_r(v_h^2,\xi)$$
$$-Gr(\theta_h,\xi) + \mathcal{L}_t(v_h,\xi) + \phi_r 2t((1-y)v_h,\xi) + \phi_r 2\frac{t^{1-\alpha}}{\Gamma(2-\alpha)}\mathcal{L}_t^{\alpha}((1-y)v_h,\xi) = (g_1,\xi), \tag{5.55}$$

$$\mathcal{R}_t^{\beta}(\theta_h,\zeta) + \frac{1}{Pr}\langle\theta,\zeta\rangle + \mathcal{L}_t(\theta_h,\zeta) = (g_2,\xi), \tag{5.56}$$

$$v_h(y,0) = 0, \quad \theta_h(y,0) = 0,$$

for all $(\xi, \zeta) \in \mathbb{V}_0^h(\Omega = [0,1])$. $\square$

The numerical/approximate solution (v_h, θ_h) to 5.55 and 5.56 are as follows:

$$v_h(y,t) = \sum_{p=1}^{M_h} v_p(t) H_h^p(y), \qquad y \in \overline{\Omega}, \tag{5.57}$$

$$\theta_h(y,t) = \sum_{p=1}^{M_h} \theta_p(t) H_h^p(y), \qquad y \in \overline{\Omega}, \tag{5.58}$$

where $\{H_h^p |\ p = 1, 2, \cdots, M_h\}$ forms a basis of $\mathcal{V}_0^h(\Omega)$ with $M_h := \dim(\mathcal{V}_0^h)$ therefor (v_p, θ_p) are to be determined. Therefore, by choosing ξ and ζ as H_h^q, for different values of q such that $q = 1, 2, \cdots, M_h$, consequently we obtain following differential algebraic system

$$\begin{cases} \mathbb{A}\mathcal{L}_t^{\alpha+1}[\mathbf{V}_h(t)] - \mathbb{A}Gr\mathcal{L}_t^{\alpha}[\mathbf{\Theta}_h(t)] + \mathbb{A}\phi\mathcal{L}_t^{\alpha}[\mathbf{V}_h(t)] + \mathbb{C}\phi_r\mathcal{L}_t^{\alpha}[\mathbf{V^2}_h(t)] + \mathbb{B}[\mathbf{V}_h(t)] + \mathbb{A}\phi[\mathbf{V}_h(t)] \\ +\mathbb{C}\phi_r[\mathbf{V^2}_h(t)] - \mathbb{A}Gr[\mathbf{\Theta}_h(t)] + \mathbb{A}\mathcal{L}_t[\mathbf{V}_h(t)] + \mathbb{D}\phi_r 2t[\mathbf{V}_h(t)] + \mathbb{D}\phi_r 2\dfrac{t^{1-\alpha}}{\Gamma(2-\alpha)}\mathcal{L}_t^{\alpha}[\mathbf{V}_h(t)] = \mathbb{G}_1, \\ \mathbb{A}_h\mathcal{R}_t^{\beta}[\mathbf{\Theta}_h(t)] + \dfrac{1}{Pr}\mathbb{B}_h[\mathbf{\Theta}_h(t)] + \mathbb{A}_h\mathcal{L}_t[\mathbf{\Theta}_h(t)] = \mathbb{G}_2, , \\ \mathbf{V}_h(0) = \mathbf{0}, \\ \mathbf{\Theta}_h(0) = \mathbf{0}, \end{cases} \tag{5.}$$

where for all $p, q = 1, 2, \cdots, M_h$:

$$(\mathbf{V}_h)_p := V_p, \quad (\mathbf{\Theta}_h)_p := \theta_p, \quad (\mathbf{W}_h)_p := H_h^p, \quad (\mathbb{A}_h)_{qp} := (H_h^p, H_h^q)\,,$$

$$\begin{aligned} (\mathbb{B}_h)_{qp} &:= \langle H_h^p, H_h^q \rangle, \\ (\mathbb{C}_h)_{qp} &:= (H_h^p, H_h^q)\,, \\ (\mathbb{D}_h)_{qp} &:= ((h-y)H_h^p, H_h^q)\,, \\ (\mathbb{G}_1)_q &:= (g_1, H_h^q)\,, \\ (\mathbb{G}_2)_q &:= (g_2, H_h^q)\,. \end{aligned}$$

With the help of 5.45-5.47 and 5.51, the algebraic system 5.59 can further be solve for a

particular time at t_k ($k \in [0, m]$) as

$$\begin{cases} \mathbb{A}_h \mathcal{L}_t^{\alpha+1}[\mathbf{V}_h(t)] - \mathbb{A}_h Gr \mathcal{L}_t^{\alpha}[\mathbf{\Theta}_h(t)] + \mathbb{A}_h \phi \mathcal{L}_t^{\alpha}[\mathbf{V}_h(t)] + \mathbb{C}_h \phi_r \mathcal{L}_t^{\alpha}[\mathbf{V^2}_h(t)] + \mathbb{B}_h[\mathbf{V}_h(t)] + \\ \mathbb{A}_h \phi[\mathbf{V}_h(t)] + \mathbb{C}_h \phi_r[\mathbf{V^2}_h(t)] - \mathbb{A}_h Gr[\mathbf{\Theta}_h(t)] + \mathbb{A}_h \mathcal{L}_t[\mathbf{V}_h(t)] \\ + \mathbb{D}_h \phi_r 2t[\mathbf{V}_h(t)] + \mathbb{D}_h \phi_r 2 \dfrac{t^{1-\alpha}}{\Gamma(2-\alpha)} \mathcal{L}_t^{\alpha}[\mathbf{V}_h(t)] = \mathbb{G}_1, \\ \mathbb{A}_h \mathcal{R}_t^{\beta}[\mathbf{\Theta}_h(t)] + \dfrac{1}{Pr} \mathbb{B}_h[\mathbf{\Theta}_h(t)] + \mathbb{A}_h \mathcal{L}_t[\mathbf{\Theta}_h(t)] = \mathbb{G}_2, \\ \mathbf{v}_h^0 = \mathbf{0}, \quad \theta_h^0 = \mathbf{0}, \end{cases} \tag{5.60}$$

For the simulation, we have developed code in MATLAB solve the system given in (5.60). Furthermore a simulation of the system has been obtain for $\mathbf{V}_h$ and $\mathbf{\Theta}_h$. Numerical solutions and discussion for velocity profile u and temperature profile T presented in section 5.4.

5.4 Numerical results and discussion

Numerical solution of time dependent velocity and temperature are obtained by using finite element method and explicit finite difference method at final time $t = 1$ and at time $t = 2$. In this article we discusses the numerical computations of physical and fractional parameters such as Forchheimer parameter ϕ_r, porous coefficient ϕ, Grashof number Gr, Prandtl number Pr, Maxwell parameters λ_1, λ_2 and fractional parameters α and β on velocity and temperature profiles. Physical parameters average skin friction coefficient and average Nusselt number also discussed in details.

5.4.1 The influence of fractional parameters

Figure 5.1(a) shows fractional parameter α effects on velocity profile. Velocity gradient increases and also thickness of the momentum boundary layer increases when we increase α values. For $\alpha = 1$ velocity boundary layer has a maximum peak. It means fractional parameter controls momentum boundary layer. Similar effects of β parameter observed on velocity profile in figure 5.1(b). Fractional parameter β effects on temperature given in figure 5.2(a). Smooth profile of temperature gradient decreases with rise of temperature

distribution and thickness of the thermal boundary layer rises when increase β values. It observe that β play an important rule in thermal boundary layer.

5.4.2 The influence of physical parameters

Physical parameters effects on dimensionless velocity and temperature profiles are discussed from figure 5.2(b)-6.5(b). Figure 5.2(b) illustrates the effects of Ptandtl number Pr on temperature. Thermal boundary layer thickness weakens with the augment of Prandtl number Pr. This means that with the rise of Pr number, we get decrease in the heat transfer and as a result we have low thermal conductivity. Grashof number Gr is the ratio between bouncy force and viscous force in fluid is shown in figure 5.3(a). Velocity boundary layer increases with the rise of Gr that means bouncy forces drive the natural convection and hot fluid goes up and cold goes down. Figure 5.4(a) describes porous parameter ϕ effects on velocity profile. Velocity boundary layer decreases monotonically when increase porous parameter ϕ. Figure 5.4(b) shows influence of Forchheimer medium parameter ϕ_r on velocity profile. As in figure, velocity gradient decreases when increase ϕ_r. It means velocity boundary layer decreases through out region when rise up ϕ_r. Maxwell parameters λ_1 and λ_2 effects on velocity and temperature shown in figures 5.5(a) and 6.5(b). Velocity gradient decreases while increasing λ_1 values. It means momentum boundary layer decreases with the increase of relaxation time. Temperature gradient increases monotonically when rise λ_2. It means increase in relaxation time enhance thermal boundary layer. Figure 5.3(b) shows variation of velocity profile on different time.

5.4.3 Skin friction coefficient

Skin friction coefficient C_f is a friction factor in duct or pipe flows, non dimensional parameter defined as the ratio of the total wall shear stress to a characteristic large kinetic energy of the fluid. In Table 5.1, average skin friction coefficient effects due to different parameter shown. As shown in table, average skin friction coefficient decreases when we increase fractional parameter α and gets smaller value at $\alpha = 1$. It means fractional parameter control average skin friction coefficient and can maximize to take

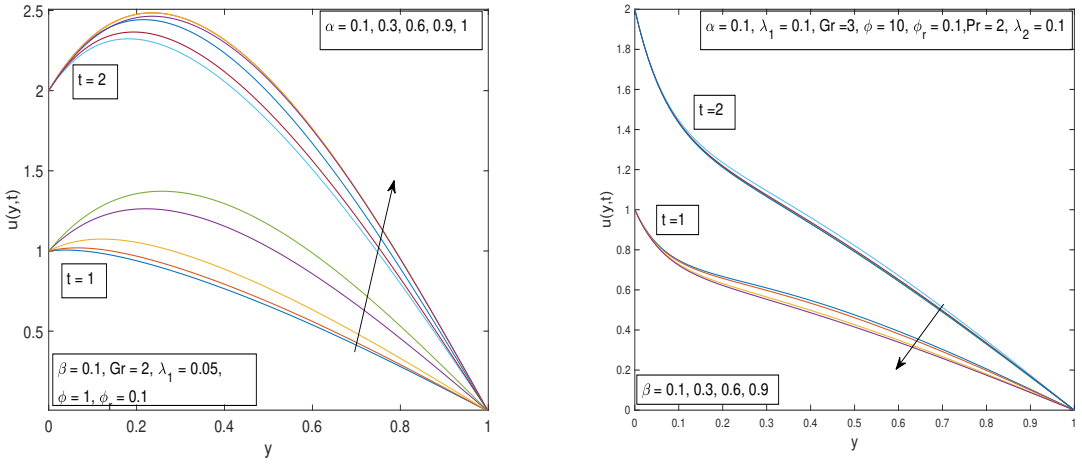

(a) Velocity variation of α.

(b) Velocity variation of β.

Figure 5.1

α values near to zero. Reynolds number has a smaller effects on average skin friction coefficient and λ_1 also decrease average skin friction coefficient when increase λ_1.

5.4.4 Nusselt number

Nusselt number is dimensionless number and is the proportion between heat transferred through convection (fluid motion) and the heat transferred through conduction (if the fluid was static). Nusselt number tell us about how much the heat transfer is enhanced because of fluid motion. It is worth to note that the fluid motion always results in increase in heat transfer rate and for convection case, Nu is always greater than 1. Average Nusselt number effects shown in Table 5.2. Fractional parameter β increase $\bar{Nu}$ when we increase β values and have a maximum $\bar{Nu}$ at $\beta = 1$. It means we can minimize and maximize average Nusselt number by using fractional parameter. Prandtl number also has similar effect and λ_2 has small increment in average Nusselt number.

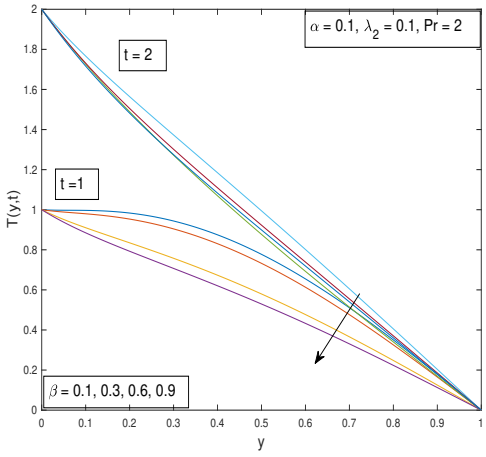

(a) Temperature variation of β.

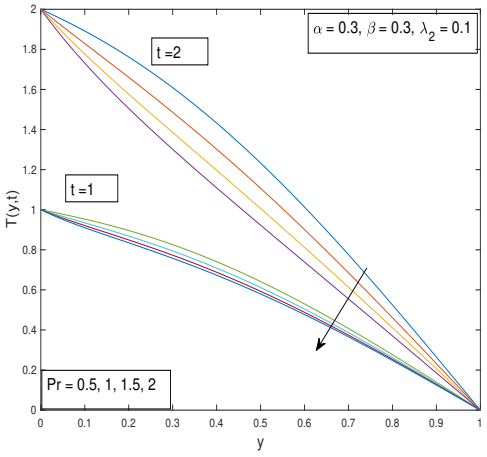

(b) Temperature variation of Prandtl number Pr.

Figure 5.2

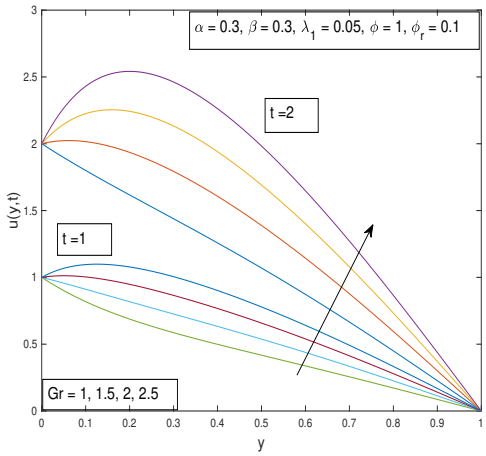

(a) Velocity variation of Grashof number Gr.

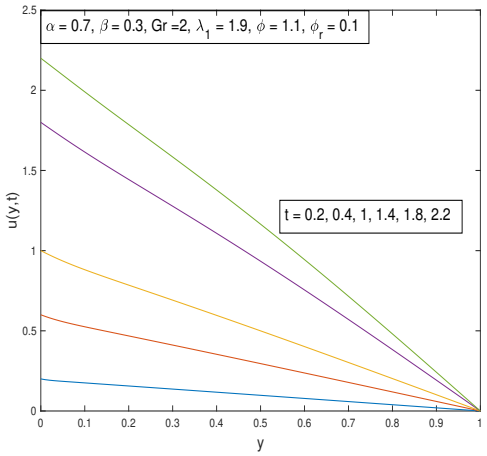

(b) Velocity variation of Re.

Figure 5.3

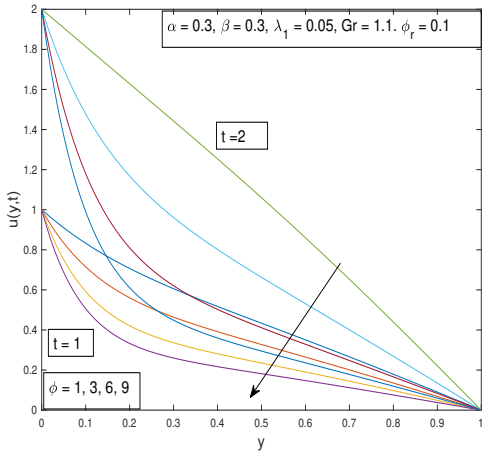

(a) Velocity variation due of ϕ.

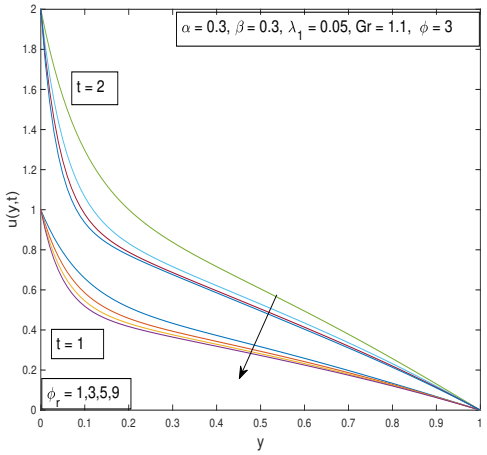

(b) Velocity variation of ϕ_r.

Figure 5.4

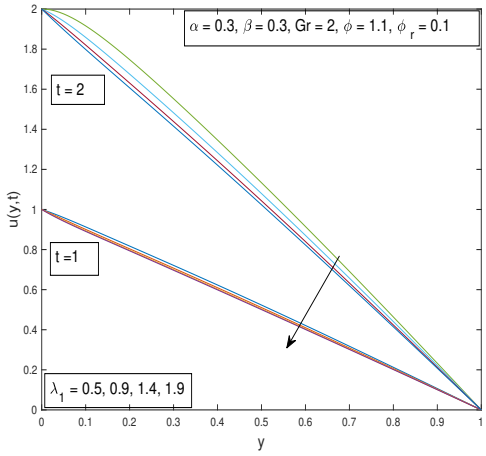

(a) Velocity variation of λ_1.

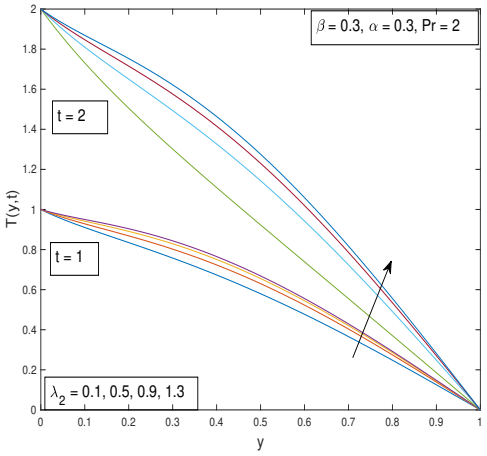

(b) Temperature variation of λ_2

Figure 5.5

5.5 Conclusion

This article studies one dimensional, unsteady boundary layer fractional Maxwell flow with heat transfer in a channel. Fluid is assumed to be incompressible and move with the

Table 5.1: Average skin friction for final time $t = 1$.

α	λ_1	Re	$\bar{C}f$
0.1	0.2	0.01	- 2.6561
0.3	0.2	0.01	- 3.0316
0.6	0.2	0.01	- 3.4775
1	0.2	0.01	- 3.8103
0.4	**0.2**	0.01	-3.7625
0.4	**0.4**	0.01	-3.9934
0.4	**0.6**	0.01	-4.1116
0.4	**0.8**	0.01	-4.1881
0.4	0.2	**0.01**	-3.1916
0.4	0.2	**0.03**	-3.2337
0.4	0.2	**0.06**	-3.2898
0.4	0.2	**0.09**	-3.3464

motion of lower plate through Darcy law of Forchheimer coefficient. Fractional derivative is employed in the constitutive equation of Maxwell model as well as to the conservation of energy equation. The governing equations of fractional Maxwell fluid and fractional heat equation are non linear. To solve these equations, we used finite element method and finite difference method to solve coupled non linear equations. Finite element discretization is used to discretize space variable (y in this problem) and finite difference scheme is used to discretize time variable t. A MATLAB code is developed for the simulation of governing equations. Fractional parameters α and β effects on velocity, temperature, average skin friction and average Nusselt number are discussed in details. Investigated heat transfer analysis with the temperature dependent thermal conductivity properties. Results show that fractional parameter α increase boundary layer thickness of the velocity and fractional parameter β decrease thermal boundary layer and weakens heat conduction. Forchheimer coefficient ϕ_r decrease the momentum boundary layer which weakens velocity profile. Average skin friction and average Nusselt number arises with the rise of fractional

Table 5.2: Average Nusselt number for final time $t = 1$.

β	λ_2	P_r	$\bar{Nu}$
0.1	1.3	0.01	0.003447
0.3	1.3	0.01	0.007057
0.6	1.3	0.01	0.073158
1	1.3	0.01	6.055115
0.3	**1.3**	0.01	0.006807
0.3	**1.5**	0.01	0.007074
0.3	**1.7**	0.01	0.007326
0.3	**2.0**	0.01	0.007681
0.3	1.3	**0.01**	0.006807
0.3	1.3	**0.03**	0.014376
0.3	1.3	**0.06**	0.023271
0.3	1.3	**0.09**	0.030406

parameter.

Chapter 6

Effects of Exponential Variable Viscosity on Heat Transfer Flow of MHD Fractional Maxwell Fluid.

This research article presents the unsteady natural convection of Maxwell viscoelastic fluid based on boundary layer heat transfer. The stretching sheet on lower wall of fluid with exponential time dependent viscosity is implemented. The fractional derivative based governing equations of Maxwell fluid model are derived. These governing equations are used to derive nonlinear coupled partial differential equations (PDEs) which involves space and time derivatives. By employing the Finite Difference Method with $L1$-algorithm, to solve system of nonlinear coupled PDEs and presented via graphically. The effects of fractional and physical parameters on velocity, temperature and particular fractional parameters effect on average skin friction coefficient $\bar{Cf}$ and average Nusselt number $\bar{Nu}$ are discussed in details. For instance, the thickness of velocity boundary layer increases in response to increase in fractional parameter α, whereas heat conduction reduces in response to increase in fractional parameter γ.

6.1 Mathematical formulation

The viscous two dimensional in-compressible unsteady Maxwell fluid with heat transfer between parallel plates separated by depth h with stretching sheet and in presence of internal heat generation and absorption. The upper plate at $y = h$ is constant where as the bottom plate at $y = 0$ moves on its own directions with velocity ax. Axes x and y are along bottom and perpendicular to it respectively. The velocity field is

$$\mathbf{U} = (u(x, y, t), v(x, y, t), 0)$$

6.1.1 Continuity equation

Continuity equation is presented as [69]

$$\frac{\partial \rho}{\partial t} + \nabla.(\rho \mathbf{U}) = 0,$$

fluid is taken as compressible due to small variation of density, there for continuity equation becomes

$$\begin{aligned} \nabla.\mathbf{U} &= 0, \\ \frac{\partial u}{\partial x} + \frac{\partial v}{\partial y} &= 0. \end{aligned} \tag{6.1}$$

Here, we investigate fluid motion along $y - axix$ there for only velocity component u is taken in this paper.

$$\mathbf{U} = (0, u(x, y, t), 0)$$

6.1.2 Momentum equation

Using the boundary layer assumption and Boussinesq approximation, momentum equations is [69]

$$\frac{\partial u}{\partial t} \quad + \quad u\frac{\partial u}{\partial x} + v\frac{\partial u}{\partial y} = \frac{1}{\rho}\frac{\partial \tau_{xy}}{\partial y} + \frac{\beta g}{\rho}(T - T_\infty), \tag{6.2}$$

where β is thermal expression coefficient, g is gravitational acceleration, ν is kinematic viscosity.

Using fractional derivative into constitutive equation of Maxwell model proposed by Friedrich [70].

$$(1+\lambda_1^{\alpha}D_t^{\alpha})\,\tau_{xy}=\mu\frac{\partial u}{\partial y}, \tag{6.3}$$

here λ_1 is the relaxation time, α is fractional parameter and τ_{xy} is shear stress. D_t^{α} is Caputo time fractional operator of order α is defined as: [71]:

$$D_t^{\alpha}g(t):=\frac{1}{\Gamma(m-\alpha)}\int_0^t\frac{g^m(\xi)}{(t-\xi)^{\alpha+1-m}}d\xi,\quad m-1<\Re e\{\alpha\}<m,\quad m\in\mathbb{N}, \tag{6.4}$$

with $\Gamma(\cdot)$ denotes Gamma function given by

$$\Gamma(z):=\int_{\mathbb{R}}\xi^{z-1}e^{-\xi}d\xi,\quad z\in\mathbb{C},\quad \Re\{z\}>0.$$

Applying operator $(1+\lambda^{\alpha}D_t^{\alpha})$ on Eq. 6.2 and also using Eq. 6.3, we get

$$\begin{aligned}\frac{\partial u}{\partial t}+u\frac{\partial u}{\partial x}+v\frac{\partial u}{\partial y}+\lambda_1^{\alpha}\frac{\partial^{\alpha+1}u}{\partial t^{\alpha+1}}+\lambda_1^{\alpha}\frac{\partial^{\alpha}}{\partial t^{\alpha}}\left(u\frac{\partial u}{\partial x}\right)+\lambda_1^{\alpha}\frac{\partial^{\alpha}}{\partial t^{\alpha}}\left(v\frac{\partial u}{\partial y}\right)\\ =\frac{1}{\rho}\frac{\partial}{\partial y}\left(\mu\frac{\partial u}{\partial y}\right)+\frac{\beta g}{\rho}(T-T_{\infty})+\frac{\beta g}{\rho}\lambda_1^{\alpha}\frac{\partial^{\alpha}}{\partial t^{\alpha}}(T-T_{\infty})\end{aligned} \tag{6.5}$$

Fluid viscosity is taken as exponential function of temperature [72]:

$$\mu=\mu_n\exp(-\gamma(T-T_{\infty})), \tag{6.6}$$

here μ_n is reference fluid velocity and γ is constant.

Using μ (as defined in 6.6) into equation 6.5

$$\begin{aligned}\frac{\partial u}{\partial t}+u\frac{\partial u}{\partial x}+v\frac{\partial u}{\partial y}+\lambda_1^{\alpha}\frac{\partial^{\alpha+1}u}{\partial t^{\alpha+1}}+\lambda_1^{\alpha}\frac{\partial^{\alpha}}{\partial t^{\alpha}}\left(u\frac{\partial u}{\partial x}\right)+\lambda_1^{\alpha}\frac{\partial^{\alpha}}{\partial t^{\alpha}}\left(v\frac{\partial u}{\partial y}\right)=\\ \frac{1}{\rho}\frac{\partial}{\partial y}\left(\mu_n\exp(-\gamma(T-T_{\infty}))\frac{\partial u}{\partial y}\right)+\frac{\beta g}{\rho}(T-T_{\infty})+\frac{\beta g}{\rho}\lambda_1^{\alpha}\frac{\partial^{\alpha}}{\partial t^{\alpha}}(T-T_{\infty}),\end{aligned} \tag{6.7}$$

6.1.3 Conservation of energy

Energy equation for temperature is [73], [74]

$$\frac{\partial T}{\partial t}+u\frac{\partial T}{\partial x}+v\frac{\partial T}{\partial y}=-\frac{1}{\rho c_p}\nabla q+\frac{Q_0}{\rho c_p}(T-T_{\infty}),$$

where q is heat flux, ρ is the density, Q_0 is heat generation $Q_0 > 0$ or absorption $Q_0 < 0$ coefficient and c_p is the specific heat capacity. Since heat flux is supposed to move vertical direction. There for the above equation can be modified as

$$\frac{\partial T}{\partial t} + u\frac{\partial T}{\partial x} + v\frac{\partial T}{\partial y} = -\frac{1}{\rho c_p}\frac{\partial q}{\partial y} + \frac{Q_0}{\rho c_p}(T - T_\infty). \tag{6.8}$$

The fractional Cattaneo model of generalized Fourier's law is employed [75].

$$(1 + \lambda_2^\gamma D_t^\gamma)\, q = -k\frac{\partial T}{\partial y} \tag{6.9}$$

Applying operator $(1 + \lambda_2^\gamma D_t^\gamma)$ on both side of Eq. 6.8 and using Eq. 6.9, we get

$$\begin{aligned}\frac{\partial T}{\partial t} + u\frac{\partial T}{\partial x} + v\frac{\partial T}{\partial y} + \lambda_2^\gamma\frac{\partial^{\gamma+1} T}{\partial t^{\gamma+1}} + \lambda_2^\gamma\frac{\partial^\gamma}{\partial t^\gamma}\left(u\frac{\partial T}{\partial x}\right) + \lambda_2^\gamma\frac{\partial^\gamma}{\partial t^\gamma}\left(v\frac{\partial T}{\partial y}\right) \\ = \frac{1}{\rho c_p}\frac{\partial}{\partial t}\left(k\frac{\partial T}{\partial y}\right) + \frac{Q_0}{\rho c_p}\left(1 + \lambda_2^\gamma\frac{\partial^\gamma}{\partial t^\gamma}\right)(T - T_\infty).\end{aligned} \tag{6.10}$$

Combining continuity, momentum and energy equations

$$\frac{\partial u}{\partial x} + \frac{\partial v}{\partial y} = 0, \tag{6.11}$$

$$\begin{aligned}\frac{\partial u}{\partial t} + u\frac{\partial u}{\partial x} + v\frac{\partial u}{\partial y} + \lambda_1^\alpha\frac{\partial^{\alpha+1} u}{\partial t^{\alpha+1}} + \lambda_1^\alpha\frac{\partial^\alpha}{\partial t^\alpha}\left(u\frac{\partial u}{\partial x}\right) + \lambda_1^\alpha\frac{\partial^\alpha}{\partial t^\alpha}\left(v\frac{\partial u}{\partial y}\right) \\ = -\frac{\mu_n\gamma}{\rho}\exp(-\gamma(T - T_\infty))\frac{\partial T}{\partial y}\frac{\partial u}{\partial y} + \frac{\mu_n}{\rho}\exp(-\gamma(T - T_\infty))\frac{\partial^2 u}{\partial y^2} + \frac{\beta g}{\rho}(T - T_\infty) \\ + \frac{\beta g}{\rho}\lambda_1^\alpha\frac{\partial^\alpha}{\partial t^\alpha}(T - T_\infty),\end{aligned} \tag{6.12}$$

$$\begin{aligned}\frac{\partial T}{\partial t} + u\frac{\partial T}{\partial x} + v\frac{\partial T}{\partial y} + \lambda_2^\gamma\frac{\partial^{\gamma+1} T}{\partial t^{\gamma+1}} + \lambda_2^\gamma\frac{\partial^\gamma}{\partial t^\gamma}\left(u\frac{\partial T}{\partial x}\right) + \lambda_2^\gamma\frac{\partial^\gamma}{\partial t^\gamma}\left(v\frac{\partial T}{\partial y}\right) = \\ \frac{k}{\rho c_p}\frac{\partial^2 T}{\partial y^2} + \frac{Q_0}{\rho c_p}\left(1 + \lambda_2^\gamma\frac{\partial^\gamma}{\partial t^\gamma}\right)(T - T_\infty),\end{aligned} \tag{6.13}$$

here λ_1, λ_2 are Maxwell fluid parameters, α and γ are fractional derivative parameters. Boundary conditions are:

$$y = 0: \quad u = ax, \quad v = 0, \quad T = T_w, \tag{6.14}$$

$$y = \infty; \quad u = 0, \quad v = 0, \quad T = T_\infty \tag{6.15}$$

Where a is stretching rate, T_w is upper and T_∞ is lower wall temperature.

6.1.4 Non-Dimensionalization

In numerical calculation, non-dimensional parameters generally used to analyze effects of different parameters on the solution. In non-dimensionalization, each term in differential equation are divided by known parameter so we may get non-dimensional groups.
We introduce length unit h and velocity unit U_0 that are small quantity. Then non-dimensional form of the Eqs. (6.11)- (6.13) are given as: (removing $*$)

$$t^* = \frac{tU_0}{h}, \quad y^* = \frac{y}{h}, \quad x^* = \frac{x}{h}, \quad u^* = \frac{u}{U_0}, \quad v^* = \frac{v}{U_0}, \quad \lambda_1^* = \lambda_1(\frac{U_0}{h}),$$
$$\lambda_2^* = \lambda_2(\frac{U_0}{h}), \quad T^* = \frac{T - T_\infty}{T_w - T_\infty}, \quad \nu^* = \frac{\mu_n h U_0}{\rho} \tag{6.16}$$

$$\frac{\partial u}{\partial x} + \frac{\partial v}{\partial y} = 0, \tag{6.17}$$

$$\frac{\partial u}{\partial t} + u\frac{\partial u}{\partial x} + v\frac{\partial u}{\partial y} + \lambda_1^\alpha \frac{\partial^{\alpha+1} u}{\partial t^{\alpha+1}} + \lambda_1^\alpha \frac{\partial^\alpha}{\partial t^\alpha}\left(u\frac{\partial u}{\partial x}\right) + \lambda_1^\alpha \frac{\partial^\alpha}{\partial t^\alpha}\left(v\frac{\partial u}{\partial y}\right) = \tag{6.18}$$
$$-\frac{\gamma}{Re}\exp(-VrT)\frac{\partial T}{\partial y}\frac{\partial u}{\partial y} + \frac{1}{Re}\exp(-VrT)\frac{\partial^2 u}{\partial y^2} + GrT + Gr\lambda_1^\alpha \frac{\partial^\alpha}{\partial t^\alpha} T,$$

$$\frac{\partial T}{\partial t} + u\frac{\partial T}{\partial x} + v\frac{\partial T}{\partial y} + \lambda_2^\gamma \frac{\partial^{\gamma+1} T}{\partial t^{\gamma+1}} + \lambda_2^\gamma \frac{\partial^\gamma}{\partial t^\gamma}\left(u\frac{\partial T}{\partial x}\right) + \lambda_2^\gamma \frac{\partial^\gamma}{\partial t^\gamma}\left(v\frac{\partial T}{\partial y}\right) = \tag{6.19}$$
$$\frac{1}{Pr}\frac{\partial^2 T}{\partial y^2} + Q\left(1 + \lambda_2^\gamma \frac{\partial^\gamma}{\partial t^\gamma}\right) T,$$

where $Pr = \frac{\mu_n C_p u_0 h}{k_n}$ is Prandtl number, $Re = \frac{hU_0}{\nu}$ is Reynolds number, $Gr = \frac{\beta g(T_w - T_\infty)}{\rho}$ is Grashof number, $Q = \frac{hQ_0}{\rho c_p U_0}$ is heat generation or absorption coefficient and $Vr = \gamma(T_w - T_\infty)$
With boundary conditions:

$$\begin{cases} y = 0: & u = ax, \quad v = 0, \quad T = 0, \\ y = \infty, & u = 0, \quad v = 0, \quad T = 1. \end{cases} \tag{6.20}$$

6.2 Numerical technique

This section is concern with numerical solution of fractional diffusion equations. For the solution of these equations, we used already developed finite difference method along with L1-algorithm to solve non linear equations 6.17-6.19 mixed with space and time

derivatives. The L1 scheme used to solve Caputo fractional derivative and is one of the most useful and successful method for discretizing one dimensional space-time derivative, introduced by Liu et al [76].

6.2.1 Discretization method

Let's define $t_k = k\delta t$, $k = 0, 1, 2, 3, ..., R$; is time step size, $x_i = i\delta x$, $i = 0, 1, 2, 3, ..., M$; $y_j = j\delta y$, $j = 0, 1, 2, 3, ..., N$, where $dx = \delta x = \frac{L}{M}$ and $dy = \delta y = \frac{h}{N}$ are space step size. Let u_{ij}^k and T_{ij}^k be numerical solutions of our problem and let $\delta u(t_k)$ be:

$$\delta u(t_k) = u(t_{k+1}) - u(t_k) \tag{6.21}$$

L1-discretization of Caputo time fractional derivative as defined in [76]:

$$\partial_t^\alpha u(t_k) := \frac{1}{\Gamma(2-\alpha)} \sum_{s=0}^{k} \int_{t_f}^{t_{f+1}} (t_{k+1} - \xi)^{1-\alpha-1} \frac{\partial u(\xi)}{\partial \xi} d\xi, \quad 0 < \Re e\{\alpha\} < 1, \tag{6.22}$$

$$= \frac{\delta t^{-\alpha}}{\Gamma(2-\alpha)} \left[u(t_k) - b_k u(t_0) - \sum_{s=1}^{k-1} (b_{s-1} - b_s) u(t_{k-s}) \right] + O(\delta t^{2-\alpha}), \tag{6.23}$$

Where $b_s = (s+1)^{1-\alpha} - (s)^{1-\alpha}$, $s = 0, 1, 2, ..., r$.

From [77] we have the following relation:

$$\frac{\partial^{\alpha+1} u(t_k)}{\partial t^{\alpha+1}} = \frac{\partial^\alpha}{\partial t^\alpha} \frac{du(t_k)}{dt} \tag{6.24}$$

Where

$$\frac{du(t_k)}{dt} = \frac{u(t_k) - u(t_{k-1})}{\delta t}$$

is backward difference.

Non fractional terms apperes in the problem discretized as in [78]:

$$\left.\frac{\partial u}{\partial t}\right|_{t=t_k} = \frac{u(x_i, y_j, t_k) - u(x_i, y_j, t_{k-1})}{\delta t} + O(\delta t), \tag{6.25}$$

$$u \left.\frac{\partial u}{\partial x}\right|_{t=t_k} = u(x_i, y_j, t_{k-1}) \frac{u(x_i, y_j, t_k) - u(x_{i-1}, y_j, t_k)}{\delta x} + O(\delta x), \tag{6.26}$$

$$v \left.\frac{\partial u}{\partial y}\right|_{t=t_k} = v(x_i, y_j, t_{k-1}) \frac{u(x_i, y_j, t_k) - u(x_i, y_{j-1}, t_k)}{\delta y} + O(\delta y), \tag{6.27}$$

$$\frac{\partial^2 u(t_k)}{\partial y^2} = \frac{u_{i,j+1}^k - 2u_{i,j}^k + u_{i,j-1}^k + u_{i,j+1}^{k-1} - 2u_{i,j}^{k-1} + u_{i,j-1}^{k-1}}{2\delta y} + O(\delta y^2) \tag{6.28}$$

Eqs from (6.24) to (6.27) are used to find the fractional derivatives as follows:

$$\frac{\partial^{\alpha+1}u(t_k)}{\partial t^{\alpha+1}} = \frac{\delta t^{-1-\alpha}}{\Gamma(2-\alpha)}\left[u_{ij}^{k} - u_{ij}^{k-1} - \sum_{s=1}^{k-1}(B_s)(u_{ij}^{k-s} - u_{ij}^{k-s-1})\right], \tag{6.29}$$

$$\frac{\partial^{\alpha}}{\partial t^{\alpha}}\left(u(t_k)\frac{\partial u(t_k)}{\partial x}\right) = \frac{\delta t^{-\alpha}}{\delta x\Gamma(2-\alpha)}\left[u_{ij}^{k-1}\left(u_{ij}^{k} - u_{i-1j}^{k}\right) - \sum_{s=1}^{k-1}(B_s)u_{ij}^{k-s-1}\left(u_{ij}^{k-s} - u_{i-1j}^{k-s}\right)\right]$$
$$+O(\delta t^{2-\alpha} + \delta x), \tag{6.30}$$

$$\frac{\partial^{\alpha}}{\partial t^{\alpha}}\left(v(t_k)\frac{\partial u(t_k)}{\partial y}\right) = \frac{\delta t^{-\alpha}}{\delta y\Gamma(2-\alpha)}\left[v_{ij}^{k-1}\left(u_{ij+1}^{k} - u_{ij}^{k}\right) - \sum_{s=1}^{k-1}(B_s)v_{ij}^{k-s-1}\left(u_{ij+1}^{k-s} - u_{ij}^{k-s}\right)\right]$$
$$+O(\delta t^{2-\alpha} + \delta y) \tag{6.31}$$

Assume that

$$B_s = (b_{s-1} - b_s), \quad r1 = \lambda_1^{\alpha}\frac{\delta t^{-\alpha}}{\Gamma(2-\alpha)}, \quad r2 = \frac{1}{2\delta y^2}, \quad r3 = \lambda_2^{\gamma}\frac{\delta t^{-\gamma}}{\Gamma(2-\gamma)}$$

$$A_1 = \sum_{s=1}^{k-1}(b_{s-1} - b_s)(u_{ij}^{k-s} - u_{ij}^{k-s-1}), \tag{6.32}$$

$$A_2 = \sum_{s=1}^{k-1}(b_{s-1} - b_s)u_{ij}^{k-s-1}\left(u_{ij}^{k-s} - u_{i-1j}^{k-s}\right), \tag{6.33}$$

$$A_3 = \sum_{s=1}^{k-1}(b_{s-1} - b_s)v_{ij}^{k-s-1}\left(u_{ij+1}^{k-s} - u_{ij}^{k-s}\right) \tag{6.34}$$

From Eq (6.22) we have:

$$A_4 = T_{ij}^{k} - \sum_{s=1}^{k-1}(b_{s-1} - b_s)T_{ij}^{k-s} \tag{6.35}$$

By using similar dicretization techniques we have the following results for temperature terms as well.

$$D_1 = \sum_{s=1}^{k-1}(c_{s-1} - c_s)(T_{ij}^{k-s} - T_{ij}^{k-s-1}), \tag{6.36}$$

$$D_2 = \sum_{s=1}^{k-1}(c_{s-1} - c_s)u_{ij}^{k-s-1}\left(T_{ji}^{k-s} - T_{i-1j}^{k-s}\right), \tag{6.37}$$

$$D_3 = \sum_{s=1}^{k-1}(c_{s-1} - c_s)v_{ij}^{k-s-1}\left(T_{ij+1}^{k-s} - T_{ij}^{k-s}\right), \tag{6.38}$$

$$D_4 = \sum_{s=1}^{k-1}(c_{s-1} - c_s)T_{ij}^{k-s}, \tag{6.39}$$

Similarly here $c_s = (s+1)^{1-\gamma} - s^{1-\gamma},\ s = 0, 1, 2, ..., r.$

Using all these differences we get Eqs. (6.17), (6.18) and (6.19) in the following form:

$$v_{ij}^k = v_{ij-1}^k + v_{ij-1}^{k-1} - v_{ij}^{k-1} + \frac{2h_y}{h_x}\left(u_{i-1j-1}^{k-1} - u_{ij-1}^{k-1} + u_{i-1j}^{k-1} - u_{ij}^{k-1} + u_{i-1j-1}^{k} - u_{ij-1}^{k} + u_{i-1j}^{k} - u_{ij}^{k}\right) \tag{6.40}$$

$$\begin{cases} u_{ij}^k\left[\frac{1}{dt} + \frac{u_{ij}^{k-1}}{dx} + \frac{v_{ij}^{k-1}}{dy} + \frac{r1}{dt} + \frac{r1u_{ij}^{k-1}}{dx} + \frac{r1v_{ij}^{k-1}}{dy} + \frac{\gamma\exp(-VrT_{ij}^{k-1})}{Re(dy)^2}\left(T_{ij}^{K-1} - T_{ij-1}^{k-1}\right)\right] \\ +u_{ij}^k\left[\frac{2(r2)\exp(-VrT_{ij}^{k-1})}{Re}\right] + u_{ij-1}^k\left[-v_{ij}^{k-1}\frac{1}{dy} - \frac{\gamma}{Redy^2}\exp(-VrT_{ij}^{k-1})(T_{ij}^{k-1} - T_{ij-1}^{k-1})\right] \\ +u_{ij-1}^k\left[-r1\frac{v_{ij}^{k-1}}{dy} - \frac{r2}{Re}\exp(-VrT_{ij}^{k-1})\right] + u_{i-1j}^k\left[-\frac{u_{ij}^{k-1}}{dx} - r1\frac{u_{ij}^{k-1}}{dx}\right] - u_{ij+1}^k\frac{r2}{Re}\exp(-VrT_{ij}^{k-1}) \\ = u_{ij}^{k-1}\left(\frac{1}{dt} + \frac{r1}{dt} - \frac{2r2}{Re}\exp(-VrT_{ij}^{k-1})\right) + \frac{r1A_1}{dt} + \frac{r1A_2}{dx} + \frac{r1A_3}{dy} + Grr1A_4 + GrT_{ij}^{k-1} \\ +\frac{r2}{Re}\exp(-VrT_{ij}^{k-1})\left(u_{ij+1}^{k-1} + u_{ij-1}^{k-1}\right), \end{cases} \tag{6.41}$$

$$\begin{cases} T_{ij}^k\left[\frac{1}{dt} + u_{ij}^{k-1}\frac{1}{dx} + \frac{v_{ij}^{k-1}}{dy} + \frac{r3}{dt} + \frac{r3}{dx}u_{ij}^{k-1} + \frac{r3}{dy}v_{ij}^{k-1} + \frac{2r2}{Pr} - Q - r3Q\right] \\ +T_{i-1j}^k\left[-\frac{u_{ij}^{k-1}}{dx} - \frac{r3u_{ij}^{k-1}}{dx}\right] + T_{ij-1}^k\left[-\frac{v_{ij}^{k-1}}{dy} - \frac{r2}{Pr} - \frac{r3v_{ij}^{k-1}}{dy}\right] - T_{ij+1}^K\frac{r2}{Pr} \\ = T_{ij}^{k-1}\left[\frac{1}{dt} - \frac{2r2}{Pr} + \frac{r3}{dt}\right] + \left(T_{ij+1}^{k-1} - T_{ij-1}^{k-1}\right)\frac{r2}{Pr} + \frac{r3}{dt}D_1 + \frac{r3}{dx}D_2 + \frac{r3}{dy}D_3 - \frac{r3Q}{dt}D4. \end{cases} \tag{6.42}$$

Skin friction coefficient which measure the surface shear stress and Nusselt number that measure heat transfer effect, are defined for integer order derivative [79].

$$C_f = \left.\frac{\mu}{\rho U_0^2}\frac{\partial u}{\partial y}\right|_{y=0}, \tag{6.43}$$

$$Nu = \left.\frac{-kh}{T_w - T_\infty}\frac{\partial T}{\partial y}\right|_{y=0} \tag{6.44}$$

Skin friction coefficient and Nusselt number for fractional Maxwell model with variable viscosity are derived by multiplying equations 6.43 and 6.44 with operators $(1 + \lambda_1^\alpha D_t^\alpha)$ and $(1 + \lambda_2^\gamma D_t^\gamma)$ respectively.

$$C_f + \lambda_1^\alpha\frac{\partial^\alpha}{\partial t^\alpha}C_f = \left.\frac{\mu_n\exp(-\gamma(T - T_\infty))}{\rho U_0^2}(1 + \lambda_1^\alpha D_t^\alpha)\frac{\partial u}{\partial y}\right|_{y=0}, \tag{6.45}$$

$$Nu + \lambda_2^\gamma\frac{\partial^\gamma}{\partial t^\gamma}Nu = \left.\frac{-kh}{T_w - T_\infty}(1 + \lambda_2^\gamma D_t^\gamma)\frac{\partial T}{\partial y}\right|_{y=0} \tag{6.46}$$

The generalized Fourier's law for fractional derivative introduced by Catteno [75].

$$(1+\lambda_1^{\alpha}D_t^{\alpha})\frac{\partial u}{\partial y}\bigg|_{y=0} = \frac{\partial u}{\partial y}\bigg|_{y=0}, \tag{6.47}$$

$$(1+\lambda_2^{\gamma}D_t^{\gamma})\frac{\partial T}{\partial y}\bigg|_{y=0} = -\frac{\partial T}{\partial y}\bigg|_{y=0} \tag{6.48}$$

Using 6.47 and 6.48 with non-dimensional form of equations 6.45 and 6.46 are given as.

$$C_f + \lambda_1^{\alpha}\frac{\partial^{\alpha}}{\partial t^{\alpha}}C_f = \frac{\exp(-\gamma T)}{Re}\frac{\partial u}{\partial y}\bigg|_{y=0}, \tag{6.49}$$

$$Nu + \lambda_2^{\gamma}\frac{\partial^{\gamma}}{\partial t^{\gamma}}Nu = k\frac{\partial T}{\partial y}\bigg|_{y=0} \tag{6.50}$$

Solving 6.49 and 6.50 at every t_k time step, skin friction coefficient and Nusselt number will become:

$$C_f = \frac{1}{1+r1}\left(r1\sum_{s=1}^{k-1}(\alpha_{s-1}-\alpha_s)C_{f(t_{k-s})} + \frac{\exp(-\gamma T)}{Re}\frac{\partial u}{\partial y}\bigg|_{y=0}\right) \tag{6.51}$$

$$Nu = \frac{1}{1+r3}\left(r3\sum_{s=1}^{k-1}(\gamma_{q-1}-\gamma_q)Nu(t_{k-q}) - k\frac{\partial T}{\partial y}\bigg|_{y=0}\right) \tag{6.52}$$

In similar, way average skin friction coefficient and average Nusselt number are:

$$\bar{C_f} = \frac{1}{1+r1}\left(r1\sum_{s=1}^{k-1}(\alpha_{s-1}-\alpha_s)\bar{C}_{f(t_{k-s})} + \frac{1}{Re}\int_0^1 \exp(-\gamma T)\frac{\partial u}{\partial y}\bigg|_{y=0}dx\right) \tag{6.53}$$

$$\bar{Nu} = \frac{1}{1+r3}\left(r3\sum_{s=1}^{k-1}(\gamma_{q-1}-\gamma_q)\bar{Nu}(t_{k-q}) - k\int_0^1 \frac{\partial T}{\partial y}\bigg|_{y=0}dx\right) \tag{6.54}$$

6.3 Results and discussion

This section explains the numerical solution for velocity $u(x,y,t)$, temperature $T(x,y,t)$, average skin friction coefficient $\bar{C}f$ and average Nusselt number $\bar{N}u$ by using Finite Difference Method combined with L1-algorithm. Also, the effects of other physical and fractional parameters analyzed in the form of numerical simulations.

6.3.1 Effects on velocity

The effects of fractional parameter α is shown in Fig. 6.1(a). It is notice that a small increment in α, gives the maximum peak in velocity profile, and velocity profile for different

α do not interest each other. This shows that the thickness of boundary layer rises when the fractional parameter α increases from 0 to 1 and decreases at 1. It means integer order Maxwell fluid boundary layer velocity has minimum thickness. This result demonstrate that fractional derivatives strengthen the effects of natural convection in viscoelastic flow. Variable viscosity parameter effects shown in figure 6.2(a), where we noticed that decreasing variable viscosity parameter Vr, gives increase in momentum boundary layer, it is because of viscosity that is inverse proportional of temperature. Physically, it is because of smaller Vr that implies temperature difference between surface and ambient fluid.

Fig. 6.2(b), shows velocity variation for different relaxation time parameter λ_1. Velocity of the fluid increases with small increment in relaxation time parameter λ_1. It means thickness of the momentum boundary layer increases through out domain. The effects of linear stretching sheet parameter a on velocity profile is shown in Fig. 6.4(b). Here, the positive increment in stretching parameter a increase the velocity profile and as a result thickness of boundary layer is increased. As shown in figure, graphs of velocity profile going towards concave up when increasing values of a. This means stretching sheet exponentially increase velocity boundary layer. Fig. 6.5(a) explains the Grashof number Gr effects on velocity. It is observed that Gr also increase velocity boundary layer through out region when rises Gr. Reynolds number Re effects shown in figure **??**. From figure, velocity increases quickly for small increment in Reynolds number parameter Re. Increasing Re values give concave down graph of velocity, this means velocity increases at start and then decrease slowly at the end.

6.3.2 Effects on temperature

As the natural convection is derived from temperature gradient. This leads us to consider the dimensionless form of temperature. In Fig. 6.1(b) effect of fractional parameter γ on temperature variation is given. The boundary thickness of temperature profile monotonically decreases when increasing γ values. The monotonic decrease in temperature boundary layer is used to establish thickness of thermal boundary layer. This result shows fractional derivative weakens heat conduction effect.

Fig. 6.3(a) shows temperature variation for different values of relaxation time λ_2. Re-

laxation time λ_2 also weaken thermal boundary layer of increasing temperature gradient. Temperature thermal boundary layer decreases with the increase in λ_2 values. Prandtl number effects on temperature profile is given in Fig. 6.3(b). Hear temperature gradient boundary layer goes up with increment in the Prandtl number Pr. Concave up graph of temperature gradient shows thermal boundary layer thickness increase quickly and decrease slowly at the end. Stretching sheet behavior on temperature gradient shown in figure 6.4(a). Increased temperature gradient thermal boundary layer decreases with the increase of stretching sheet parameter a. Heat generation or absorption coefficient Q effects shown in figures 6.7(a) and 6.7(b). The absorption of heat formation coefficient $Q < 0$ increase thermal conductivity rate which increase temperature of the fluid. Increase in temperature also increase fluid velocity and decrease fluid viscosity due to increase in thermal buoyancy force. The generation of heat $Q > 0$ has opposite effects on temperature profile. In heat generation $Q > 0$ decreases thermal boundary layer when increases $Q > 0$. Decrease in thermal boundary layer also decrease buoyancy forces that further decrease fluid velocity.

6.3.3 Effects on average skin friction coefficient

Fig. 6.6(a) illustrates the effect of fractional parameter α on average skin friction coefficient. In figure, increase in fractional parameter α, the average skin friction coefficient $\bar{C}f$ goes down. It is found that average skin friction coefficient decreases when we increase fractional parameter α. The effect of fractional order on average skin friction coefficient is irrelevant to velocity gradient because Fig. 6.1(a) present opposite tendency. As in equation 6.49 skin friction coefficient is a function of velocity gradient.

Effects on average Nusselt number

Figure 6.6(b) shows effect of fractional parameter γ on average Nusselt number. A small increment in fractional parameter γ, the average Nusselt number graph increases monotonically. This shows that increasing fractional parameter also increase heat transfer rate. Here γ showed that average Nusselt number behavior is opposite to the temperature gradient because in figure 6.2(a) temperature variation goes down when increase fractional

γ. As from equation 6.50 we know that Nusselt number is temperature gradient function.

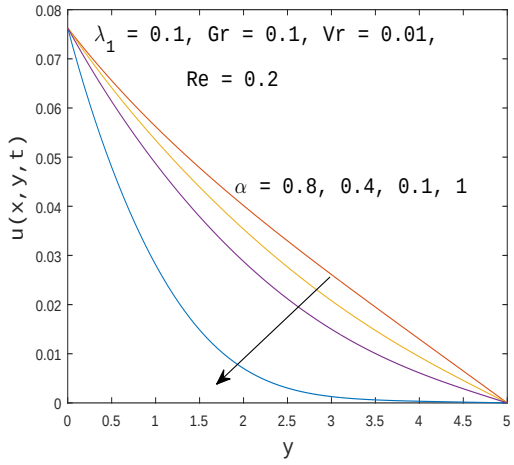

(a) Velocity variation of α

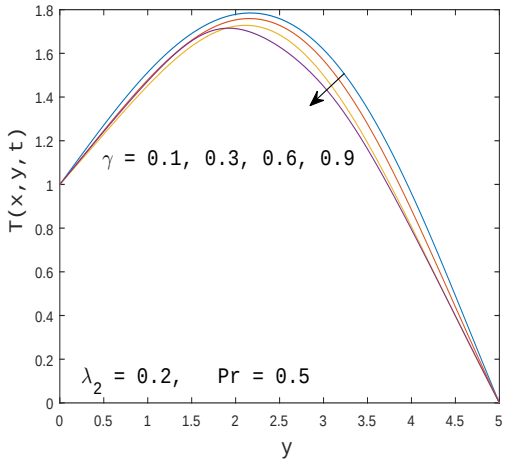

(b) Temperature variation of γ.

Figure 6.1

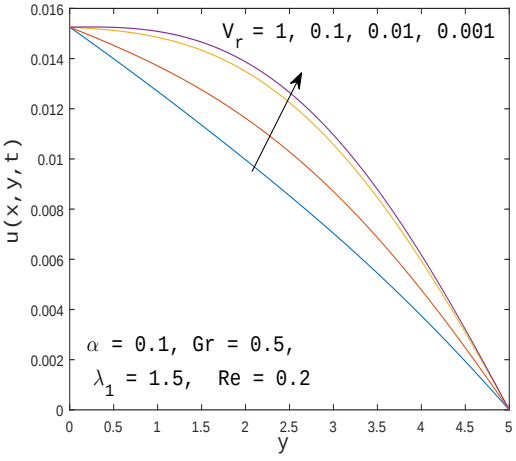

(a) Velocity variation of variable viscosity parameter.

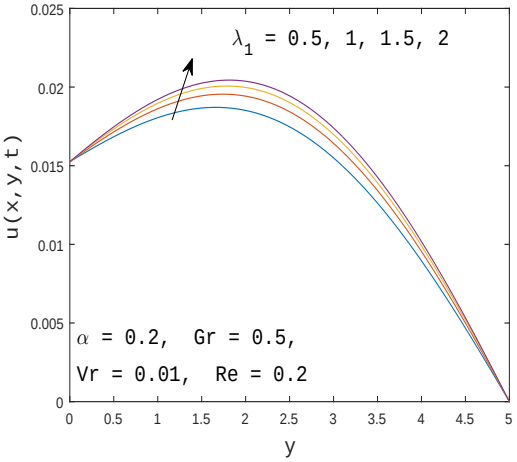

(b) Velocity variation of λ_1.

Figure 6.2

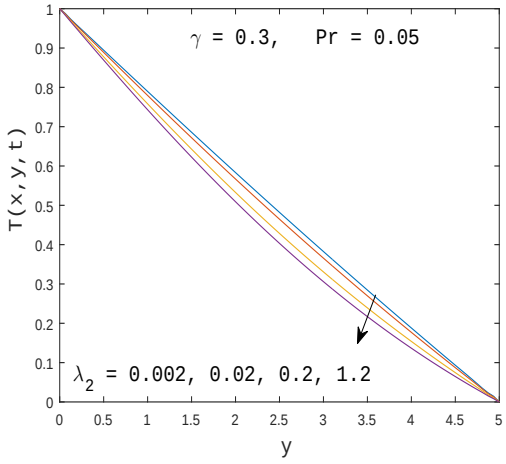

(a) Temperature variation of λ_2.

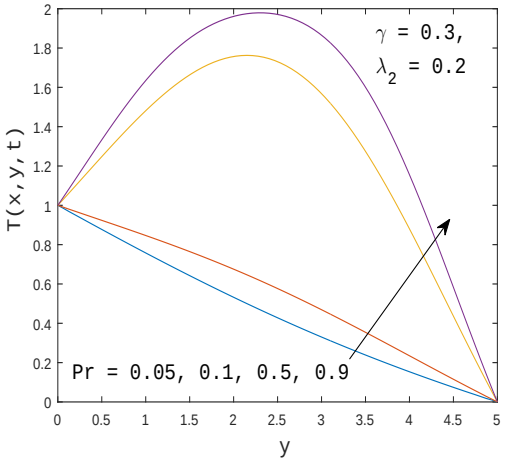

(b) Temperature variation of Pr.

Figure 6.3

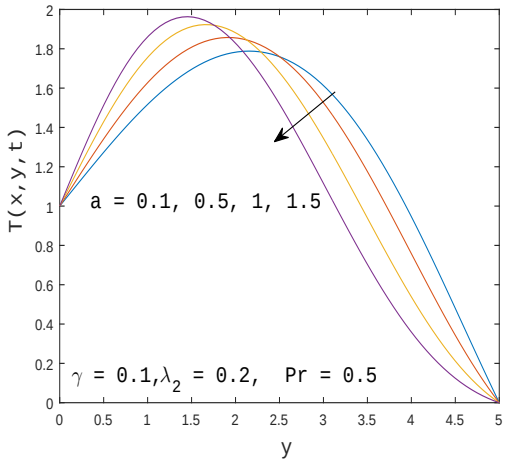

(a) Temperature variation of stretching sheet parameter a.

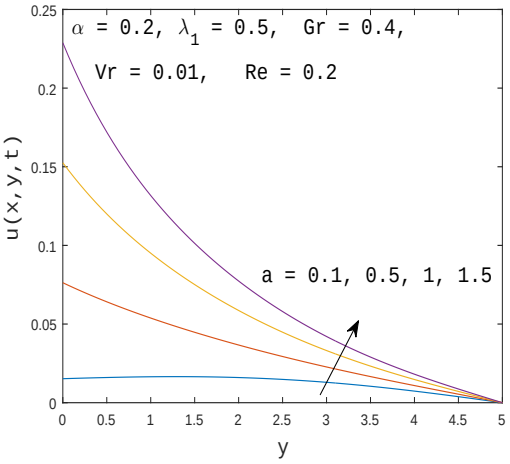

(b) Velocity variation of stretching sheet parameter a.

Figure 6.4

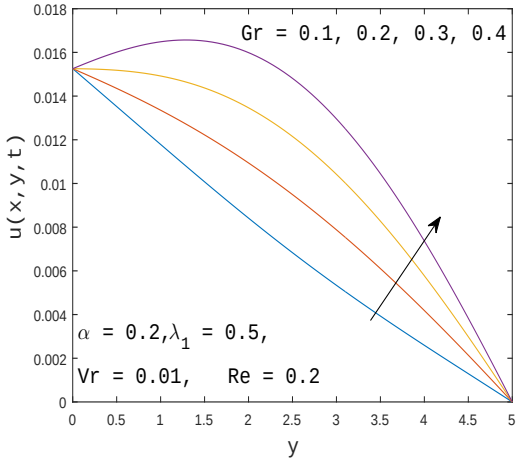

(a) Velocity variation of Gr.

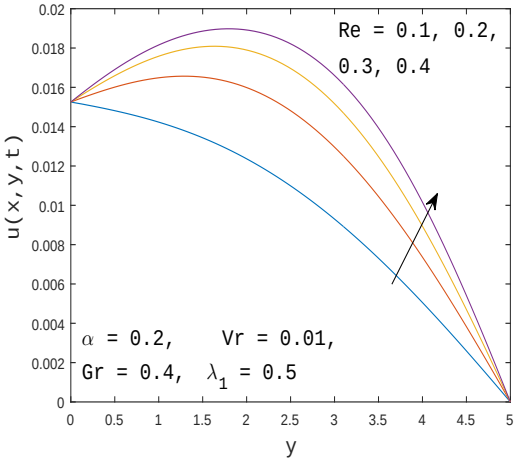

(b) Velocity variation of Re.

Figure 6.5

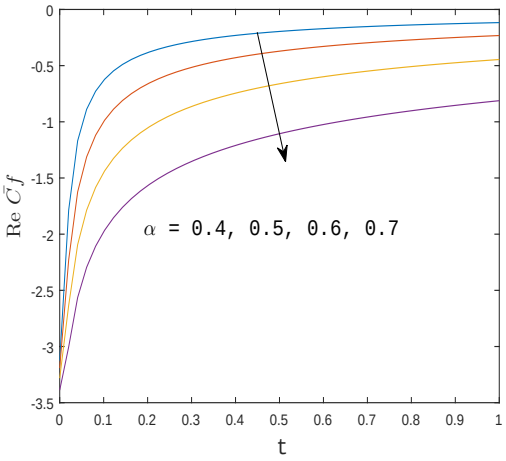

(a) Average skin friction coefficient for different α.

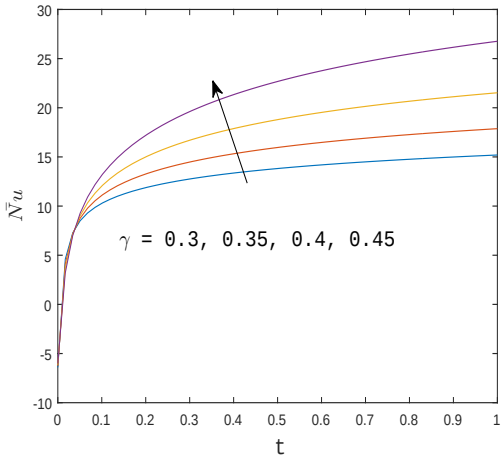

(b) Average Nusselt number for different γ.

Figure 6.6

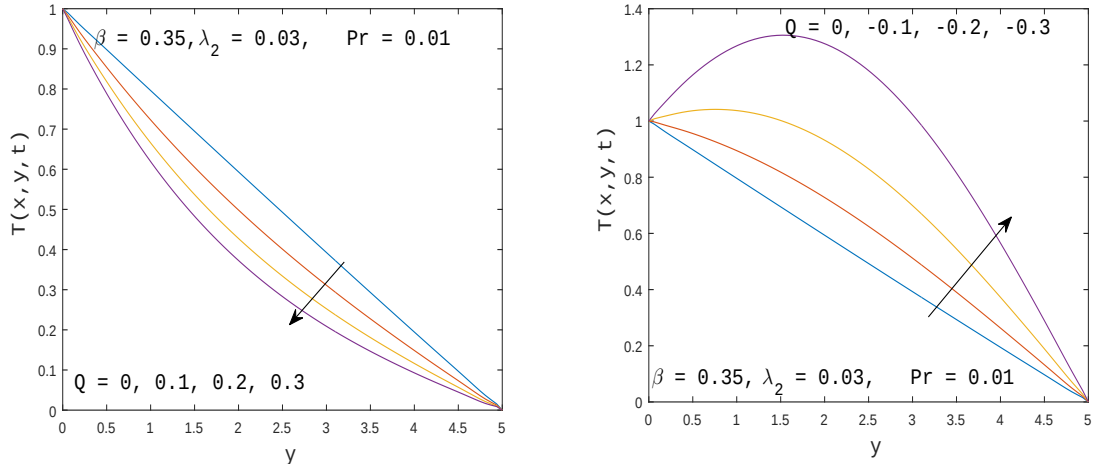

(a) Temperature variation due to heat generation $Q > 0$.

(b) Temperature variation due to heat absorption $Q < 0$.

Figure 6.7

6.4 Conclusion

In this paper we discuss variable viscosity effects on unsteady boundary layer natural convection flow with stretching sheet on lower plate. Fractional Maxwell viscoelastic fluid with heat transfer rate between parallel plates are considered. The fractional derivative introduced in constitutive equation of a Maxwell model. The derived model of fractional boundary layer governing equations are formulated and solved by Finite Difference Method combined with L1-algorithm. Effect of different physical and fractional parameters on velocity, temperature, average skin friction and Nusselt number are discussed graphically. Results indicates that fractional parameter α increase thickness of velocity profile, while γ decrease thermal boundary layer. Stretching sheet parameter a decrease thickness of velocity while increase thermal boundary layer. Temperature dependent exponential viscosity parameter Vr enhance the flow of heat transfer and λ_1 increase velocity boundary layer. A similar effect of Reynolds number Re and Grashof number Gr observed, where velocity boundary layer enhanced with positive increment of Re. Maxwell parameter for relaxation time λ_2 increase temperature that enhance heat conduction of the flow. Increasing Prandtl number Pr leads to increase in temperature profile. Skin

friction coefficient decreases with respect to fractional parameter α and Nusselt number increases with fractional parameter γ.

Chapter 7

Future work

In future, I am planing to develop Immersed Interface Method (IIM) for heat equation with fractional time derivative, to get the approximate solution of the fractional differential equation on uniform Cartesian grids with boundary conditions, we used finite difference scheme for regular grid points (grid points where interface does not lie) and derived jump relation across the interface and modified difference method for irregular grid points by using jump conditions. we consider heat equation with fractional derivative in a bounded domain $\Omega = (0, 1)$ which contains interface $\alpha \in \Omega$.

$$\frac{\partial u(x,t)}{\partial t} = \frac{\partial}{\partial x}\left(\beta \frac{\partial u(x,t)}{\partial x}\right) + \partial_x^{\gamma} u(x,t) + f(x,t), \quad x \in \Omega, t \in [0,1],$$

where $\Omega = [0, 1]$ is domain in which one or more then one discontinuities occurs. For simplicity, we assume that source term $f(x, t)$ is continuities and function β is discontinuities at $\alpha \in \Omega$. Term ∂_x^{γ} represent fractional derivative of $u(x, t)$ with non integer order γ between $0 < \gamma < 1$.

$$\partial_x^{\gamma} u(x,t) = \frac{1}{\Gamma(1-\gamma)} \int_0^x \frac{\partial_s u(s,t)}{(x-s)^{\gamma}} ds, \quad 0 < \gamma < 1,$$

For $\gamma = 1$ then ∂_x^{γ} will reduce to standard derivative.

There are many applications of Interface problems, when there are more than one or two different materials, such as oil and water, or the same material but at different states, such as ice and water, then we have an interface problem. In the modeling of these problems, we get partial or ordinary differential equations. The interface problems are, whose

input data and solutions are non-smooth or discontinuous across some interfaces. The parameters (coefficient of unknown, unknown or some times source term) in the governing differential equations are discontinuous (space or time) across the interface breaking up two states or two materials, and the source terms are often singular to reflect source/sink distributions along codimension interfaces. Because of these irregularities, the solutions to the differential equations are typically no smooth/discontinuous. For the solution of interface problems, it is difficult to find analytic solutions of such problems. There for, to find approximate/numerical solutions of such problems, standard finite difference methods on regular/simple grids will likely give error or lead to loss of accuracy in a neighborhood of interfaces. Beside this, the limitations of possible mesh generation processes for complicated geometries/domains at every or every other time step are also major concerns for moving interface or free boundary problems. Mathematically, interface problems usually lead to differential equations whose input data and solutions are non-smooth or discontinuous across some interfaces. There for, to find the solution of such problems we are using Immersed Interface Method (IIM). The IIM is a sharp interface method based on Cartesian grids. The IIM makes use of the jump conditions across the interface so that the finite difference/element discretization can be accurate . In numerical algorithms for differential equations the concern is the growth of round-off errors and/or initially small fluctuations in initial data which might cause a large deviation of final answers from the exact solution. In numerical analysis, von Neumann stability analysis is a procedure used to check the stability of finite difference schemes as applied to linear partial differential equations. The von Neuman stability analysis is based on the decomposition of numerical errors of numerical approximations into Fourier series. Fourier series decomposes any periodic function or periodic signal into the sum of a (possibly infinite) set of simple oscillating functions, namely sines and cosines (or, equivalently, complex exponentials). Immersed interface methods (IIMs) is numerical second order finite difference method to solve initial-boundary value problems on domains with complex geometries. The immersed interface method determine a solution at every grid point within domain Ω on both sides of the interfaces. Immersed interface method was developed first by LeVeque and Li for elliptic partial differential equations [80]. In this paper, they solved elliptic PDEs for

one and two dimensions with discontinuous coefficients and used jump conditions that are imposed in the finite difference discretization of the partial differential equations. This method was extended to Navier-Stokes equations [81]-[83] and Stokes equations [84]-[85]. In Paper [82], Lai and Li proposed an immersed interface method for the Navier–Stokes equations with singular forces and in paper [81] they derived jump conditions for velocity and for normal derivatives of three dimensional Navier-Stokes Equations, as well as the pressure and its first normal derivative at the moving interface. They solved the Navier-Stokes equations with a second-order accurate projection algorithm and illustrate that the jump conditions were appropriate to achieve full second order accuracy for the velocity and also nearly second order accuracy for the pressure in the maximum norms. Li and Ito [86] provided details on immersed interface method in their book which is used in the simulation of different physical phenomena.

Bibliography

[1] R. I. Tanner, K. Walters, (1998) Rheology: a historical perspective. Elsevier, Amsterdam

[2] J.C. Maxwell, On the dynamical theory of gases, Philosophical Transactions of the Royal Society London A157 (1866) 26-78.

[3] T. Hayat, M. I. Khan, M. Imtiaz, A. Alsaedi, Heat and Mass Transfer Analysis in the Stagnation Region of Maxwell Fluid With Chemical Reaction Over a Stretched Surface, ASME. J. Thermal Sci. Eng. Appl,(2017).

[4] Z. Cao, J. Zhao, Z. Wang, F. Liu, L. Zhen, MHD flow and heat transfer of fractional Maxwell viscoelastic nanofluid over a moving plate, Journal of Molecular Liquids, 222 (2016) 1121–1127.

[5] Y. Liu, B. Guo, Effects of second-order slip on the flow of a fractional Maxwell MHD fluid. Journal of the Association of Arab Universities for Basic and Applied Sciences (2017).

[6] Y. Mashud, N. A. Shah, D. Vieru, Influence of time-fractional derivatives on the boundary layer flow of Maxwell fluids, Chinese Journal of Physics 55 (2017).

[7] M. Madhu, N. Kishan, A. J. Chamkha, Unsteady flow of a Maxwell nanofluid over a stretching surface in the presence of magnetohydrodynamic and thermal radiation effects, Propulsion and Power Research,(2017).

[8] D. Vieru, A. Rauf, Stokes flows of a Maxwell fluid with wall slip condition, Can. J. Physics, 89 (2011) 1061–1071.

[9] K. L. Hsiao, Combined electrical MHD heat transfer thermal extrusion system using Maxwell fluid with radiative and viscous dissipation effects, Applied Thermal Engineering 112 (2017) 1281–1288.

[10] P. A. Davidson, Magnetohydrodynamics in material processing.//Annu. Rev. Fluid Mech.- 1999.-Vol.31.-pp.273-300

[11] P. A. Davidson, An Introduction to Magnetohydrodynamics. – New York: Cambridge university press, 2001. - 431 pp.

[12] V. M. Ivlev, N. N. Baranov, Research and Development in the Field of MHD devices Utilizing Liquid Working Medium for Process Applications.: In Metallurgical Technologies, Energy Conversion, and Mgnetohydrodynamic Flows. (Progress in Astronautics and Aeronautics). Edited by Herman Branover and Yeshajahu Unger.- Washington DC: American Institute of Aeronautics and Astronautics.- 1993.-Vol. 148.- pp.3-23.

[13] Y. R. Fautrelle, Metallurgical Applications of Magnetohydrodynamics.: In Metallurgical Technologies, Energy Conversion, and Mgnetohydrodynamic Flows (Progress in Astronautics and Aeronautics). Edited by Herman Branover and Yeshajahu Unger.- Washington DC: American Institute of Aeronautics and Astronautics.- 1993.-Vol. 148.- pp.3-23.

[14] K. Bhattacharyya, S. Mukhopadhyay, G.C. Layek and I. Pop, Effects of thermal radiation on micropolar fluid flow and heat transfer over a porous shrinking sheet, Int. J. Heat Mass Transfer, 55 (2012), 2945-2952

[15] K. Bhattacharyya, MHD stagnation point flow of Casson fluid and heat transfer over a stretching sheet with thermal radiation, J. Thermodyn. (2013), 169674.

[16] T. Hayat, M. Waqas, S.A. Shehzad and A. Alsaedi, Mixed convection radiative flow of Maxwell fluid near a stagnation point with convective condition, J. Mech., 29 (2013), 403-409

[17] S. U. S. Choi, J. A. Eastman, Enhancing Thermal Conductivity of Fluids with Nanoparticles. Argonne National Lab, IL (United States), 1995.

[18] M.A. Akhavan-Behabadi, Mohamad Shahidi, M.R. Aligoodarz., An experimental study on heat transfer and pressure drop of MWCNT–water nano-fluid inside horizontal coiled wire inserted tube, International Communications in Heat and Mass Transfer 63 (2015) 62–72.

[19] M. Khoshvaght-Aliabadi, M. Tavasoli, F. Hormozi, Comparative analysis on thermal hydraulic performance of curved tubes: Different geometrical parameters and working fluids, Energy 91 (2015) 588-600.

[20] M. Rakhsha, F. Akbaridoust, A. Abbassi, S. A. Majid, Experimental and numerical investigations of turbulent forced convection flow of nano-fluid in helical coiled tubes at constant surface temperature, Powder Technology 283 (2015) 178–189.

[21] H. Bahremand, A. Abbassi, M. Saffar-Avval, Experimental and numerical investigation of turbulent nanofluid flow in helically coiled tubes under constant wall heat flux using Eulerian–Lagrangian approach, Powder Technology 269 (2015) 93–100.

[22] S. Venkatachalapathy, G. Kumaresan, S. Suresh, Performance analysis of cylindrical heat pipe using nanofluids – An experimental study, International Journal of Multiphase Flow 72 (2015) 188–197.

[23] P. Naphon, L. Nakharintr, Turbulent two phase approach model for the nanofluids heat transfer analysis flowing through the minichannel heat sinks, International Journal of Heat and Mass Transfer 82 (2015) 388–39.

[24] K. G. Kumar, B. J. Gireesha, M. R. Krishnamurthy, B. C. Prasannakumara,Impact of Convective Condition on Marangoni Convection Flow and Heat Transfer in Casson Nanofluid with Uniform Heat Source Sink, 2018.

[25] M. Turkyilmazoglu, I. Pop, Heat and mass transfer of unsteady natural convection flow of some nanofluids past a vertical infinite flat plate with radiation effect, International Journal of Heat and Mass Transfer, Volume 59, April 2013, Pages 167-171.

[26] A. J. E. J. Dupuit, Etudes Theoriques et Pratiques sur le Mouvement des Eaux dans les Canaux Decouverts et a Trovers les Terrains Permeables. Victor Dalmont, Paris 1863

[27] P, Forchheimer, Wasserbewegung durch Boden. VDIZ. 45, 1782-1788.

[28] M. A. Seddeek, Influence of viscous dissipation and thermophoresis on Darcy–Forchheimer mixed convection in a fluid saturated porous media, J. Colloid Interface Sci. 293 (2006) 137–142.

[29] M. A. Sadiq, T. Hayat, Darcy–Forchheimer flow of magneto Maxwell liquid bounded by convectively heated sheet, Results Phys. 6 (2016) 884–890.

[30] M. S. Anwar, A. Rasheed, A microscopic study of MHD fractional inertial flow through Forchheimer medium, Chinese Journal of Physics 55 (2017) 1690–1703.

[31] K. B. Oldham, J. Spanier, The Fractional Calculus. London: Academic Press c1974. 225 p.

[32] Y. F. Zakariya, Y.O. Afolabi, R.I. Nurudeen, I.O. Sarumi, Analytical Solutions to Fractional Fluid Flow and Oscillatory Process Models, Fractal Fract, 2018.

[33] Y. Zhang, H. Zhao, F. Liu, Y. Bai, Analytical and numerical solutions of the unsteady 2D flow of MHD fractional Maxwell fluid induced by variable pressure gradient, Computers and Mathematics with Applications, 2018.

[34] N. Cusimano, L. Gerardo-Giorda, A space-fractional Monodomain model for cardiac electrophysiology combining anisotropy and heterogeneity on realistic geometries, Journal of Computational Physics, 2018.

[35] J. M. Cruz-Duarte, J. Rosales-Garcia, C. R. Correa-cely, A. Garcia-Perez, J. G. Avina-Cervantes, A closed form expression for the Gaussian–based Caputo–Fabrizio fractional derivative for signal processing applications, Commun Nonlinear Sci Numer Simulat, 2018.

[36] C. Fetecau, D. Vieru, W.Azhar, Natural Convection Flow of Fractional Nanofluids Over an Isothermal Vertical Plate with Thermal Radiation, Applied Sciences, 2017.

[37] N. A. Shah, D. Vieru, C. Fetecau, Effects of the fractional order and magnetic field on the blood flow in cylindrical domains, Journal of Magnetism and Magnetic Materials, 2016.

[38] I, Podlubny, fractional differential equations, Academic press, New York - London, 1974

[39] J. N. Reddy, An introduction to the Finite Element Method, third edition, MeGraw Hill, 2006.

[40] S. Schneiderbauer, M. Krieger, What do the Navier–Stokes equations mean, 2014 Eur. J. Phys. 35 015020

[41] Z. Li, Z. Qiao, T. Tang, Numerical Solution of Differential Equations, Cambridge University Press, 2017

[42] C. Friedrich, Relaxation and retardation functions of the Maxwell model with fractional derivatives, Rheol. Acta 30 (1991) 151–158

[43] Z. Q. Chen, Time fractional equations and probabilistic representation, Chaos Solitons Fract. 102 (2017), 168–174.

[44] C. Cattaneo. Sur une forme de l'équation de la chaleur éliminant le paradoxe d'une propagation instantanée, Comptes rendus Acad. Sci. Paris Sér. A-B 247, (1958) 431.

[45] T. Hayat, S. Asad, A. Alsaedi, Flow of variable thermal conductivity fluid due to inclined stretching cylinder with viscous dissipation and thermal radiation, Appl Math Mech- Engl Ed., 35, 2014 717–728.

[46] H.F. Oztop, E. Abu-Nada, Numerical study of natural convection in partially heated rectangular enclosures filled with nanofluids, Int. J. Heat Fluid Flow 29 (5) (2008) 1326–1336.

[47] V. E. Lynch et. al., Numerical methods for the solution of partial differential equations of fractional order, Journal of Computational Physics, 192 (2003) 406–421.

[48] F. Liu, P. Zhuang, V. Anh, I. Turner, K. Burrage, Stability and convergence of the difference methods for the space–time fractional advection–diffusion equation, Appl. Math. Comput., 191 (2007) 12–20.

[49] J. Zhao, L. Zheng, X. Zhang, F. Liu, Unsteady natural convection boundary layer heat transfer of fractional Maxwell viscoelastic fluid over a vertical plate, International Journal of Heat and Mass Transfer 97 (2016) 760–766.

[50] P. Ganesan, G. Palani, Finite difference analysis of unsteady natural convection MHD flow past an inclined plate with variable surface heat and mass flux, Int. J. Heat Mass Transfer 47 (2004) 4449–4457.

[51] J. Crepeau, R. Clarksean, Similarity solutions of natural convection with internal heat generation, J. Heat Transf. 119 (1) (1997) 183–185.

[52] A.J. Chamkha, A.R.A. Khaled, Similarity solutions for hydromagnetic simultaneous heat and mass transfer by natural convection from an inclined plate with internal heat generation or absorption, Heat Mass Transfer 37 (2–3) (2001) 117–123.

[53] C.H. Chen, Combined heat and mass transfer in MHD free convection from a vertical surface with ohmic heating and viscous dissipation, Int. J. Eng. Sci. 42 (7) (2004) 699–713.

[54] J. Buongiorno, Convective Transport in Nanofluids, J. Heat Transfer. 128 (2006)240

[55] F. Salah, Z. A. Aziz, M. Ayem, D. L. Chuan Ching, MHD Accelerated Flow of Maxwell Fluid in a Porous Medium and Rotating Frame, ISRN Math. Phys. vol. 2013

[56] C. Friedrich, Relaxation and retardation functions of the Maxwell model with fractional derivatives, Rheol. Acta 30 (1991)151–158.

[57] C. C. Wang, Mathematical principles of mechanics and electromagnetism, Part A, Analytical and continuum mechanics, Springer Science and Business Media, 2013 Mar 9.

[58] M. Shen, S. Chen, F. Liu, Unsteady MHD flow and heat transfer of fractional Maxwell viscoelastic nano fluid with Cattaneo heat flux and different particle, Chin. J. Phys. 56(2018) 1199-1211

[59] C. Friedrich, Relaxation and retardation functions of the Maxwell model with fractional derivatives, Rheol. Acta 30 (1991) 151–158.

[60] I. Pop, D.B. Ingham, Transport Phenomena in Porous Media II, Pergamon, 2002

[61] A. Q. Khan, A. Rasheed, Mixed Convection Magnetohydrodynamics Flow of a Nanofluid with Heat Transfer: A Numerical Study, Math. Probl. Eng. Volume 2019, 8129564.

[62] C. Cattaneo. Sur une forme de l'équation de la chaleur éliminant le paradoxe d'une propagation instantanée, Comptes rendus Acad. Sci. Paris Sér. A-B 247, (1958) 431.

[63] J. Zhao, L. Zheng, X. Zhang, F. Liu, Unsteady natural convection boundary layer heat transfer of fractionalMaxwell viscoelastic fluid over a vertical plate, International Journal of Heat and Mass Transfer 97 (2016) 760-766 Fourier's and Fick's laws, Eur. Phys. J. Plus (2018) 133: 63

[64] F. Liu, P. Zhuang, V. Anh, I. Turner, K. Burrage, Stability and convergence of the difference methods for the space–time fractional advection–diffusion equation, Appl. Math. Comput., 191 (2007) 12–20.

[65] Y. Lin and C. Xu, Finite difference/spectral approximations for the time-fractional diffusion equation, J. Comput. Phys. 225, 2007.

[66] R.L. Bagley, P.J. Torvik, A theoretical basis for the application of fractional calculus toviscoelasticity, J. Rheology, 1983.

[67] A. Heibig, L. I. Palade, Well posedness of a linearized fractional derivative fluid model, J. Math. Anal. Appl. 380, 2011.

[68] R. A. Adams, Sobolev Spaces, Academic Press, New York, 1975.

[69] L. Liu, F. Liu, Boundary layer flow of fractional Maxwell fluid over a stretching sheet with variable thickness, Applied Mathematics Letters 79 (2018) 92–99

[70] C. Friedrich, Relaxation and retardation functions of the Maxwell model with fractional derivatives, Rheol. Acta 30 (1991) 151–158.

[71] M. Caputo, Linear models of dissipation whose Q is almost frequency independent. Part II. J Roy Austral Soc.;13:529-539,1967.

[72] I. Khan, S. Fatima, M.Y. Malik, T. Salahuddin, Exponentially varying viscosity of magnetohydrodynamic mixed convection Eyring-Powell nanofluid flow over an inclined surface, Results in Physics 8(2018)1194-1203

[73] J. Zhao, L. Zheng, X. Chen, X. Zhang, F. Liu, Unsteady Marangoni convection heat transfer of fractional Maxwell fluid with Cattaneo heat flux, Applied Mathematical Modelling 44 (2017) 497–507

[74] A.H. Srinivasa, A.T. Eswara, Effect of internal heat generation or absorption on MHD free convection from an isothermal truncated cone, Alexandria Engineering Journal (2016) 55, 1367–1373

[75] C. Cattaneo. Sur une forme de l'équation de la chaleur éliminant le paradoxe d'une propagation instantanée, Comptes rendus Acad. Sci. Paris Sér. A-B 247, (1958) 431.

[76] F. Liu, P. Zhuang, V. Anh, I. Turner, K. Burrage, Stability and convergence of the difference methods for the space–time fractional advection–diffusion equation, Appl. Math. Comput., 191 (2007) 12–20.

[77] I. Podlubny, Fractional Differential Equations, Academic Press, San Diego, 1999, pp. 78–85.

[78] P. Ganesan, G. Palani, Finite difference analysis of unsteady natural convection MHD flow past an inclined plate with variable surface heat and mass flux, Int. J. Heat Mass Transfer 47 (2004) 4449–4457.

[79] A. Q. Khan, A. Rasheed, Mixed Convection Magnetohydrodynamics Flow of a Nanofluid with Heat Transfer: A Numerical Study, Mathematical Problems in Engineering Volume 2019, Article ID 8129564

[80] R. J. LeVeque, Z. Li. The immersed interface method for elliptic equations with discontinuous coefficients and singular sources. SIAM J Numer Anal 1994;31:1019–1044.

[81] M.-C. Lai, Z. Li, A remark on jump conditions for the three-dimensional Navier–Stokes equations involving an immersed moving membrane, Appl Math Lett 14 (2) (2001) 149–154.

[82] Z. Li, M.-C. Lai, The immersed interface method for the Navier–Stokes equations with singular forces, J Comput Phys 171 (2) (2001) 822–842.

[83] L. Lee, R. J. LeVeque, An immersed interface method for incompressible Navier–Stokes equations, SIAM J Sci Comput 25 (3) (2003) 832–856.

[84] R. J. LeVeque, Z. Li, Immersed interface methods for stokes flow with elastic boundaries or surface tension, SIAM J Sci Comput 18 (3) (1997) 709–735.

[85] Z. Li, K. Ito, M.-C. Lai, An augmented approach for stokes equations with a discontinuous viscosity and singular forces, Comput Fluids 36 (3) (2007) 622–635.

[86] Z. Li, K. Ito, The immersed interface method: numerical solutions of PDEs involving interfaces and irregular domains, SIAM, 2006.